Structural biology

Studies of the shape and architecture of biological macromolecules, including in particular proteins and nucleic acids

Proper functioning of macromolecules (RNA) requires that they adopt the correct spatial structure

Macromolecules are able to perform their functions due to the precise arrangement of chemical groups in their structure

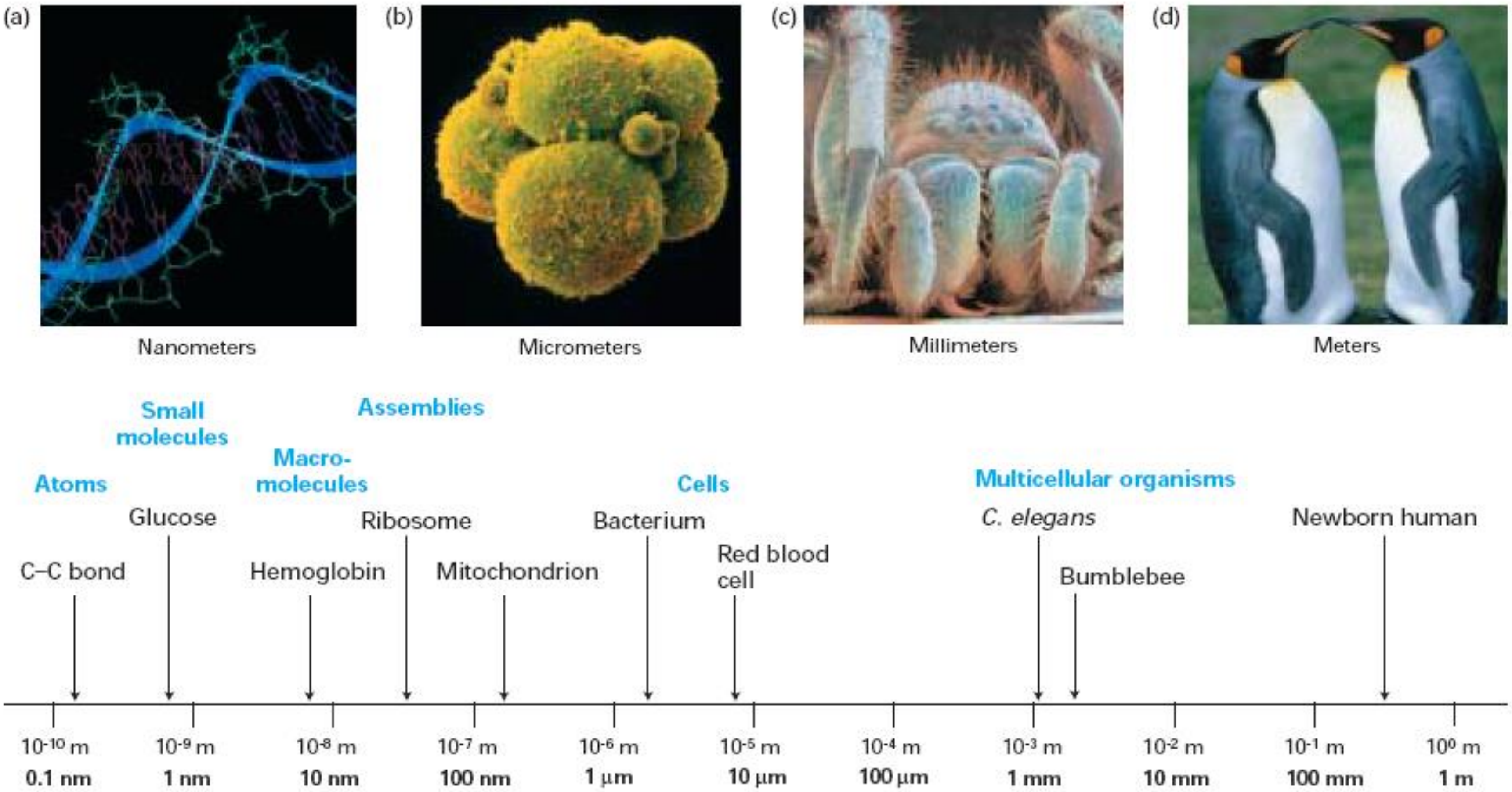

1 Å 10 Å 100 Å 1000 Å

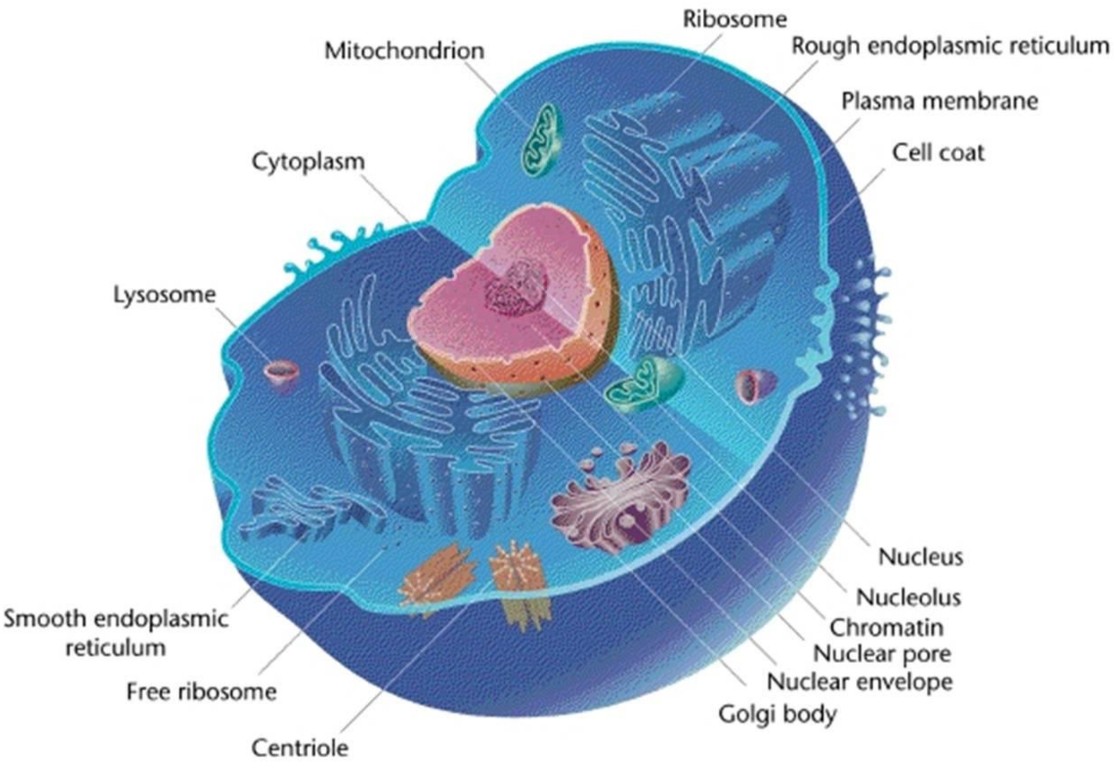
Ribosome
Mitochondrion
Rough endoplasmic reticulum
Plasma membrane
Cytoplasm
Cell coat
Lysosome
Nucleus
Nucleolus
Smooth endoplasmic reticulum
Chromatin
Nuclear pore
Free ribosome
Nuclear envelope
Golgi body
Centriole

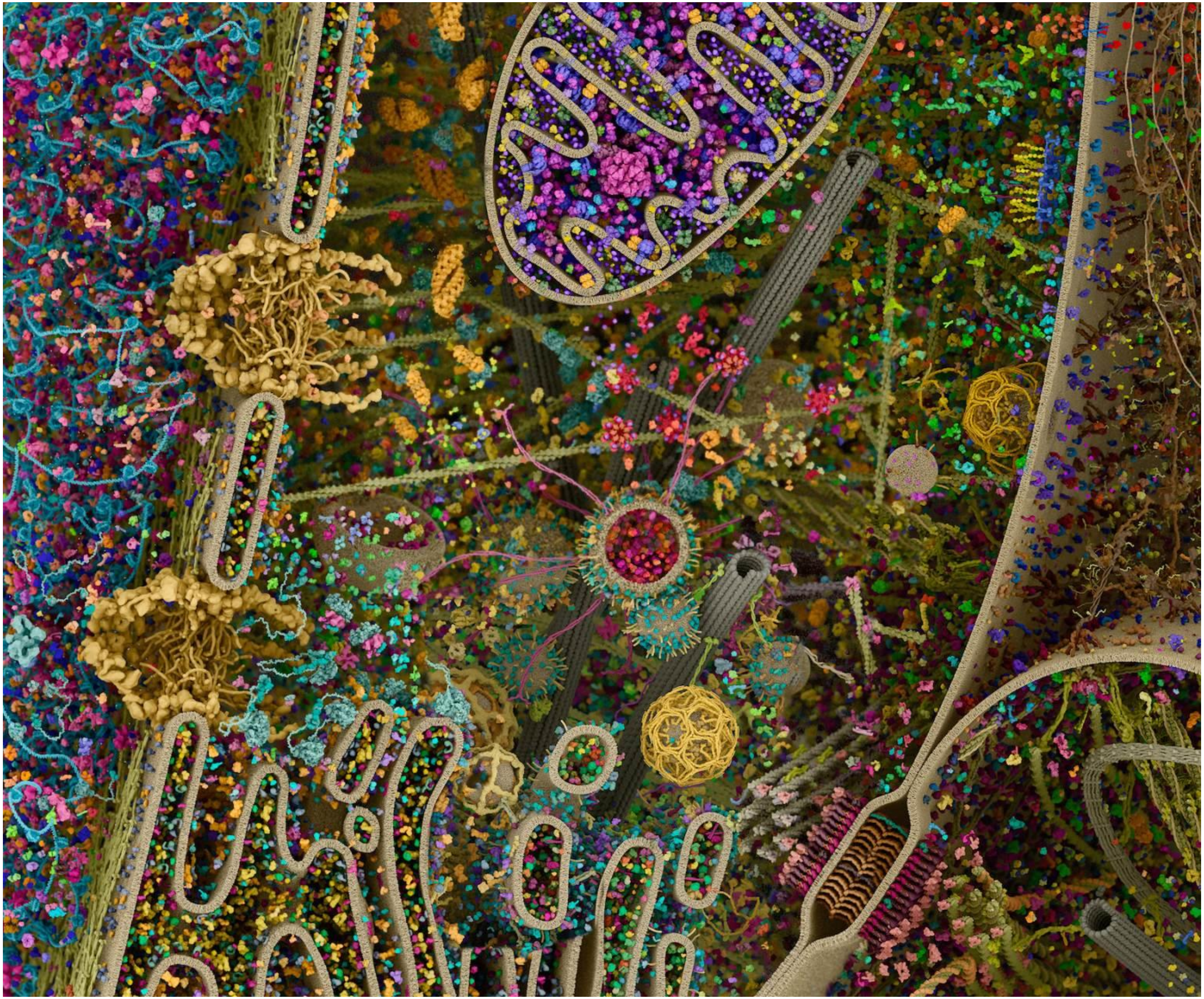

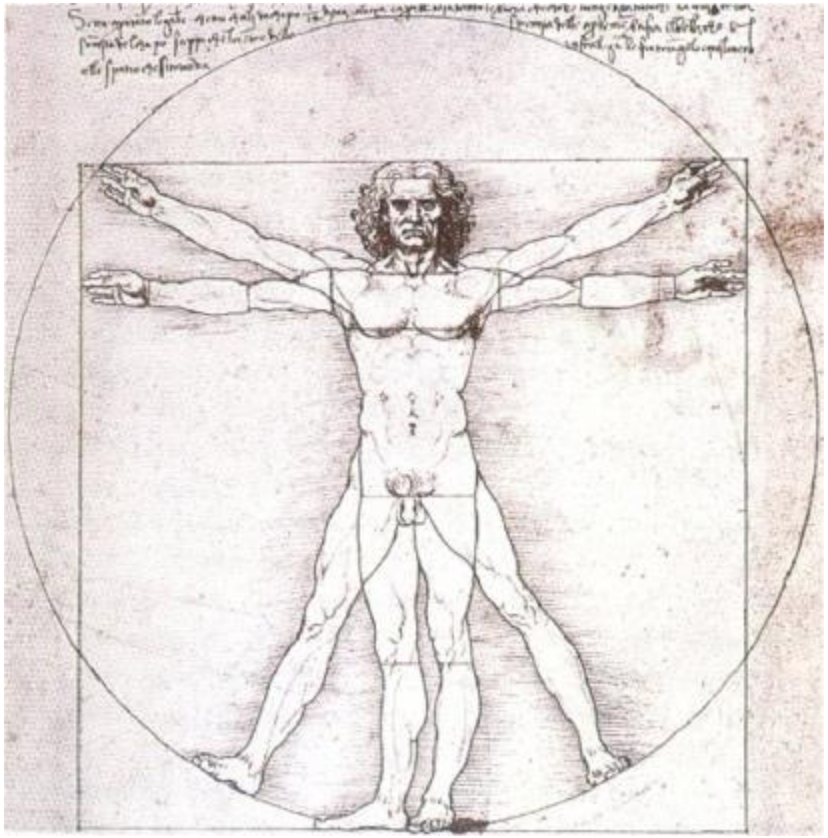

20 000 km

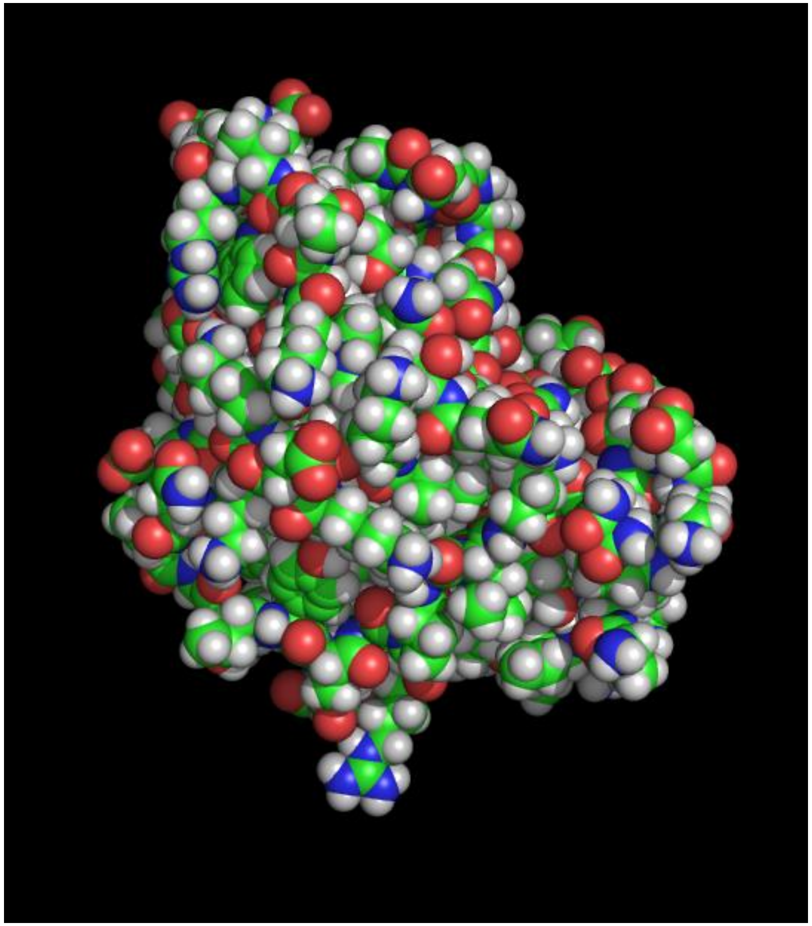

5 cm

[redacted]

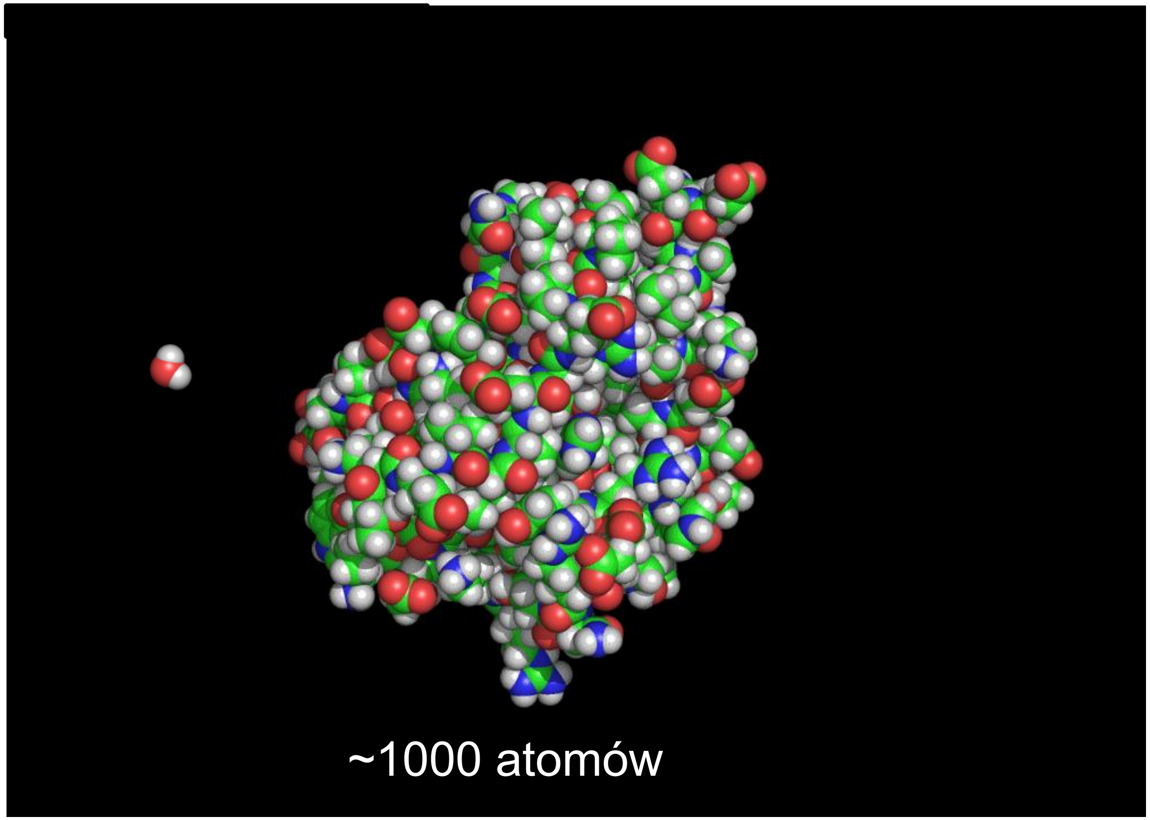

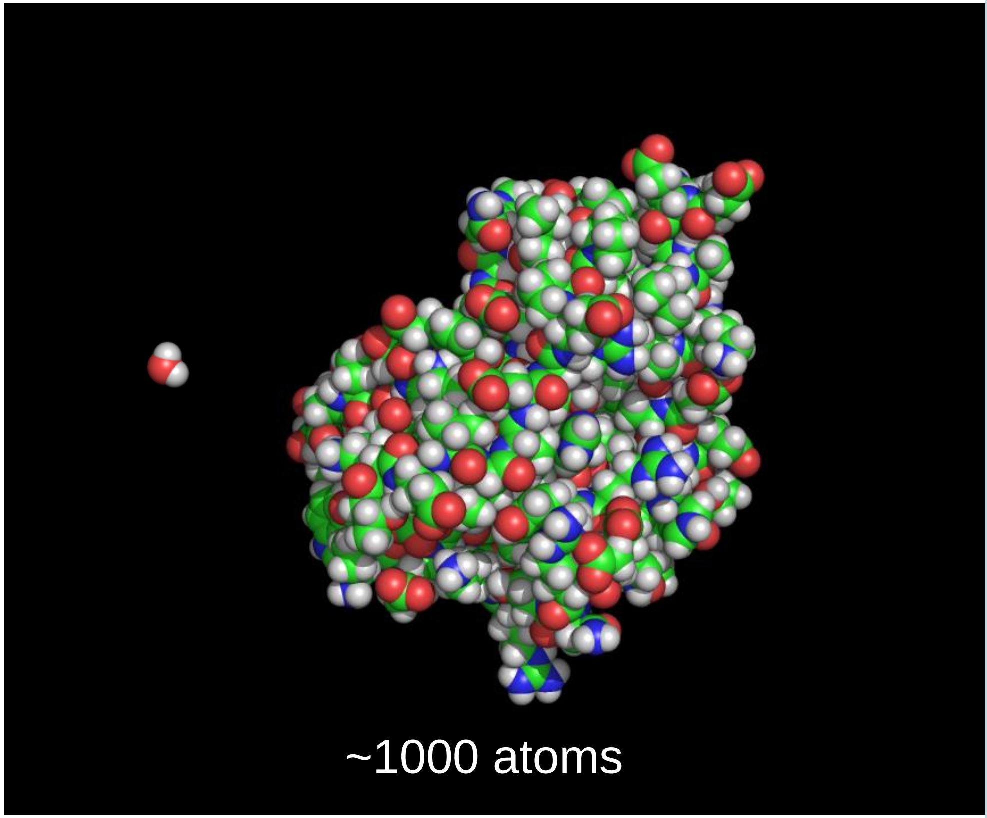

~1000 atoms

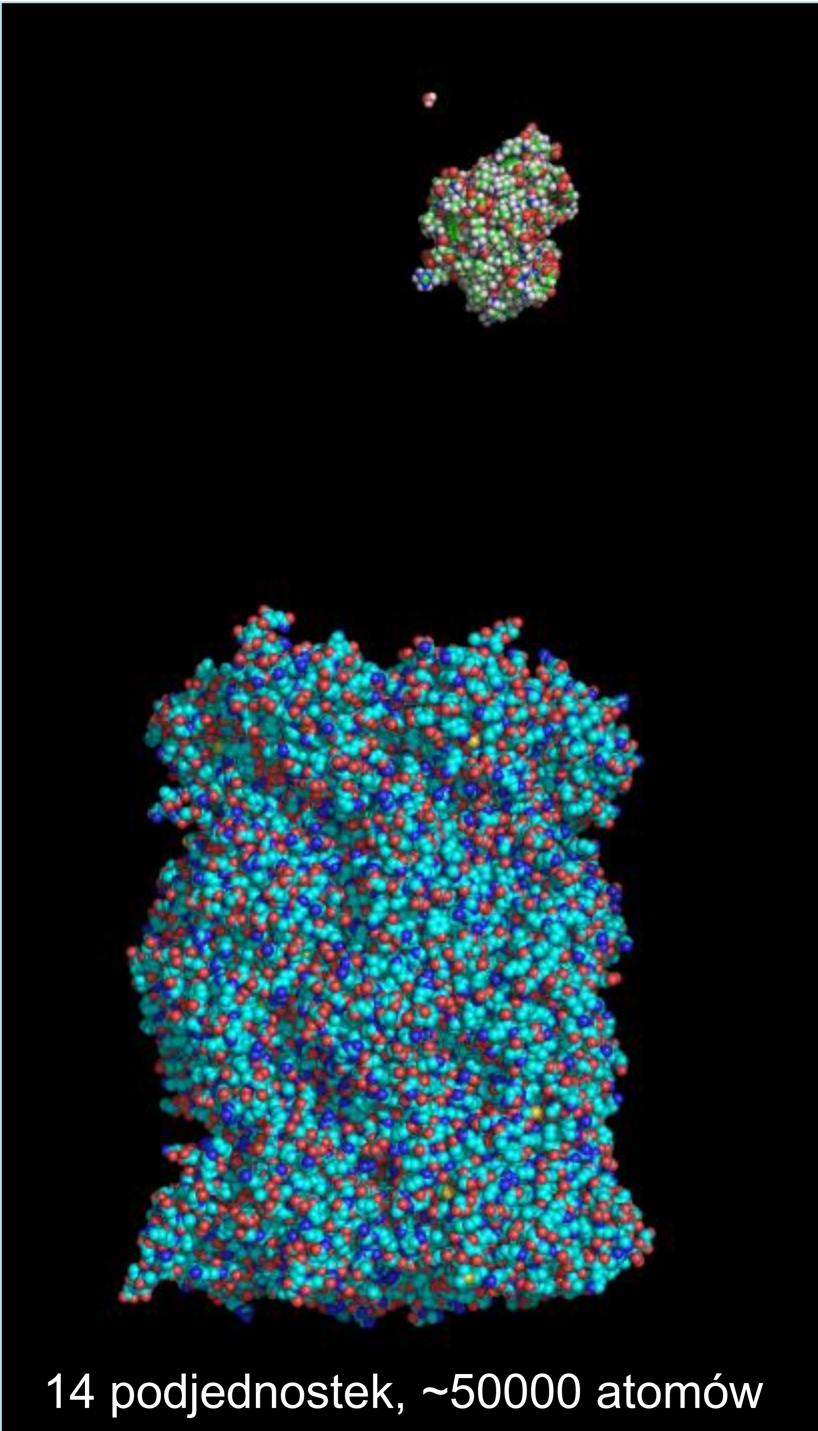

14 podjednostek, ~50000 atomów

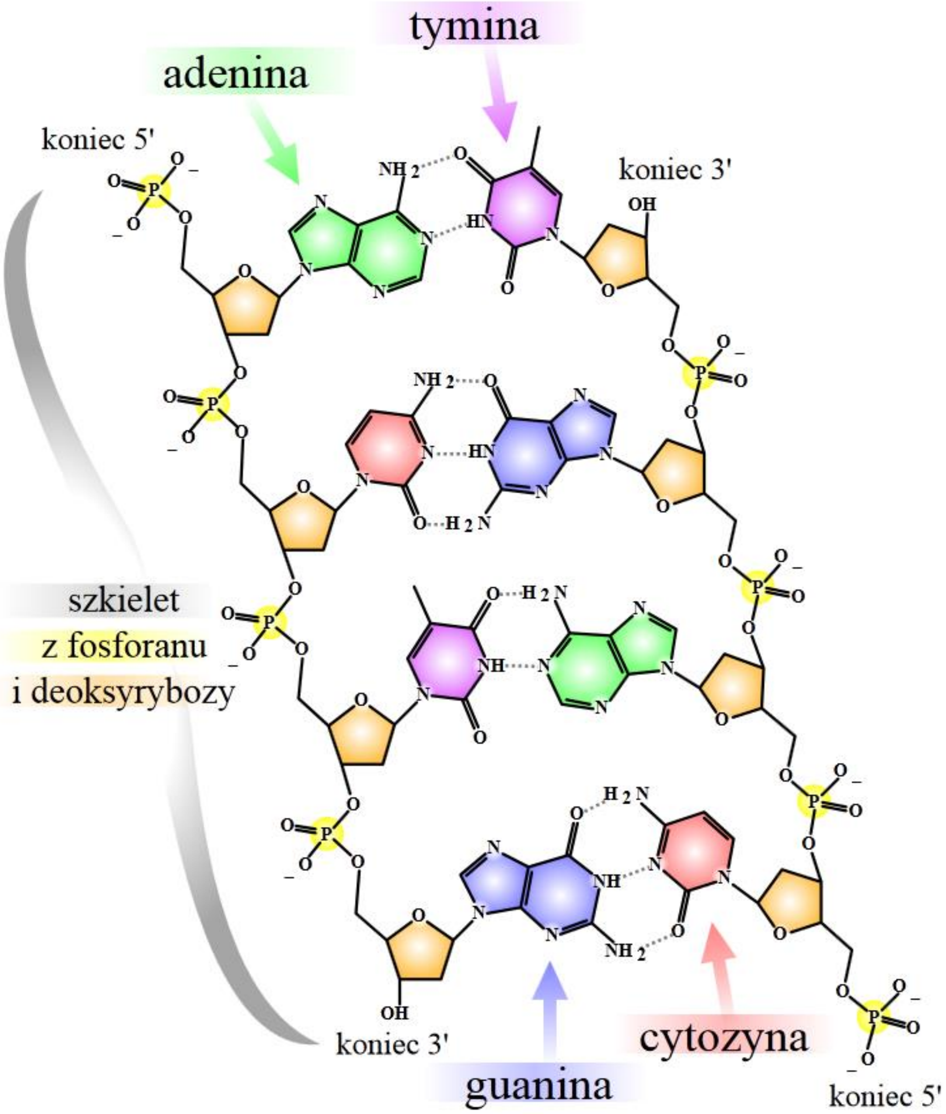
tymina
adenina
koniec 5'
koniec 3'
szkielet
z fosforanu
i deoksyrybozy
koniec 3'
cytozyna
guanina
koniec 5'

chemical structures of DNA and RNA: similar or different?

DNA:

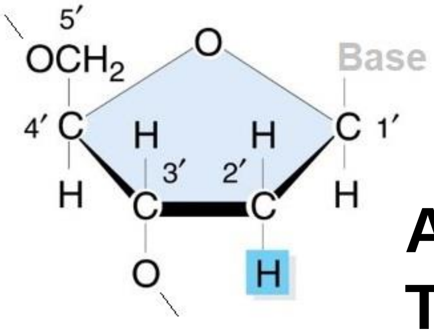

deoxyribose

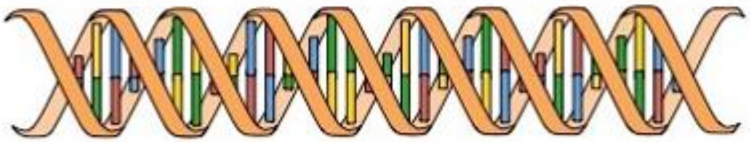

A, G, C, T
Two complementary strands forming an antiparallel double helix

RNA:

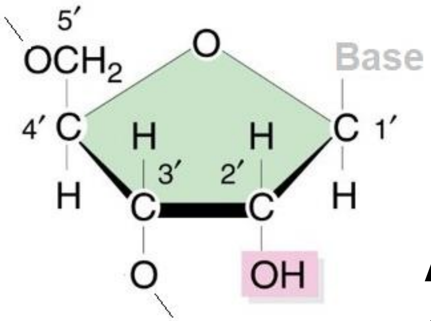

ribose

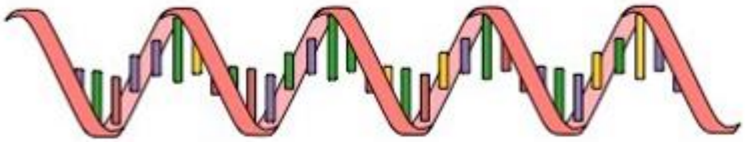

A, G, C, U
One strand
forming… what exactly?

RNA can form canonical A-U & C-G pairs and fold into helical regions divided by loops

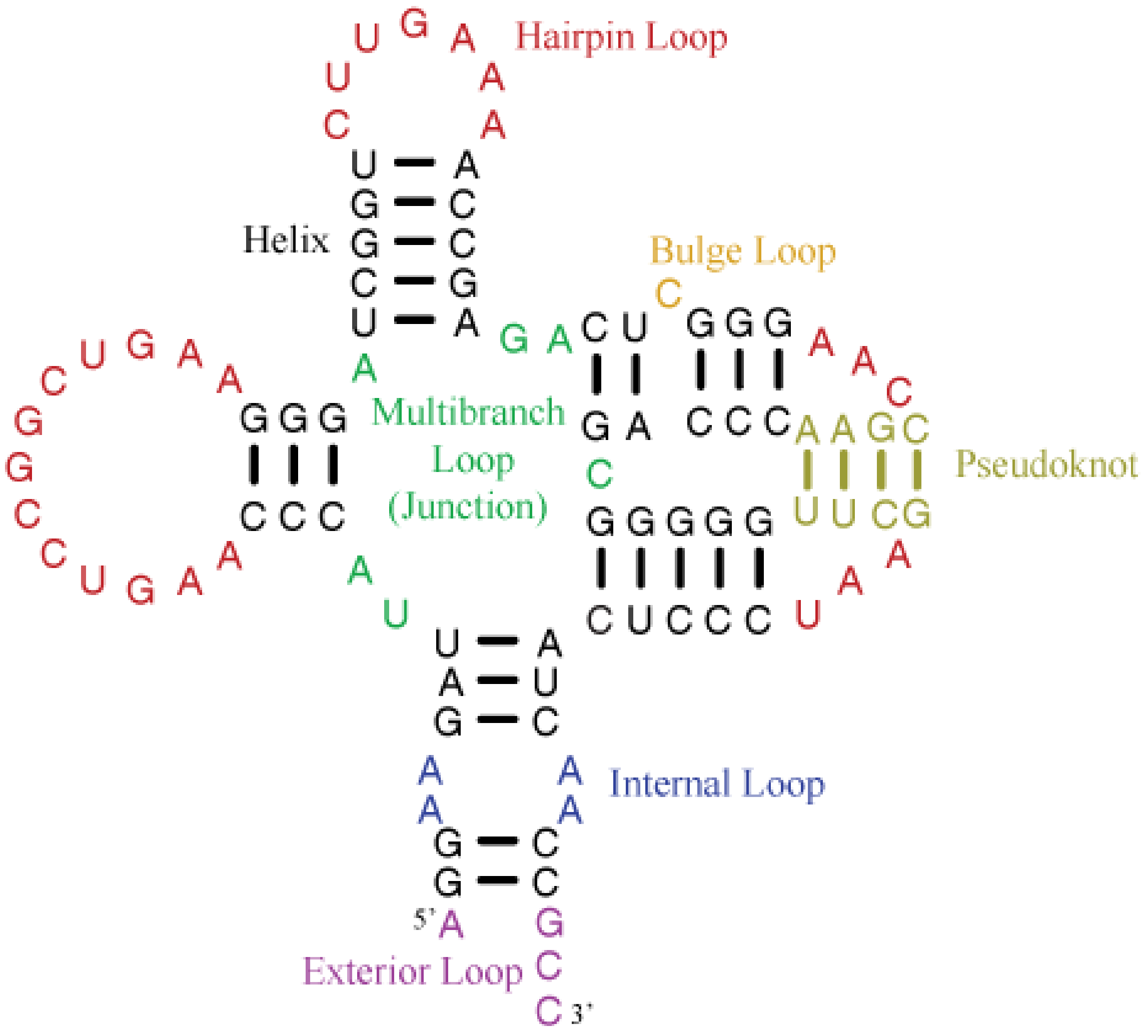

https://x3dna.org/articles/exterior-loop-in-rna-secondary-structure

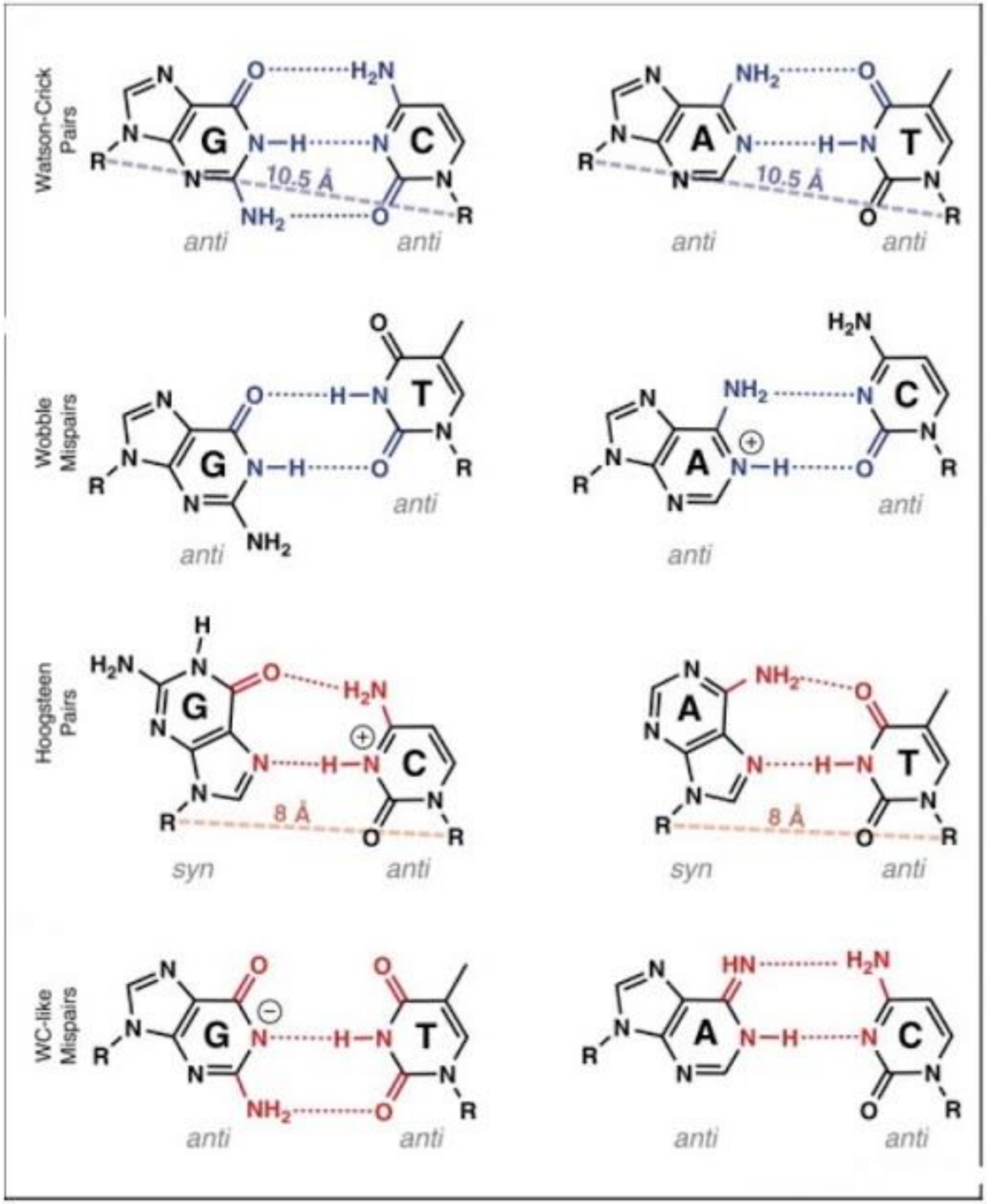

RNA can form non-canonical A-U & C-G pairs

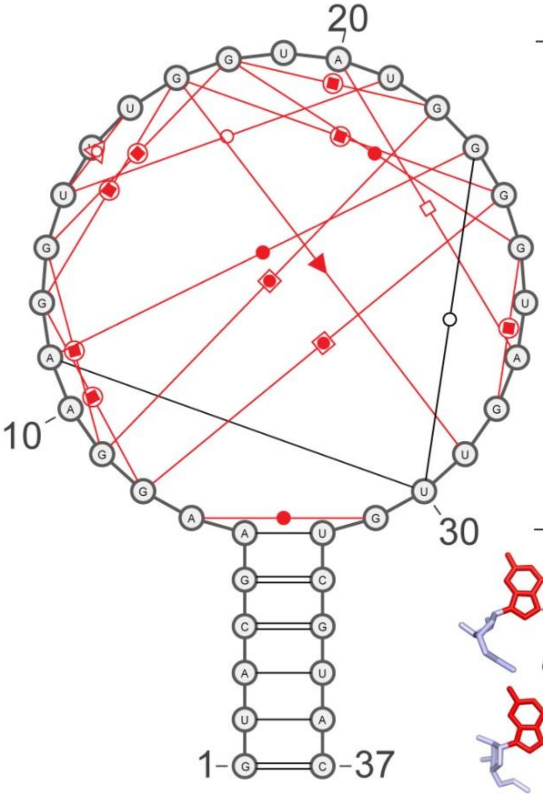

This region *is not*
'unstructured'
(as the 'empty loop'
within the
secondary
structure model
shown in black
might suggest)

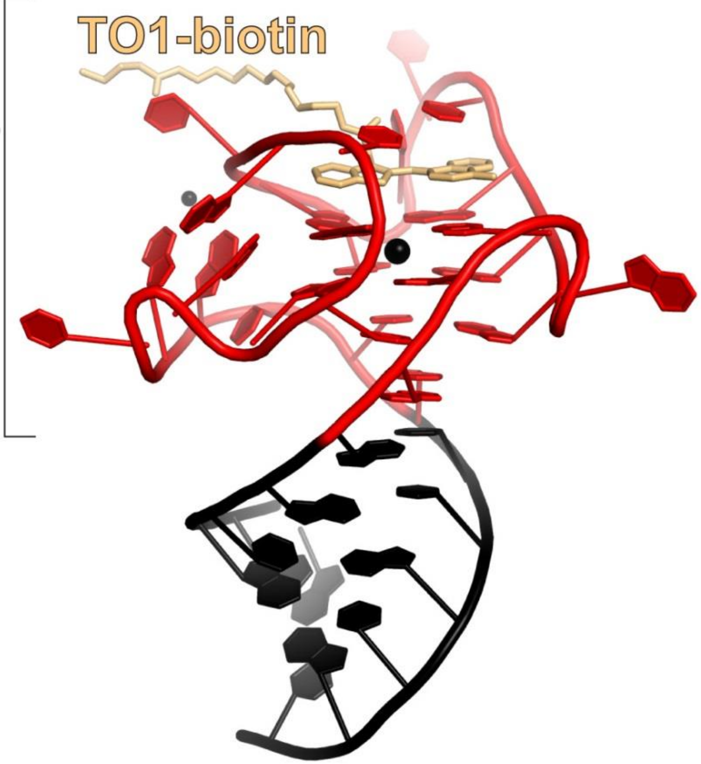

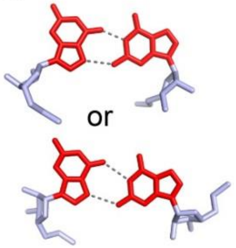

iMango-III fluorescent aptamer

PDB ID 6PQ7

Canonical and non-canonical pairs and other interactions lead to complex 3D motifs

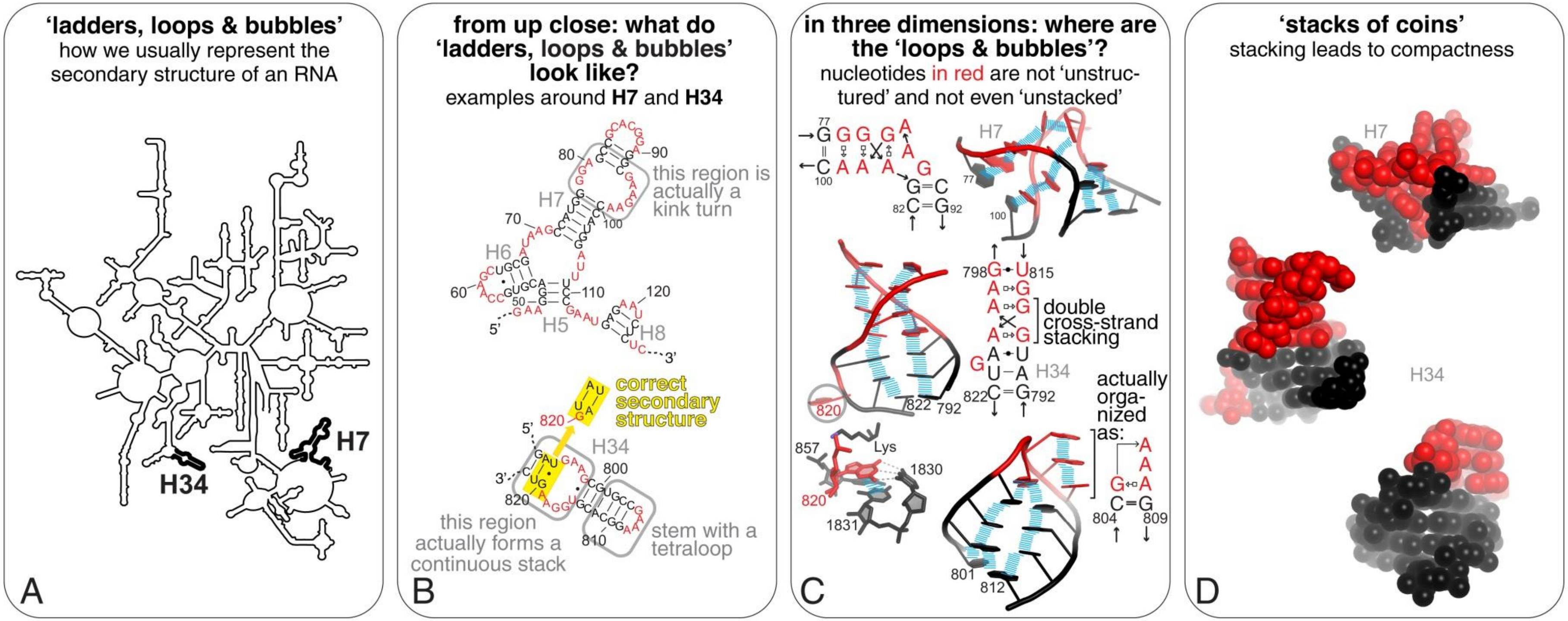

Thoughts on how to think (and talk) about RNA structure

Quentin Vicens, Jeffrey S Kieft, Proc Natl Acad Sci U S A, 2022 Apr 26;119(17):e2112677119.

RNA molecules can form alternative, different structures

5′–GGCGUUUUCGCCUUCGGGCGAUUUUUAUCGCU –3′

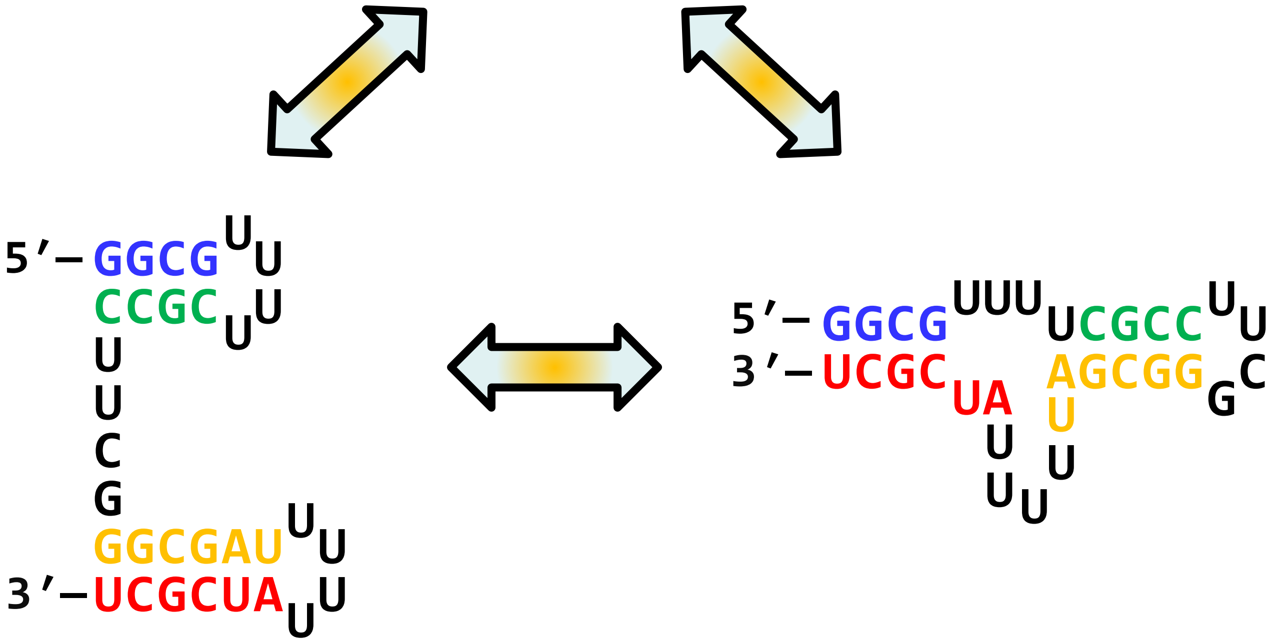

5′– GGCG^{U}U
CCGC$_{U}$U
U
U
C
G
GGCGAU^{U}U
3′–UCGCUA$_{U}$U

5′– GGCG^{UUU}UCGCC^{U}U
3′– UCGC UA AGCGG $_{G}$C
U U
U U
U U

RNA molecules
can form alternative, different structures

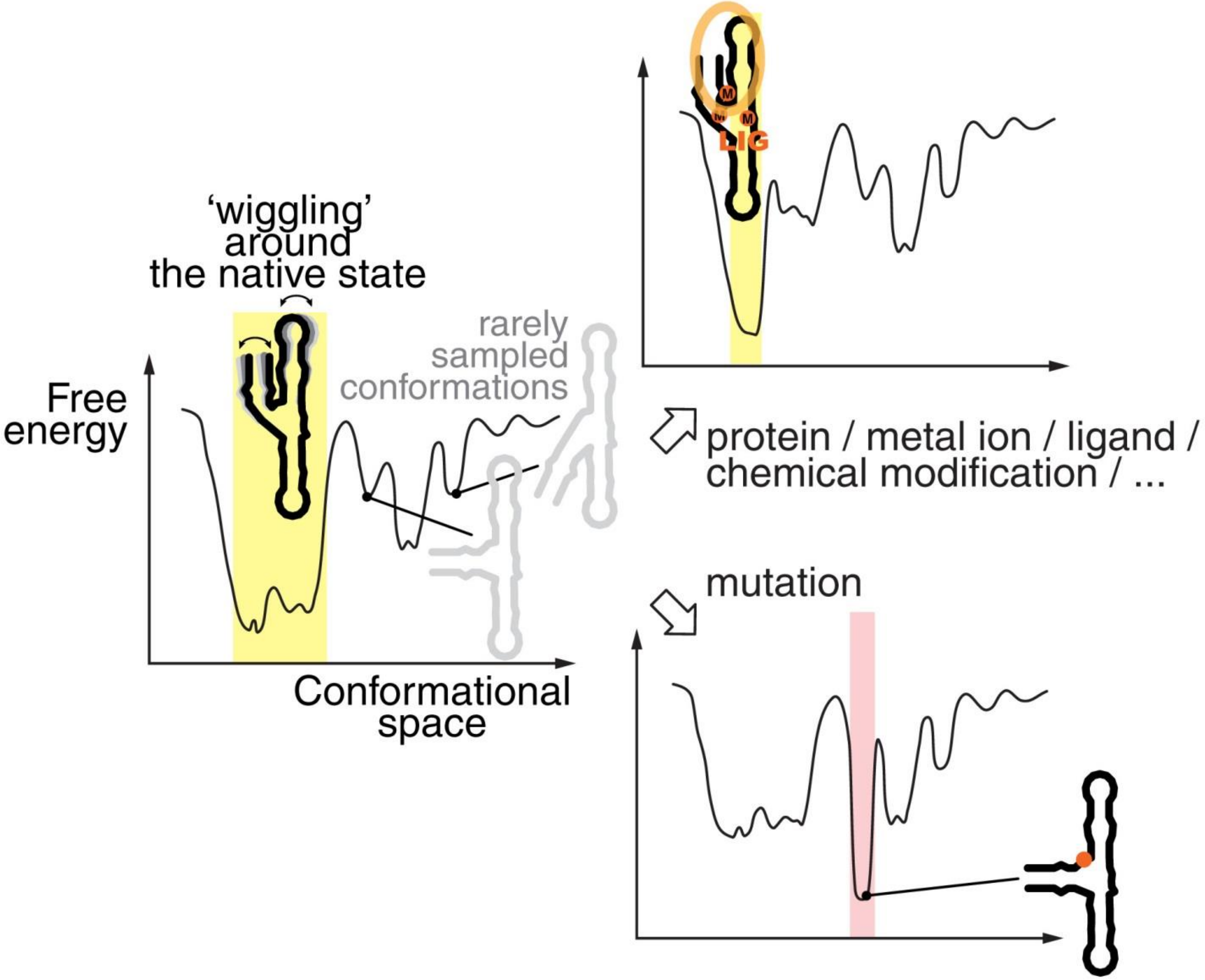

Thoughts on how to think (and talk) about RNA structure
Quentin Vicens, Jeffrey S Kieft, Proc Natl Acad Sci U S A, 2022 Apr 26;119(17):e2112677119.

Functional RNAs
have undergone evolutionary selection to form a restricted number of relatively stable structures

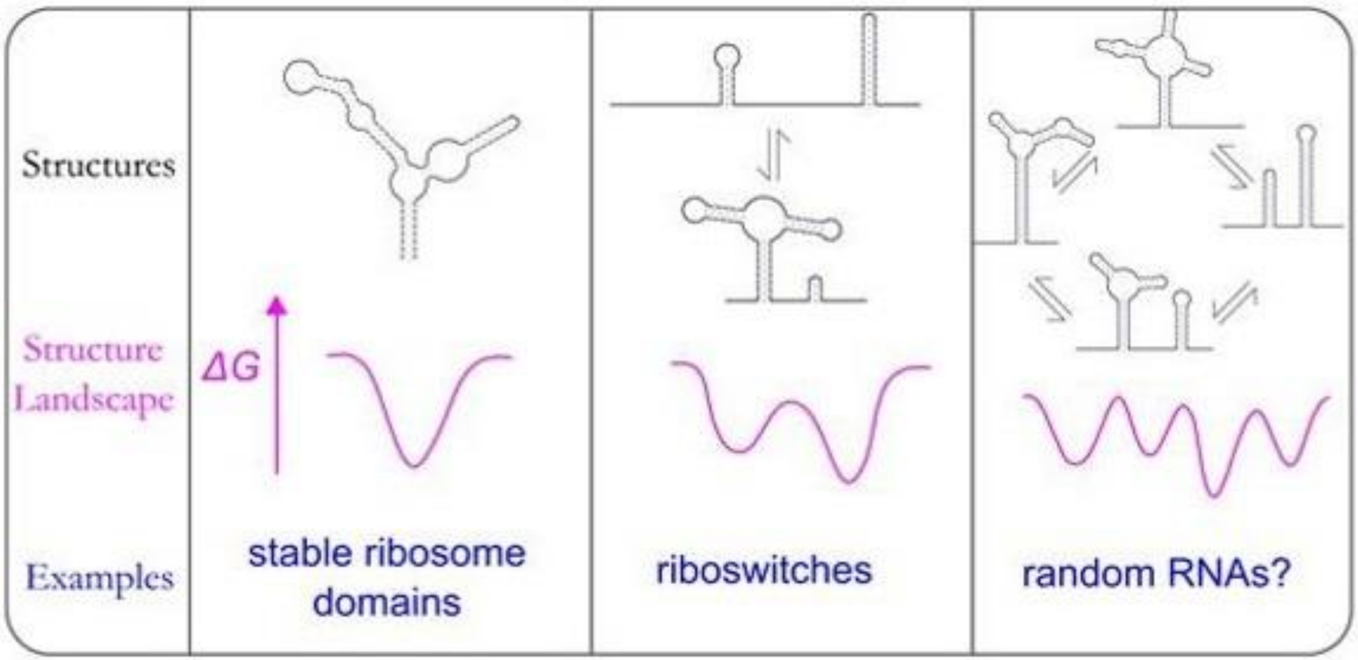

Cordero P, Das R
Rich RNA structure landscapes revealed by mutate-and-map analysis
PLoS Comput Biol 11(11): e1004473.

Dynamic RNA structures play important roles in biological processes

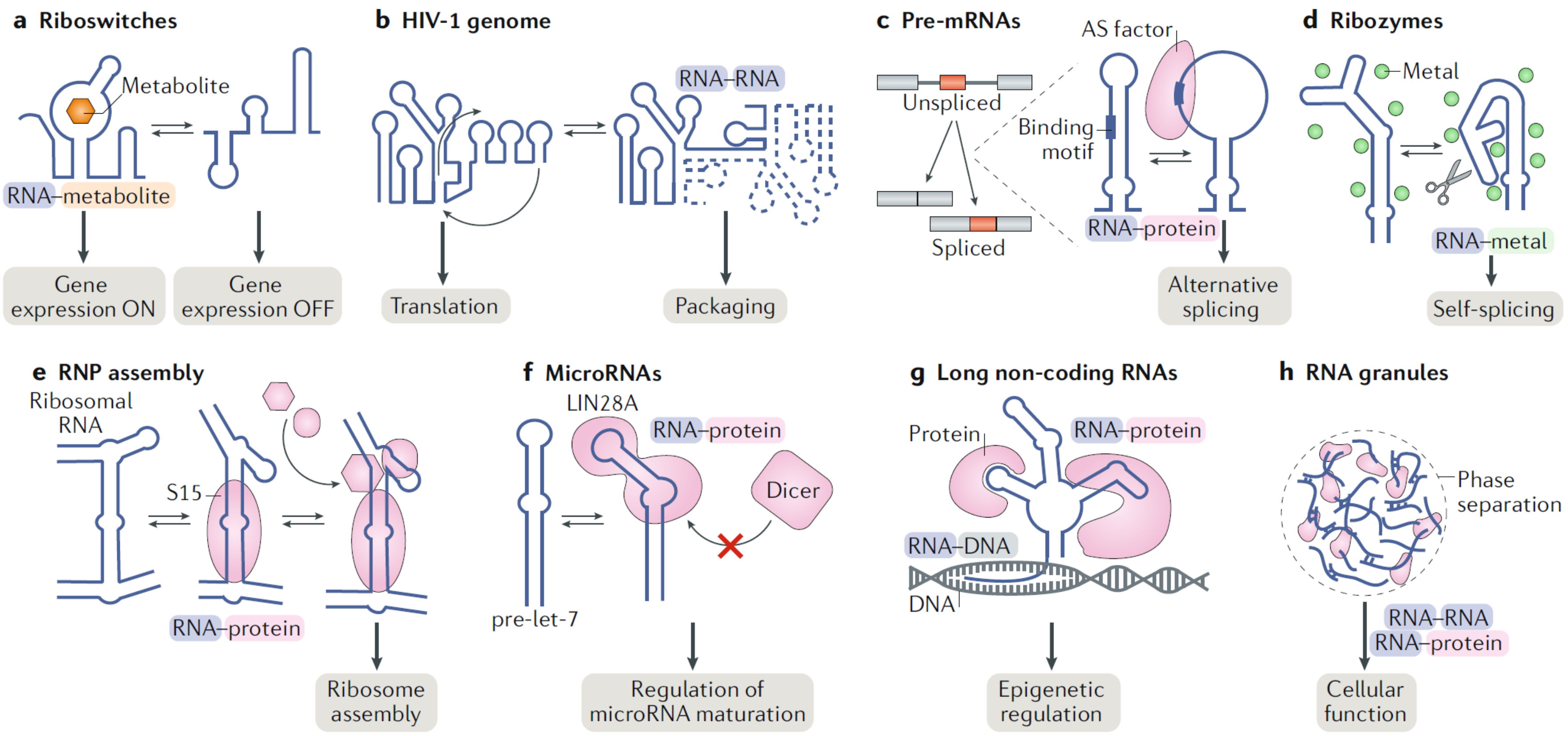

Ganser LR, Kelly ML, Herschlag D, Al-Hashimi HM
The roles of structural dynamics in the cellular functions of RNAs
Nature Rev Mol Cell Biol 2019, 20, 474–489

RNA structure is stabilized mainly by stacking interactions

Structured RNA is not static

RNA is often compact

Watson-Crick pairing is important, but not the only one

Non-canonical base pairs play a key role

Simple diagrams based on W-C pairs - treat with care

Thoughts on how to think (and talk) about RNA structure
Quentin Vicens, Jeffrey S Kieft, Proc Natl Acad Sci U S A, 2022 Apr 26;119(17):e2112677119.

Rybozym

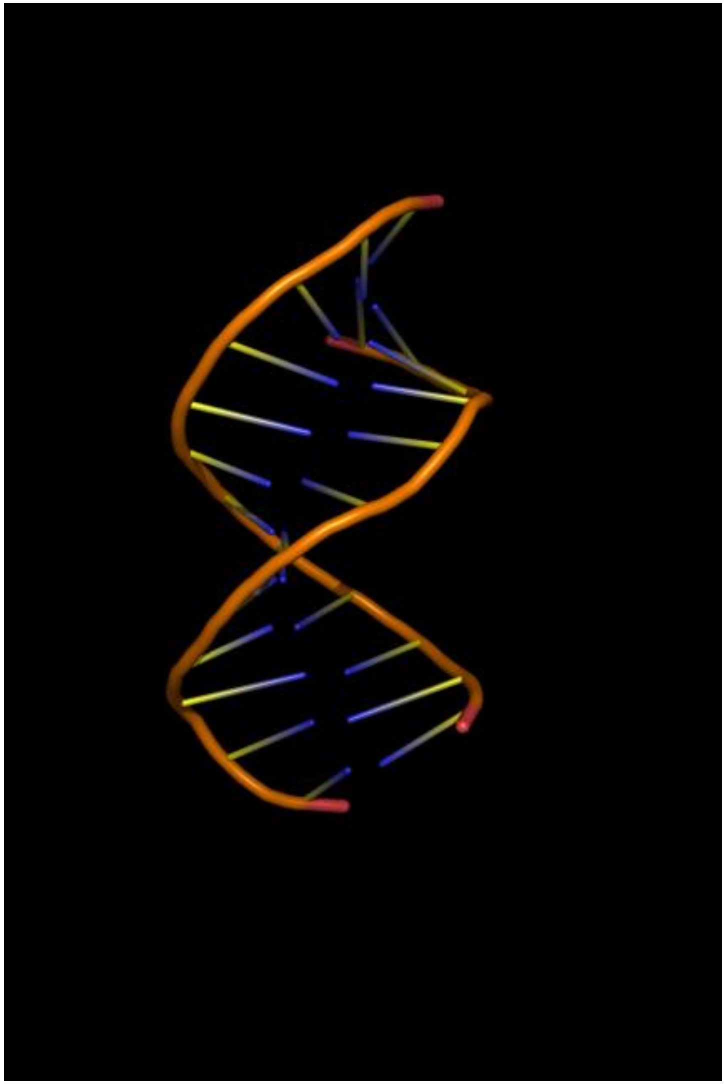

Rybozym

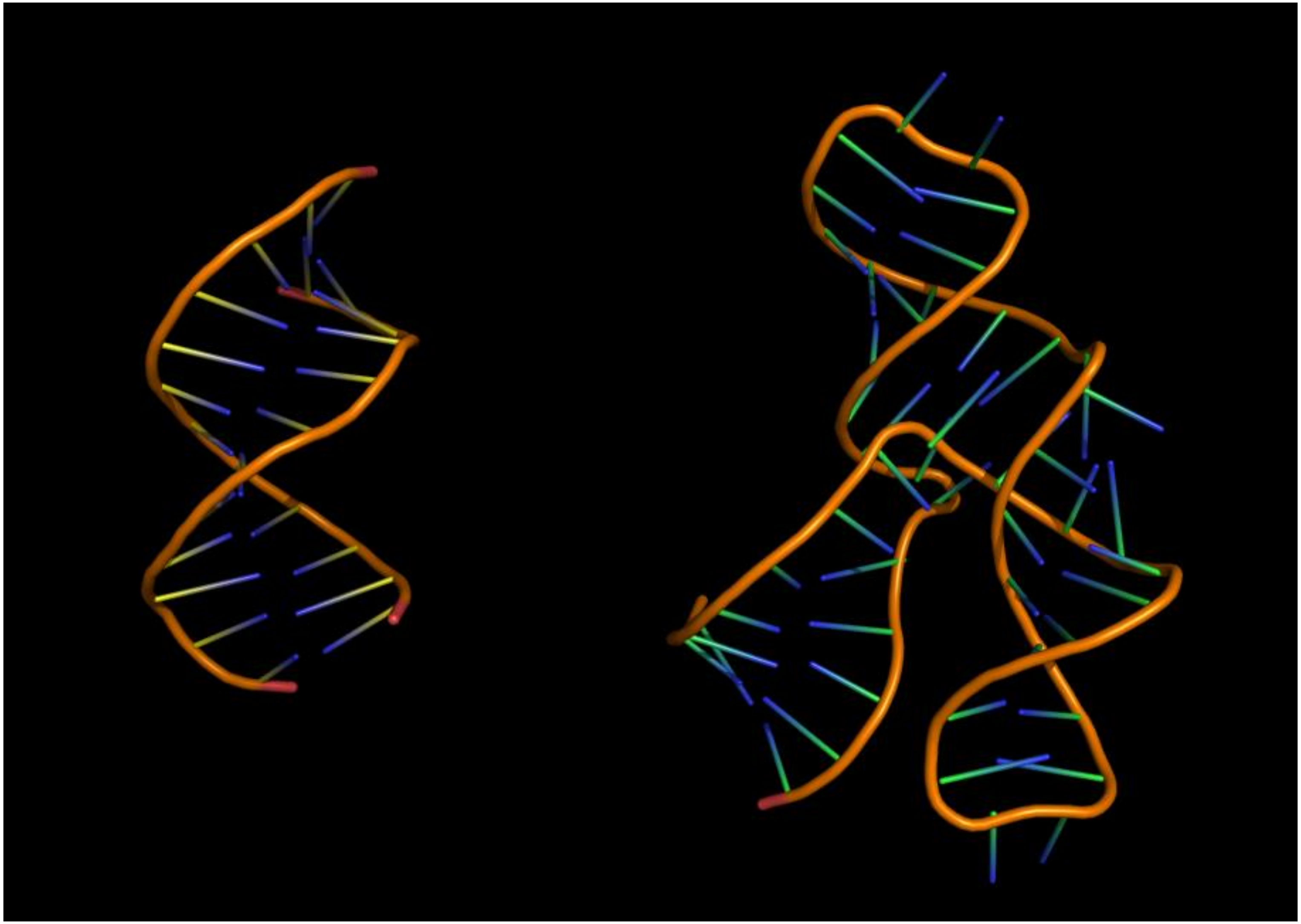

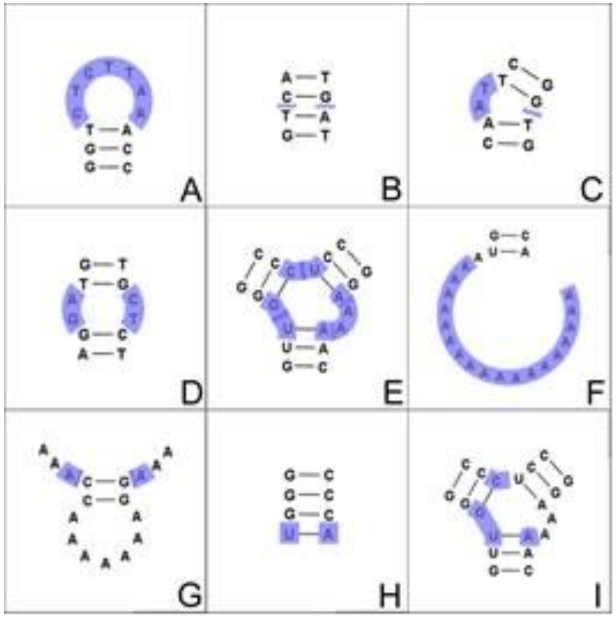
A
B
C
D
E
F
G
H
I

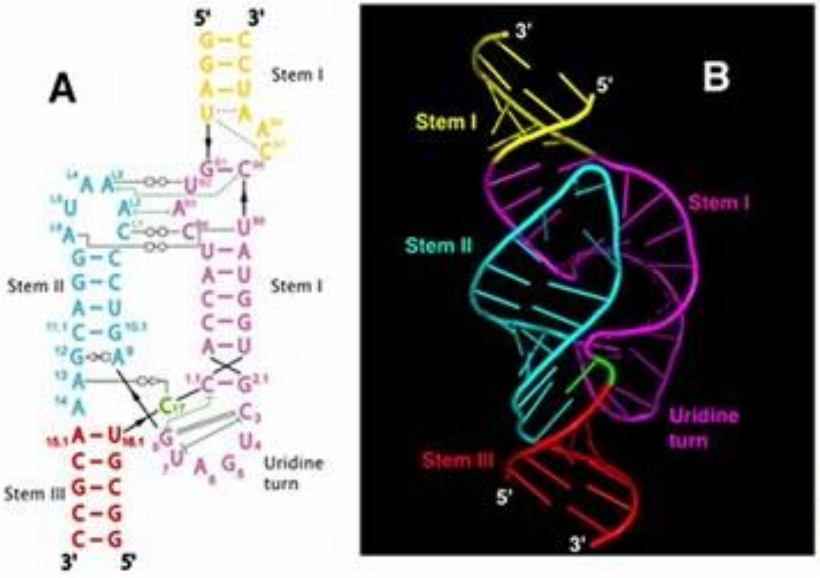
A
5'
3'
Stem I
Stem II
Stem I
Stem III
Uridine turn
3'
5'
B
3'
5'
Stem I
Stem I
Stem II
Uridine turn
Stem III
5'
3'

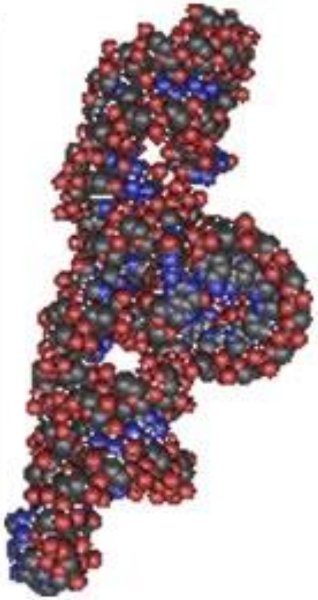

Podstawy struktury RNA

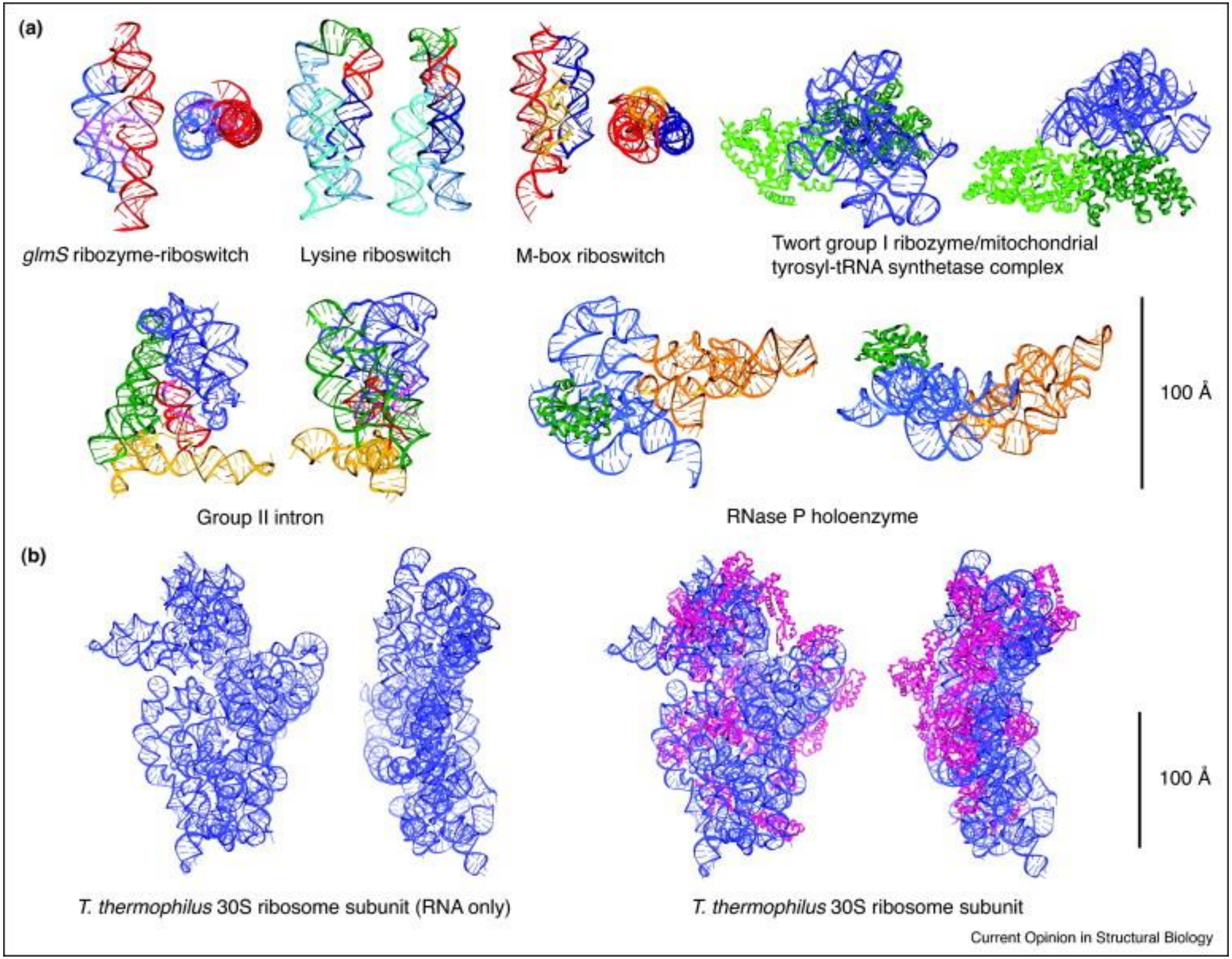

RNase P

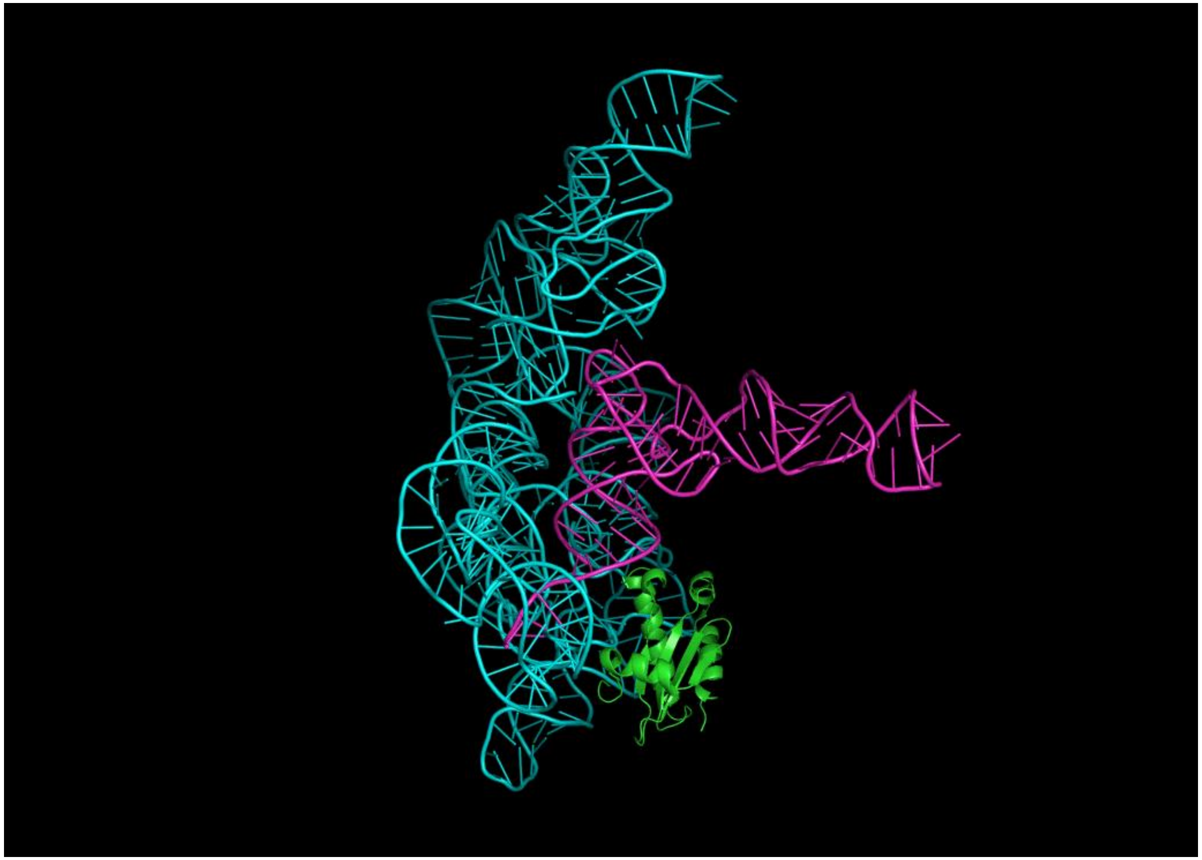

RNA secondary structure can be predicted relatively accurately by sequence comparison or thermodynamic methods

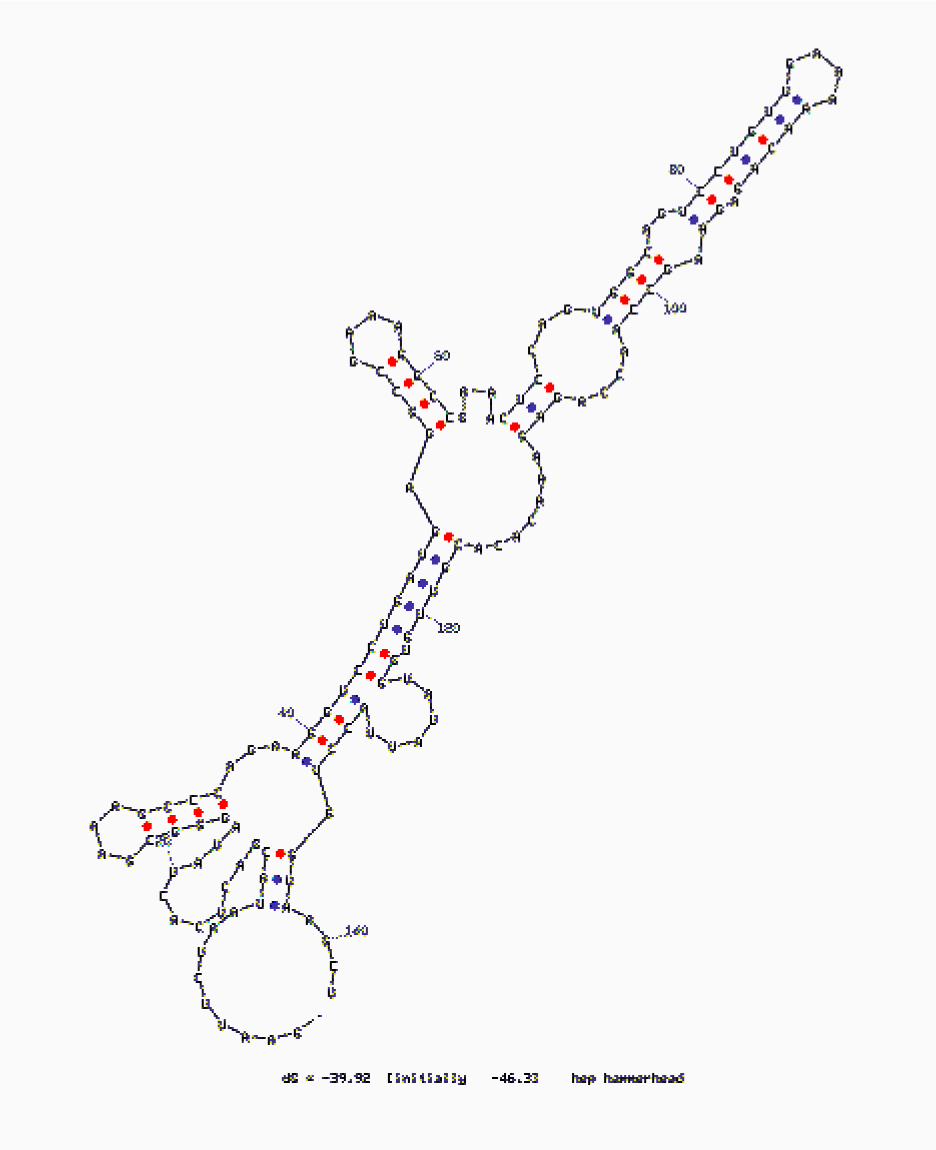

Chemical methods

Small angle X-ray scattering (SAXS)

Electron microscopy (EM)

Nuclear Magnetic Resonance (NMR).

Crystallography

Computational methods

Specialized methods (e.g., FRET)

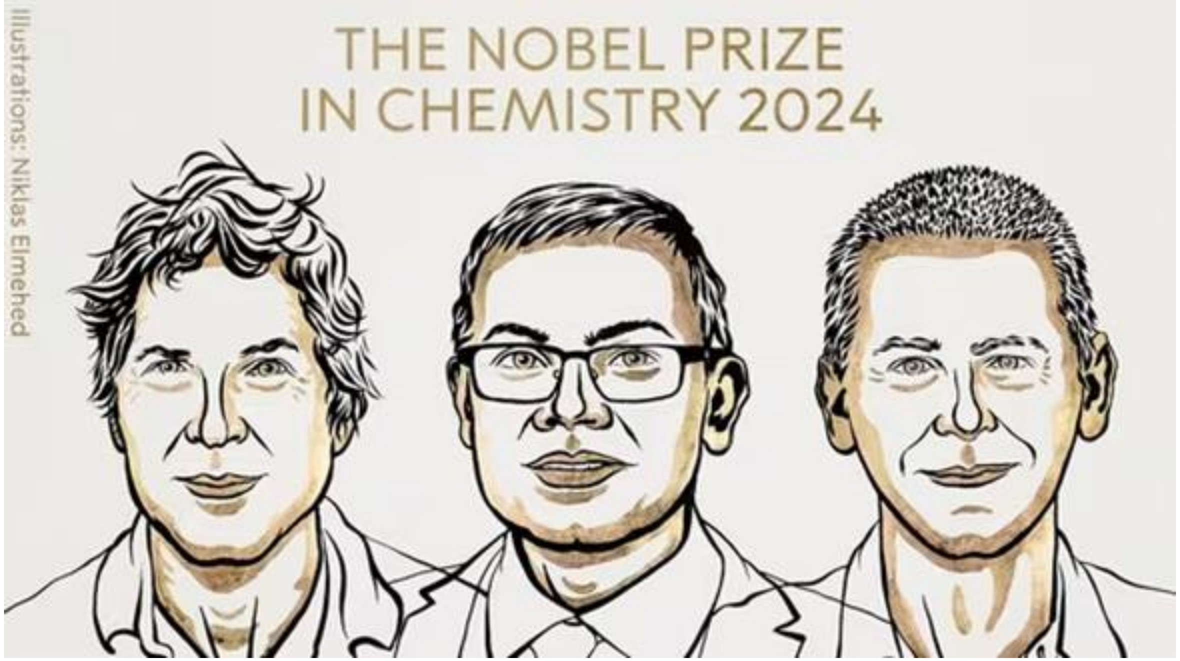

David Baker, Demis Hassabis and John M Jumper

Alphafold2

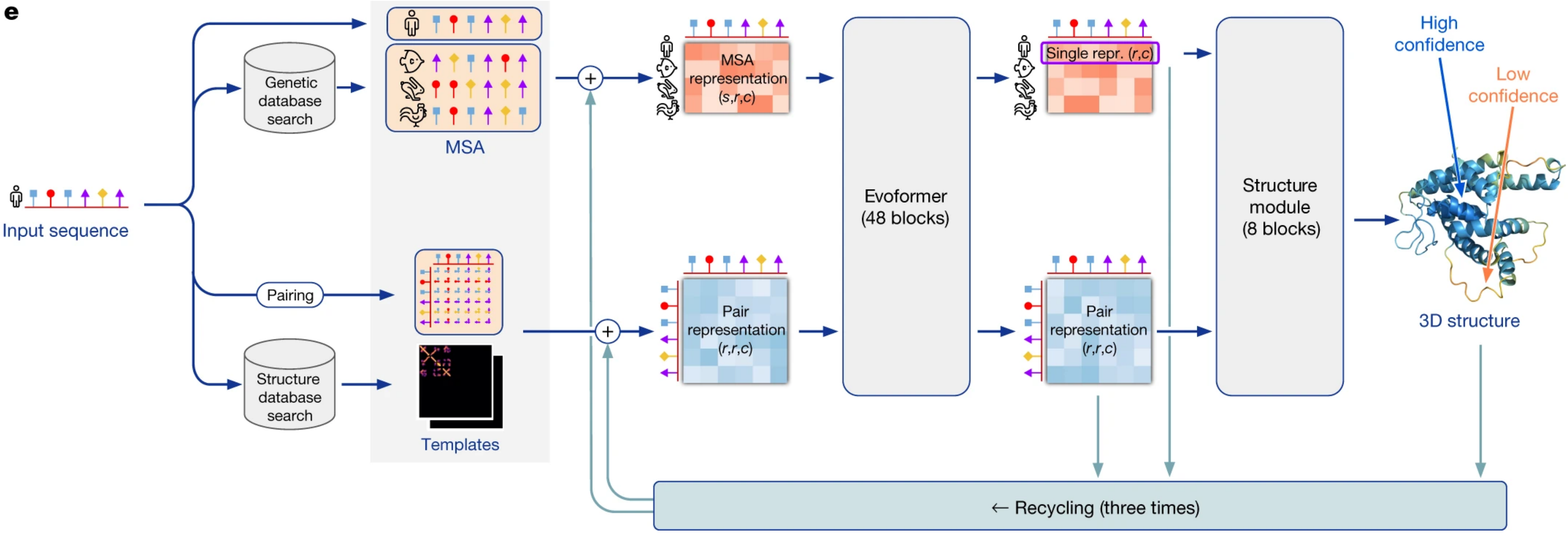

Jumper, J., *et al.* Highly accurate protein structure prediction with AlphaFold. *Nature* **596**, 583–589 (2021)

Alphafold2

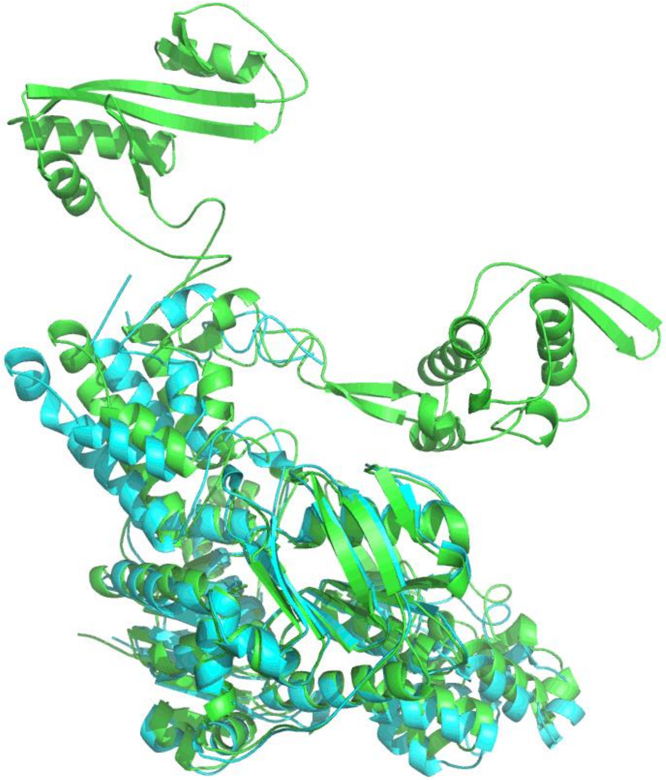

Struktura
Model AF2

RNA production:
Synthesis (up to a few ten nucleotides)
In vitro transcription
Natural sources

Purification under denaturing conditions:
HPLC
Sequential gels

Purification under native conditions:
Chromatographic methods (gel filtration)

Chemical methods

Small angle X-ray scattering (SAXS)

Electron microscopy (EM)

Nuclear Magnetic Resonance (NMR).

Crystallography

Computational methods

Specialized methods (e.g., FRET)

Chemical methods for RNA testing (chemical probing)

Enzymes

Nuclease S1 available nucleotides in single-stranded regions
Ribonuclease V1 nucleotides in forming stacking or paired interactions
T1 ribonuclease available (unpaired) guanines, sequencing for guanines (under denaturing conditions)
U2 ribonuclease Available (unpaired) adenines, sequencing for adenines (under denturating conditions)

Chemical reagents

Imidazole Single-stranded regions available
Lead Single-stranded regions available
Ethylnitrosourea ENU Ethylates available phosphates
Hydroxyl radicals (reaction of Fe(II)-EDTA with NaOH or synchortron radiation) - cut the main chain of RNA where C1' or C4' ribose is available
Dimethylsulfate DMS Methylates available N1 adenine, N3 cytosine, N7 guanine
CMCT Modifies available N3 uridine, N1 guanine
DEPC Available N7 adenine
Kethoxal Available N1 and N2 guanines

SHAPE

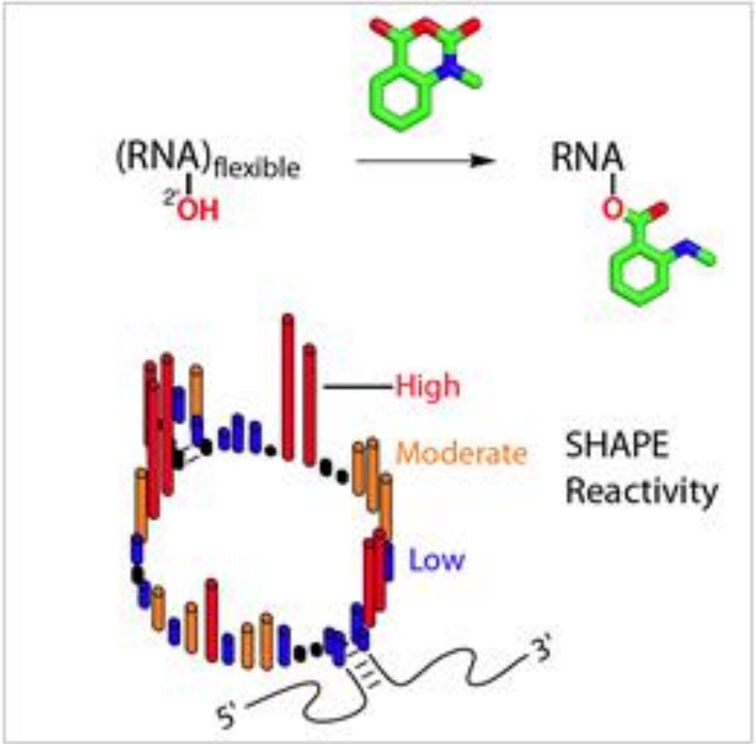

1-methyl-7-nitroisatoic anhydride

Reactivity independent of the type of base, but strongly dependent on the mobility/availability of the nucleotide.

The formation of the reaction product is detected by stopping the DNA primer elongation reaction using reverse transcriptase and comparing with the unmodified control

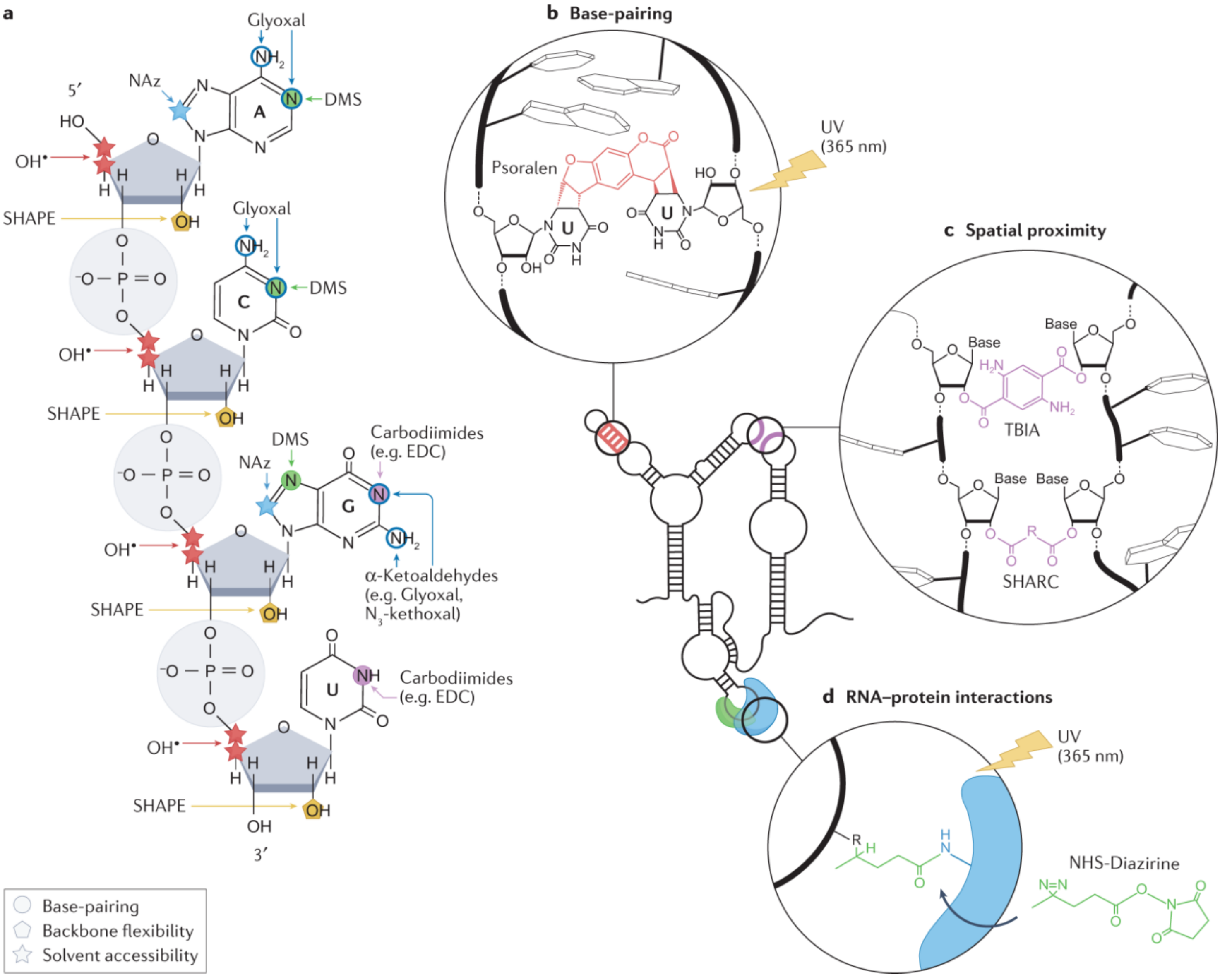

https://www.nature.com/articles/s41576-022-00546-w

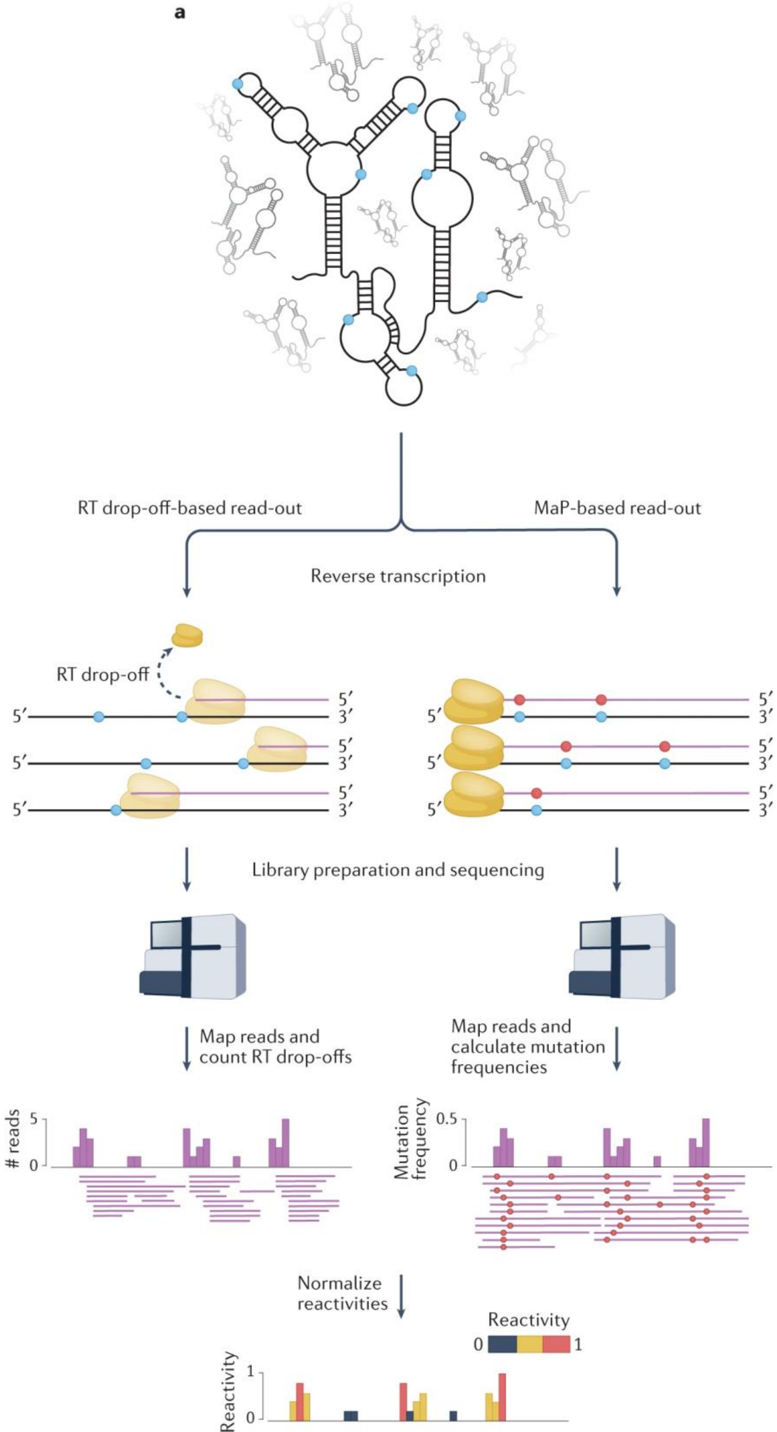

https://www.nature.com/articles/s41576-022-00546-w

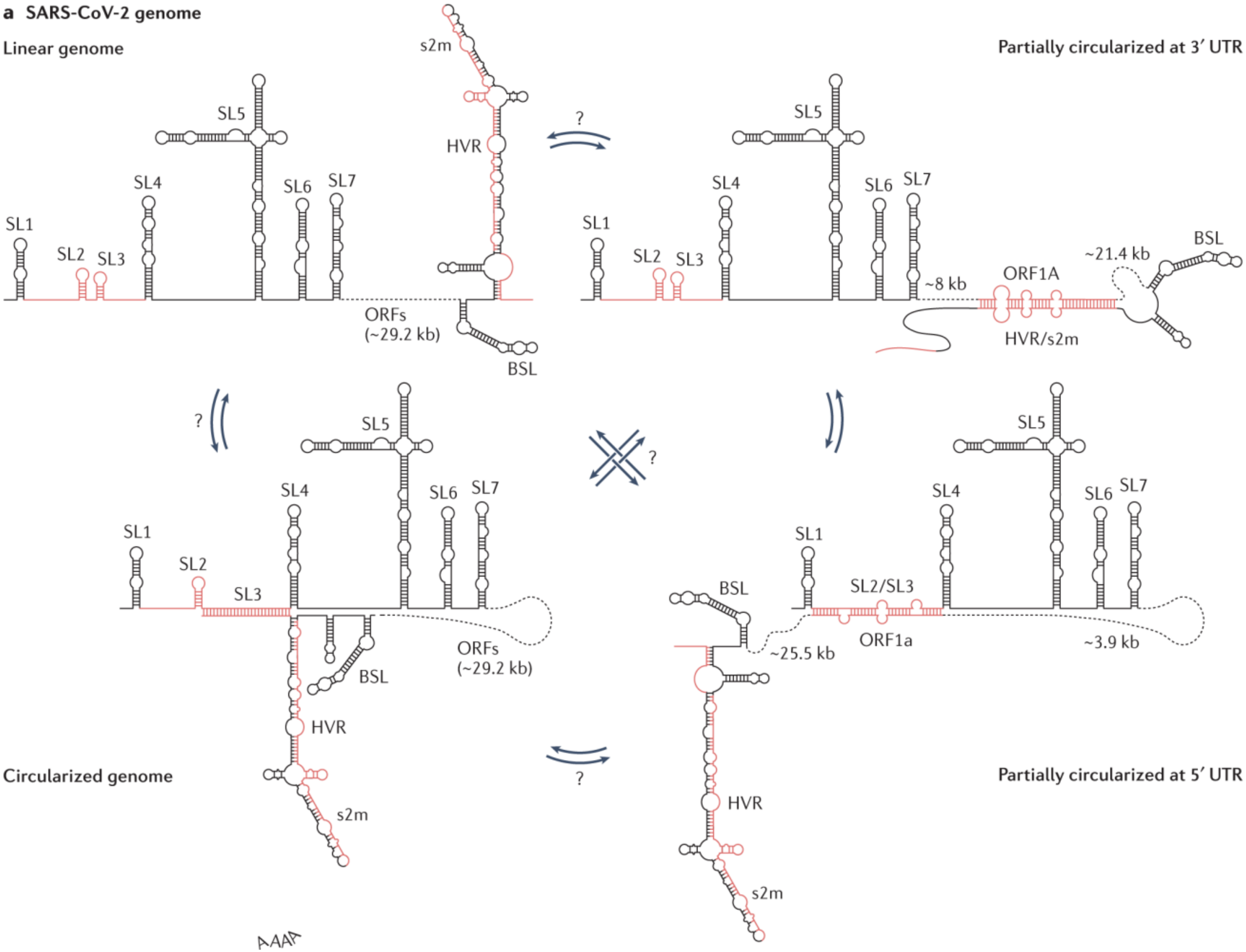
a SARS-CoV-2 genome
Linear genome
s2m
SL5
HVR
SL4
SL6
SL7
SL1
SL2
SL3
ORFs
(~29.2 kb)
BSL
?
Partially circularized at 3′ UTR
SL5
SL4
SL6
SL7
SL1
SL2
SL3
~8 kb
ORF1A
~21.4 kb
BSL
HVR/s2m
?
?
SL5
SL4
SL6
SL7
SL1
SL2
SL3
ORFs
(~29.2 kb)
BSL
HVR
Circularized genome
s2m
AAAA
SL5
SL4
SL6
SL7
SL1
BSL
SL2/SL3
~25.5 kb
ORF1a
~3.9 kb
HVR
s2m
?
Partially circularized at 5′ UTR

Chemical methods are used to confirm the correctness of crystallographic structures

They have the advantage of being used in solution under physiological conditions

These methods have been applied to whole cells (mapping the structure of 16S rRNA and RNase P in bacteria (Adilkshmi, NAR, 2006)

Nuclear magnetic resonance

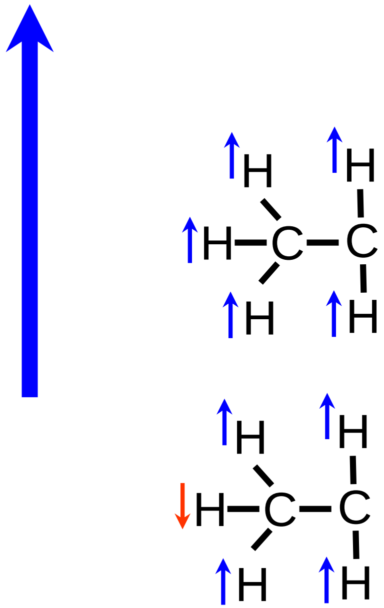

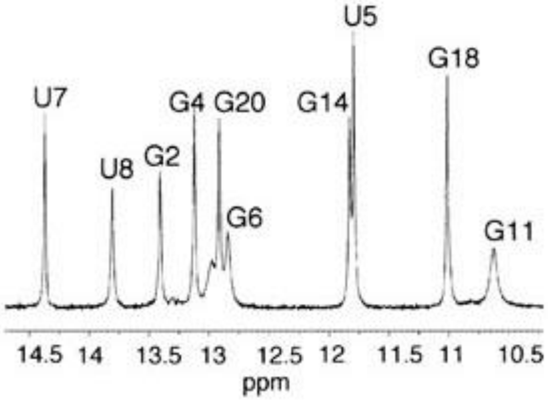

SAXS

SAXS

Provides low-resolution structural information

Advantages: in solution, simple measurement, measurements possibly from a dozen kDa to a few Mda.

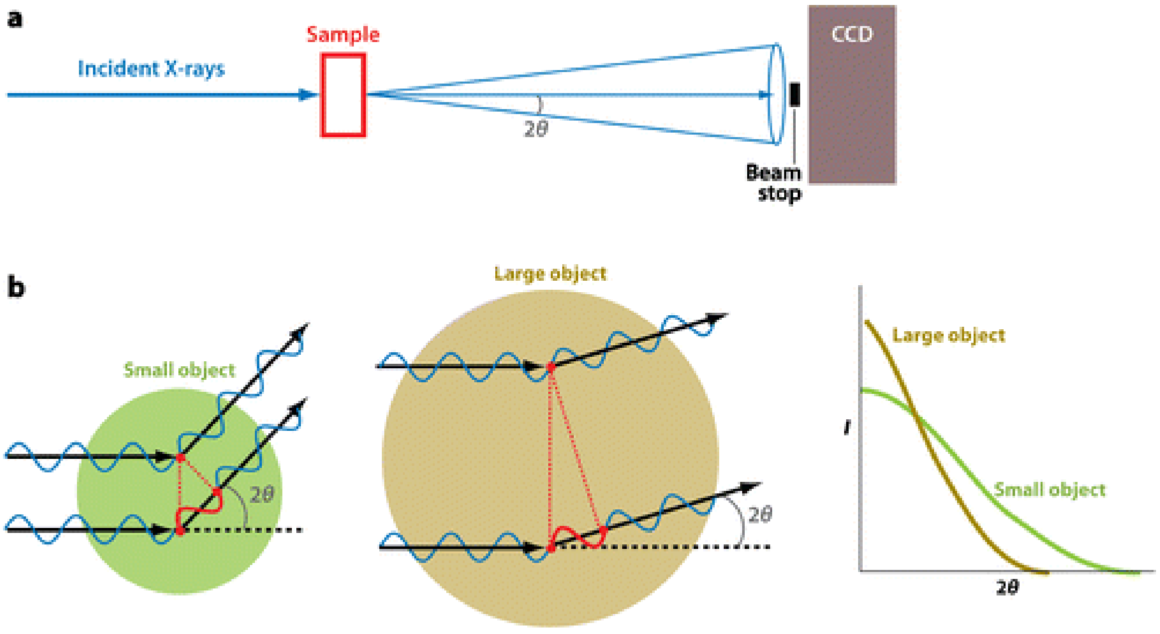

Pollack L. 2011.
Annu. Rev. Biophys. 40:225–42

<u>Possible types of analysis:</u>

Comparison of the theoretical SAXS curve with the experimental curve

Calculating the shape of a molecule

Docking the RNA model into shape

Determination of shape ab initio

A given volume is filled with spheres.

Each sphere can be assigned to a molecule or solution.

The initial assignments are random.

The assignments are randomly shifted until a shape corresponding to the experimental curve is obtained.

Conditions can be imposed that ensure the compactness of the molecule

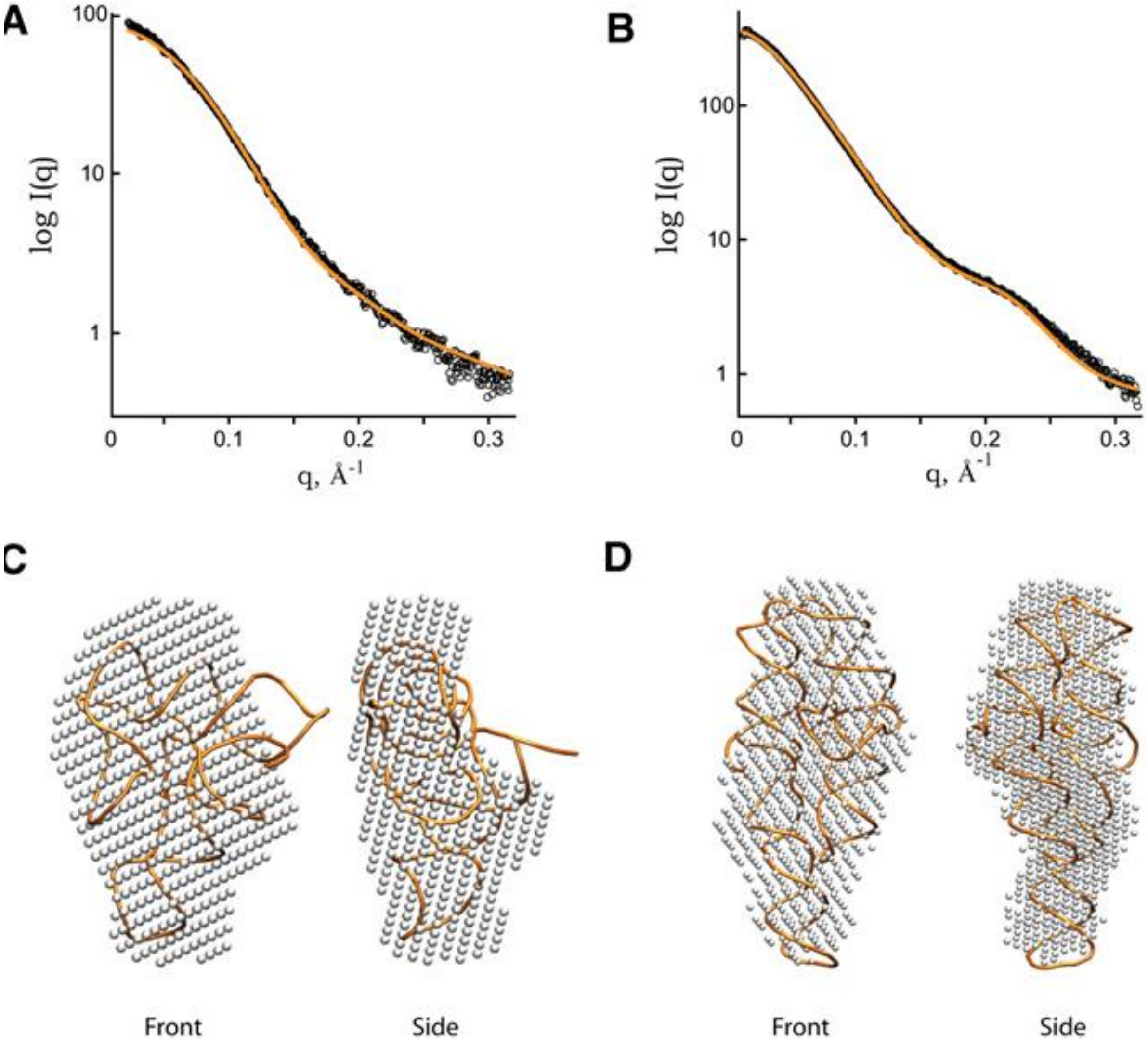

$q = 4\pi(\sin \Theta)/\lambda$

SAM-I
riboswitch

D(C209)P4-P6 domain
of the group I intron

CRYSTALLOGRAPHY

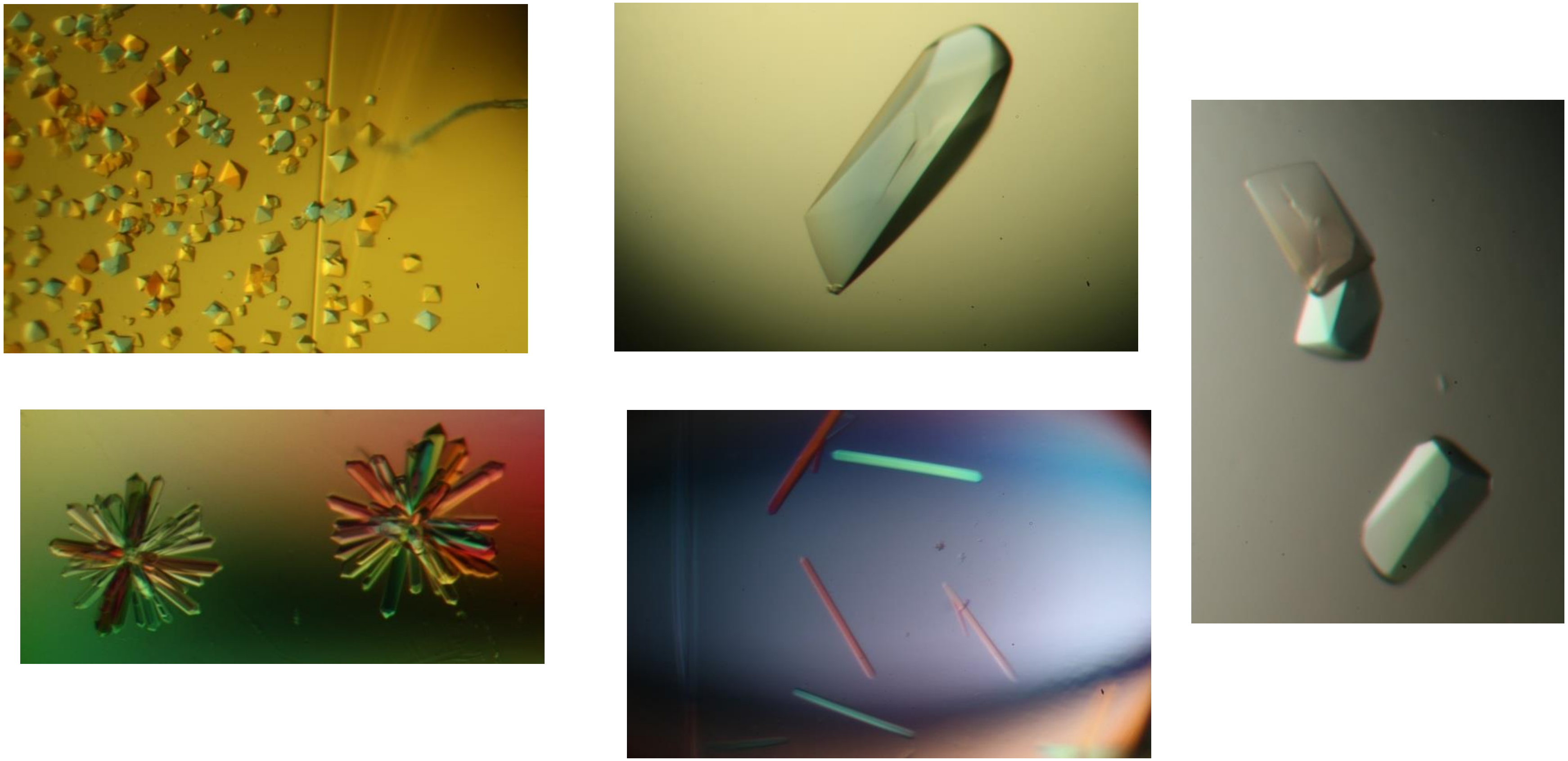

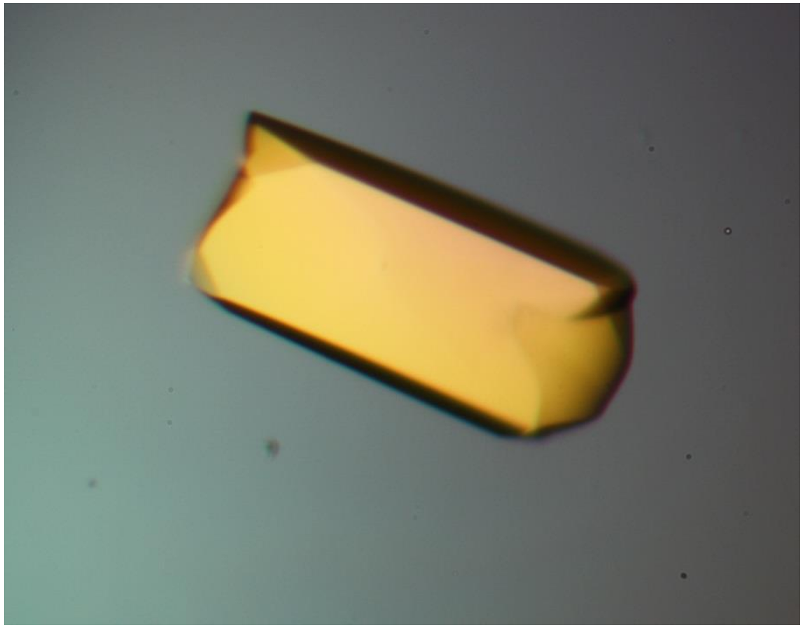

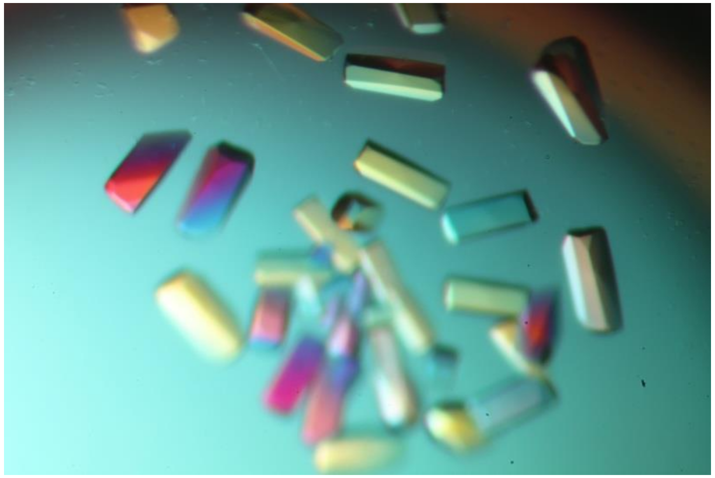

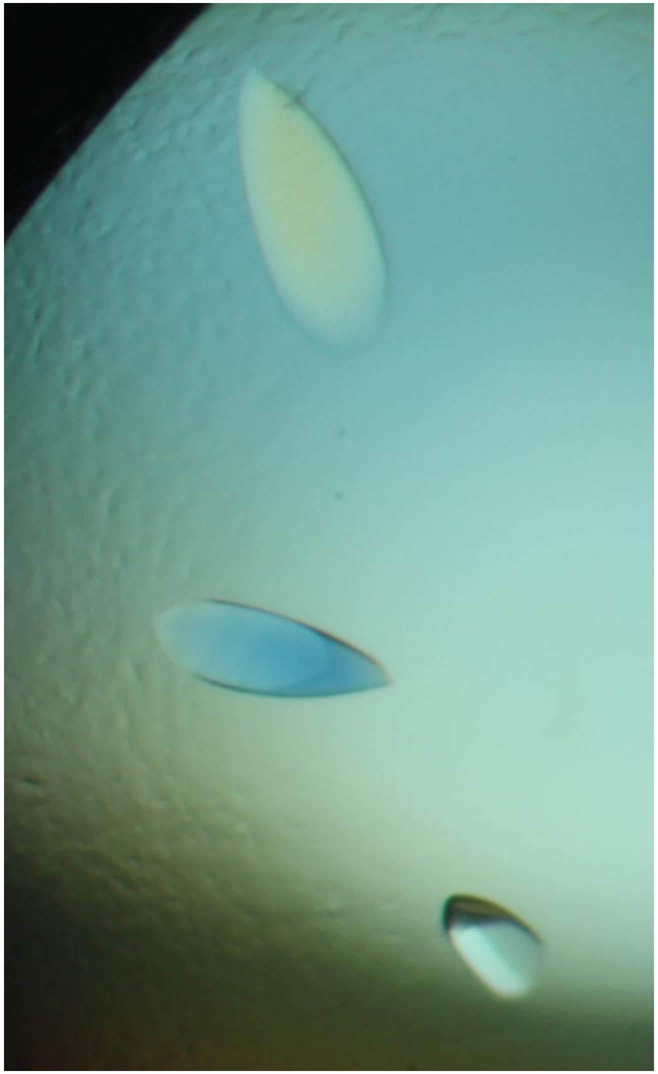

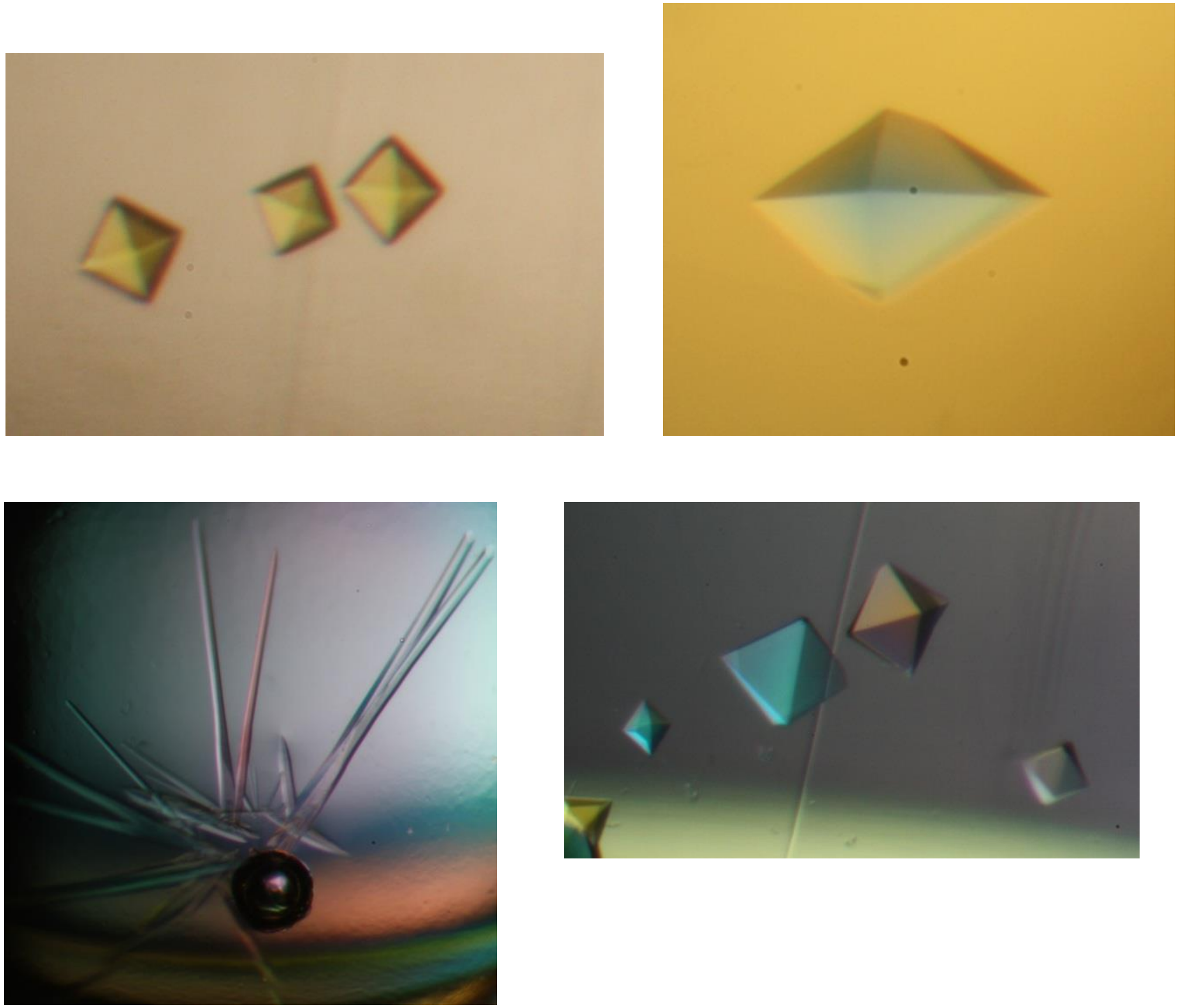

Kryształy dużej podjednostki rybosomu

Crystals

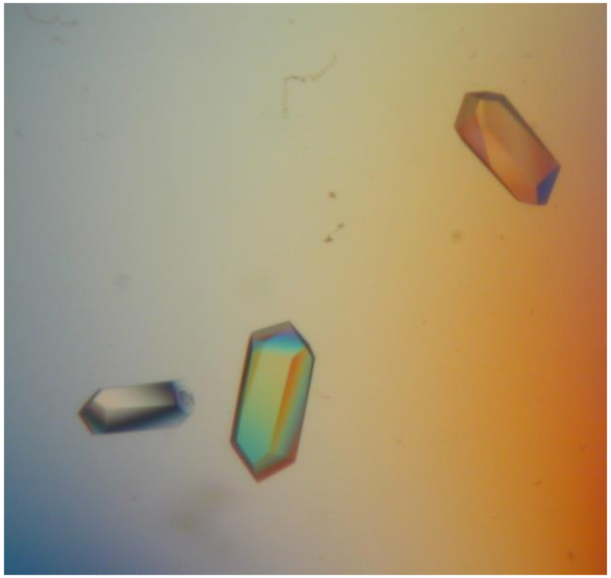

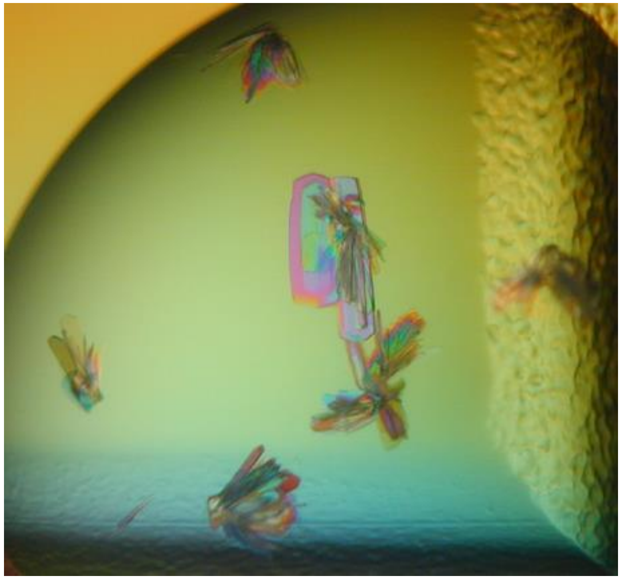

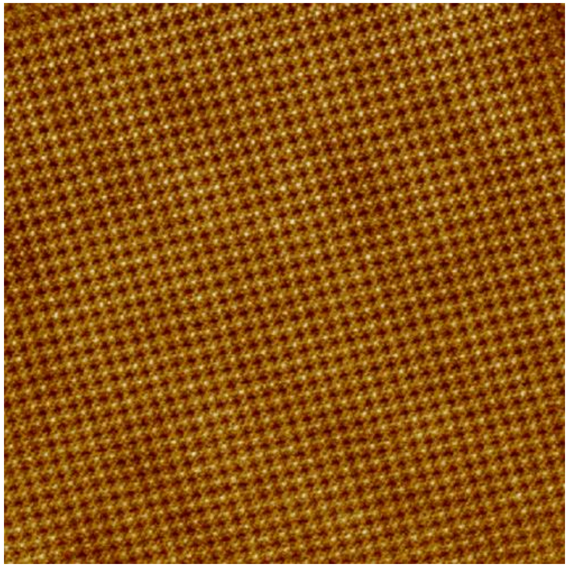

Crystallization

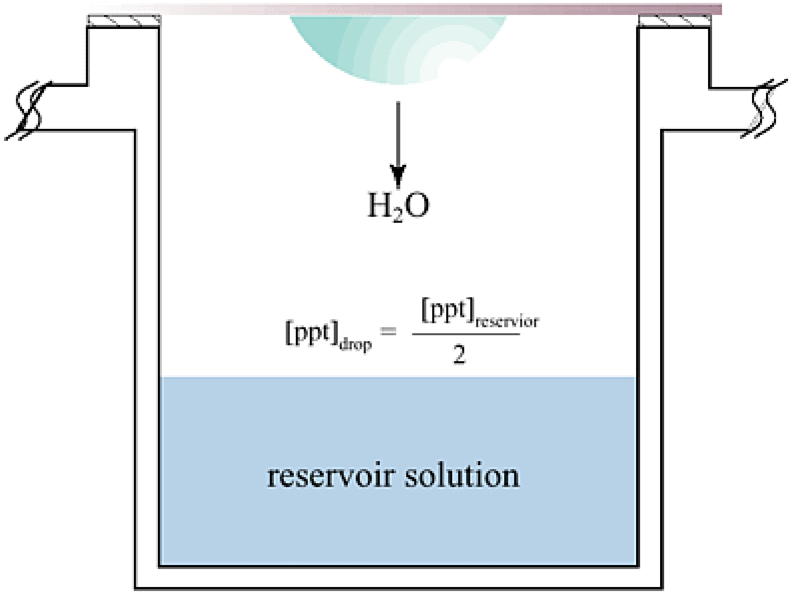

Precipitants:
salts
PEGs
organic solvents

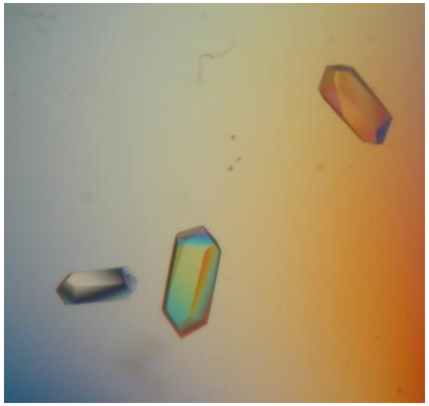

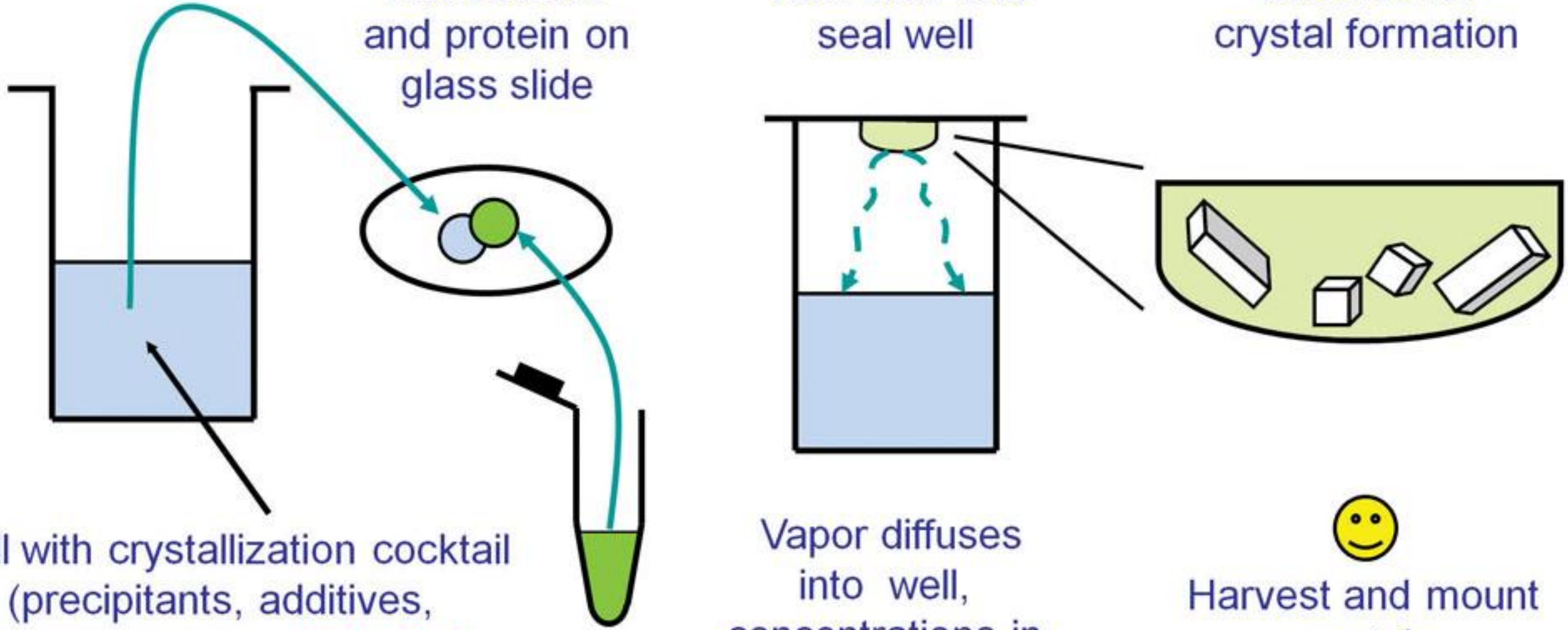

Well with crystallization cocktail (precipitants, additives, detergents, etc. – unlimited combinations possible)

Mix cocktail and protein on glass slide

Turn slide and seal well

Vapor diffuses into well, concentrations in drop increase

Observe for crystal formation

Harvest and mount crystals

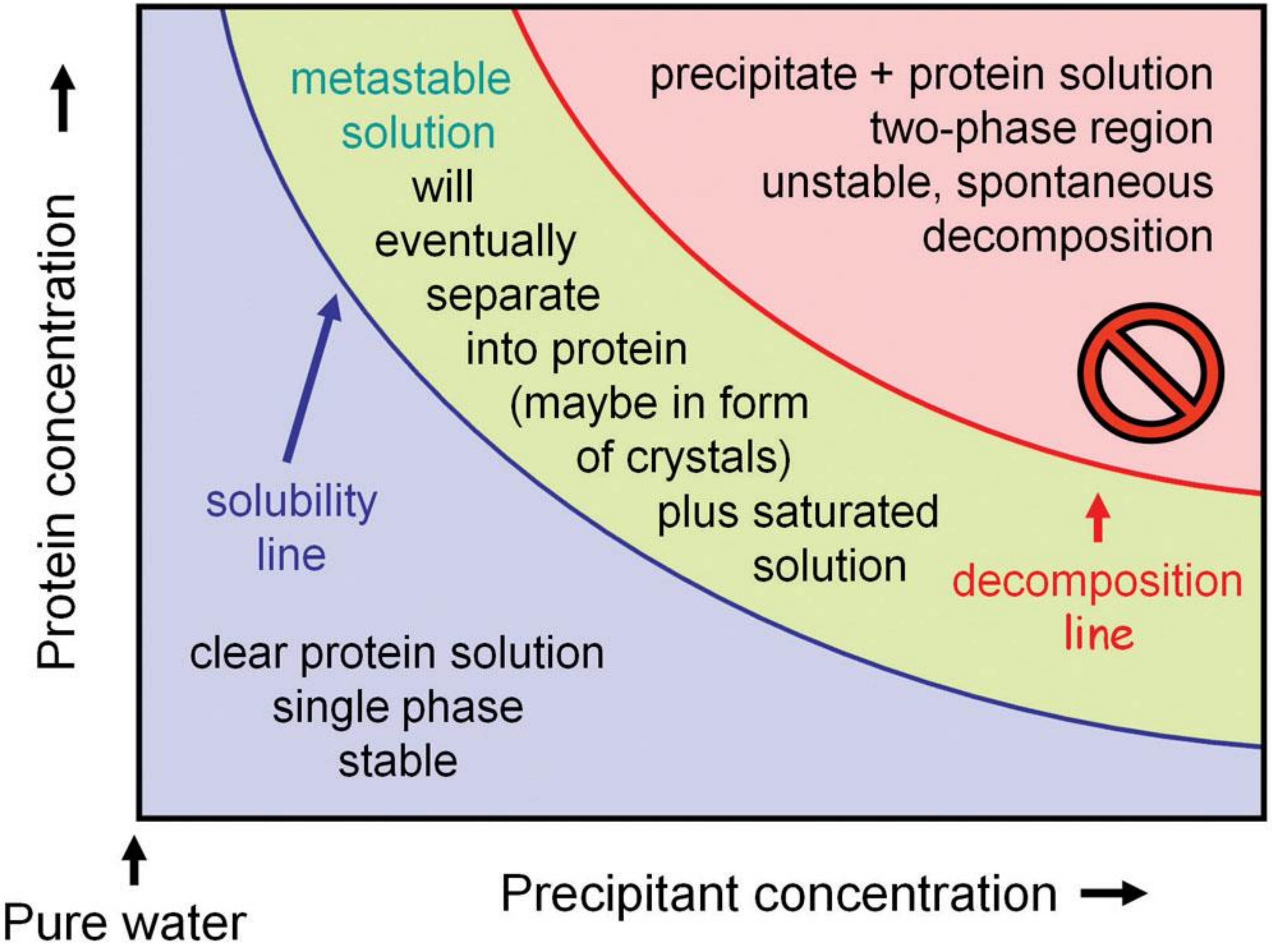
metastable solution
will eventually separate into protein (maybe in form of crystals) plus saturated solution
precipitate + protein solution
two-phase region
unstable, spontaneous decomposition
solubility line
decomposition line
clear protein solution
single phase
stable
Protein concentration
Precipitant concentration
Pure water

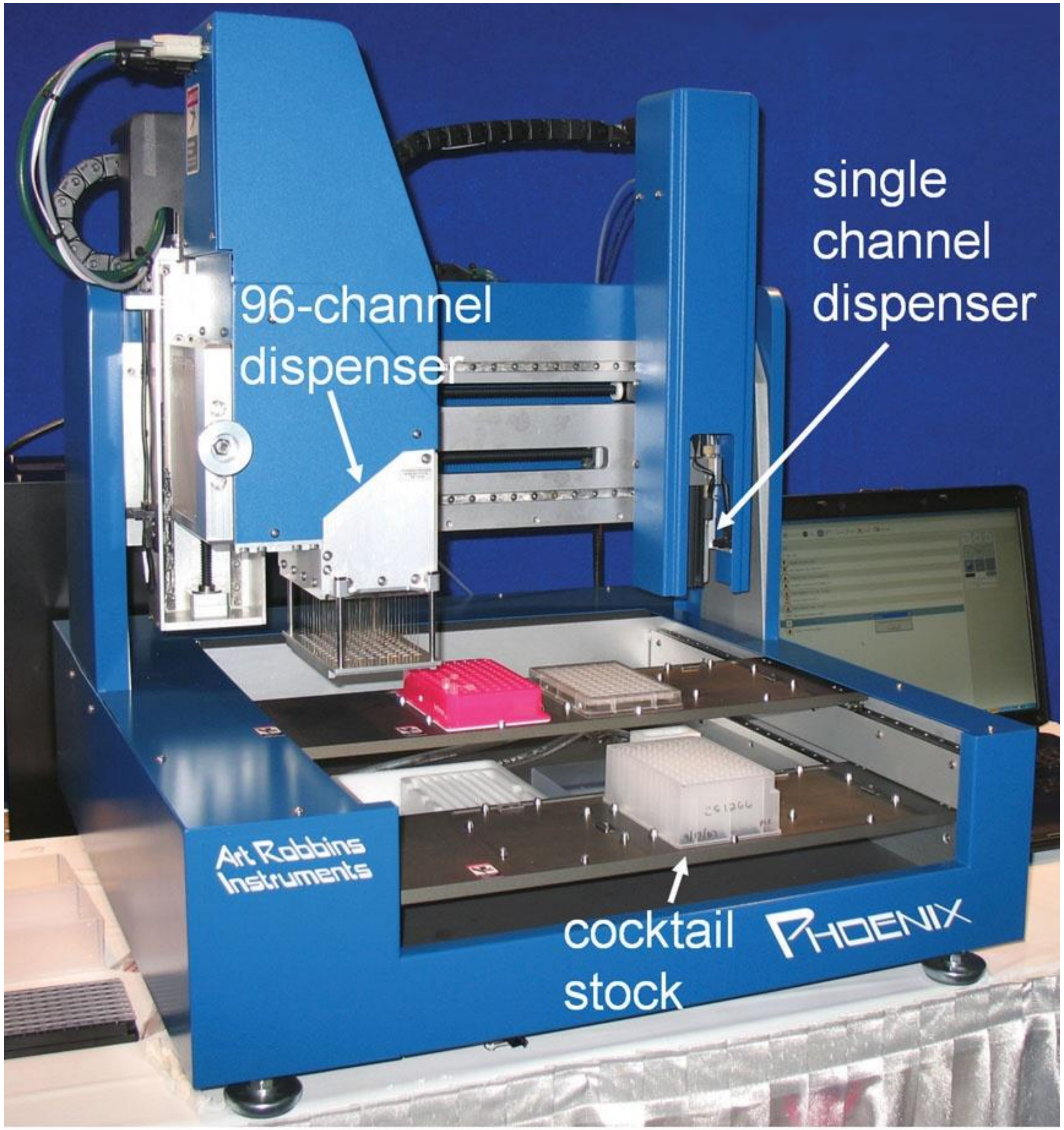
single
channel
dispenser
96-channel
dispenser
cocktail
stock
Art Robbins
Instruments
PHOENIX

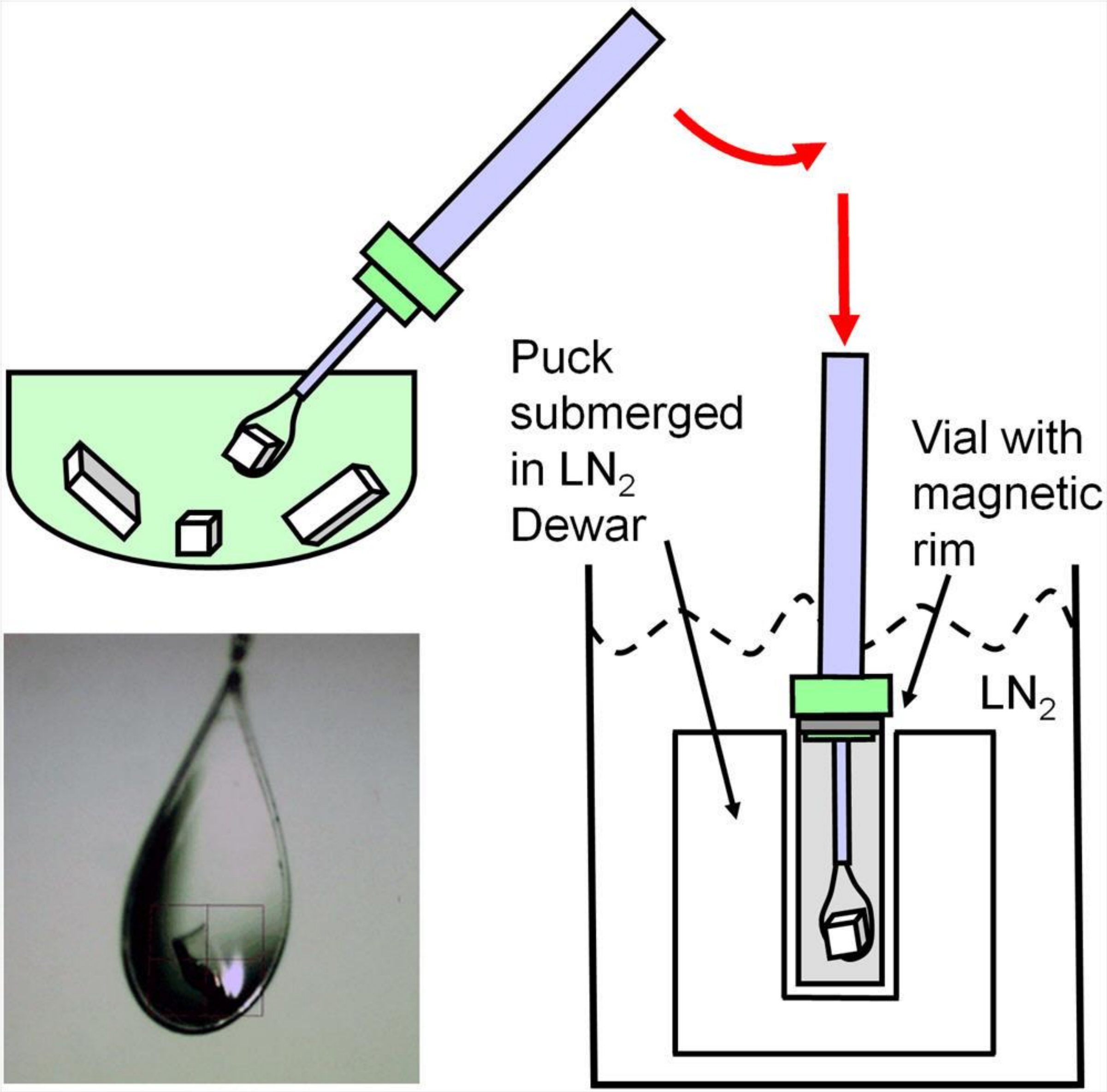
Puck submerged in LN$_2$ Dewar
Vial with magnetic rim
LN$_2$

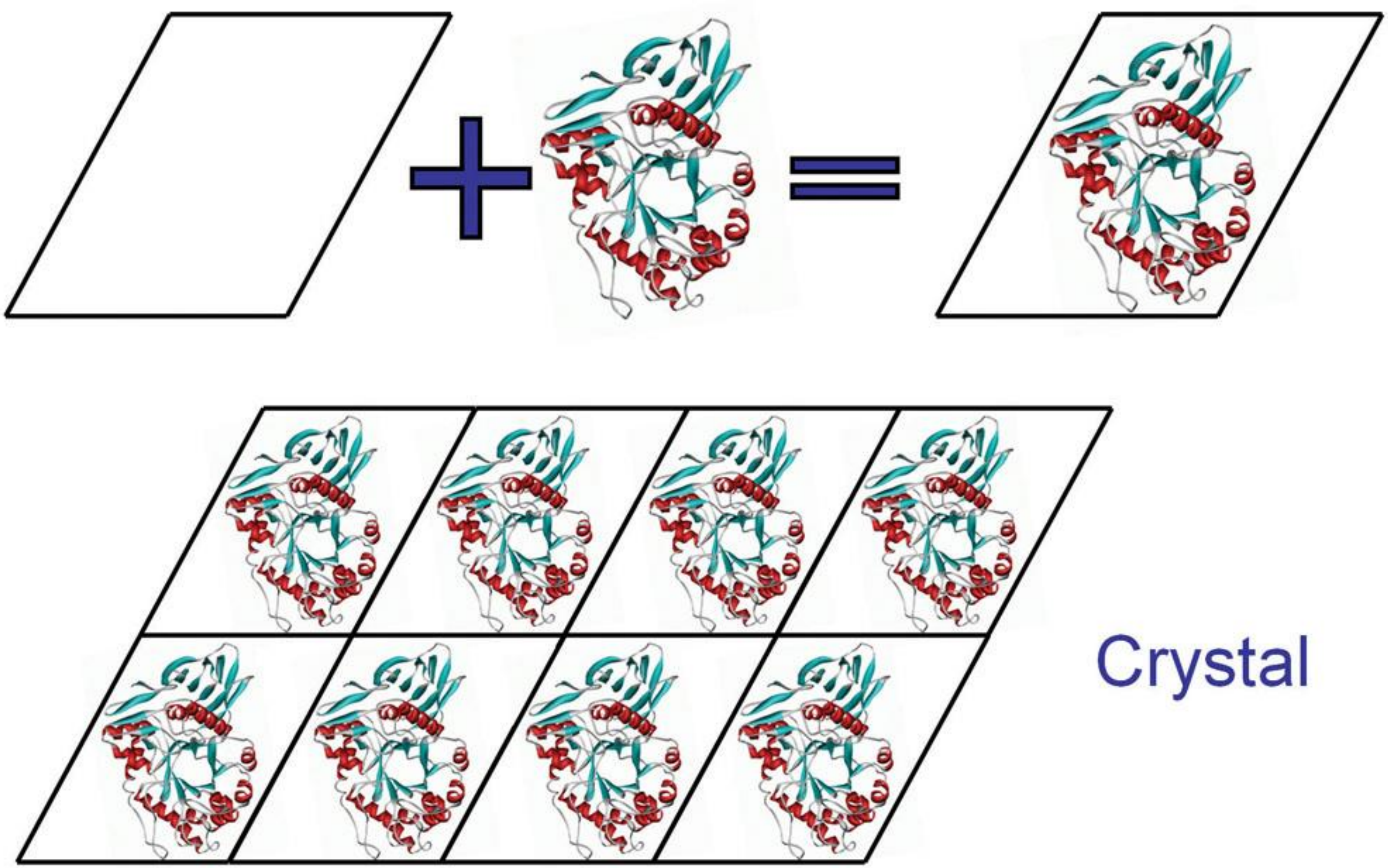

Unit lattice

Motif

Unit cell

Crystal

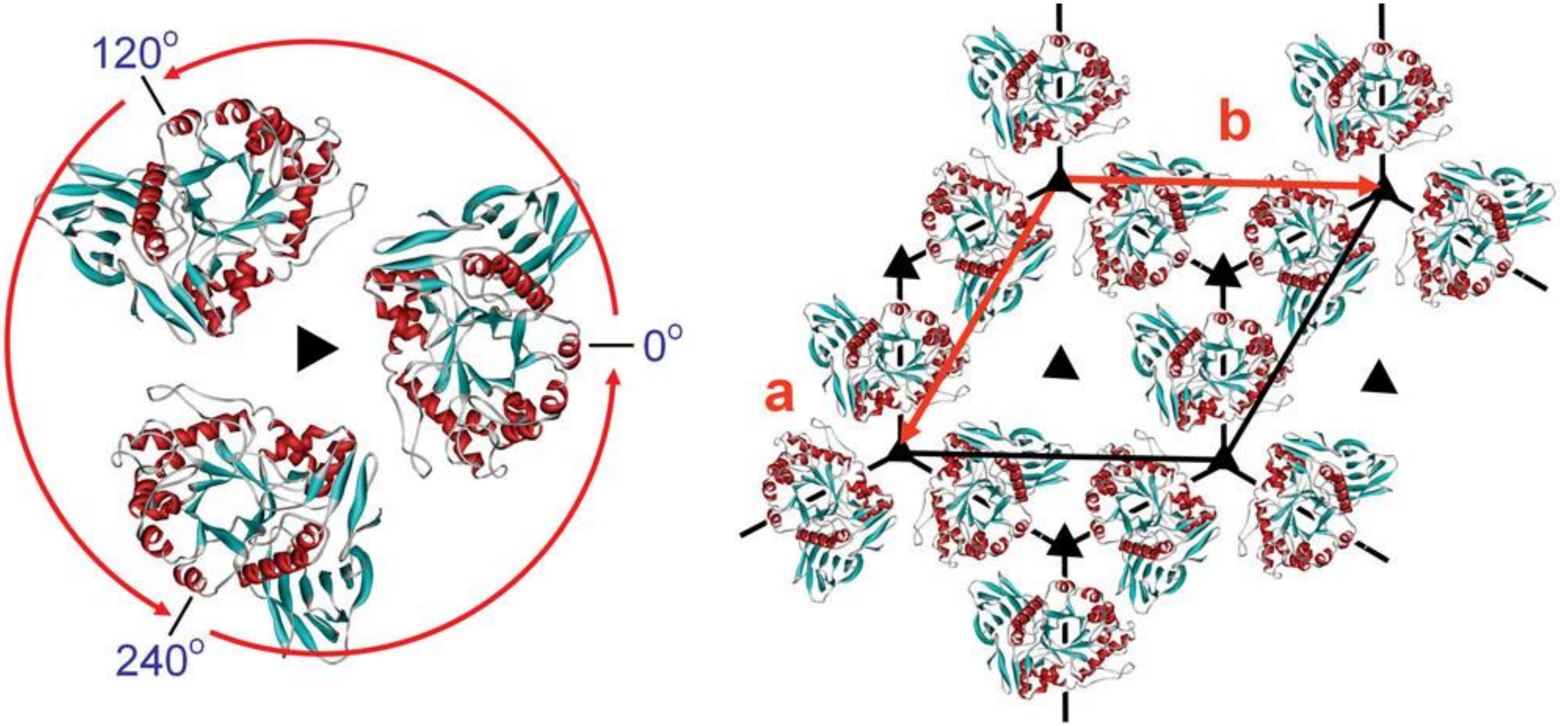
120°
0°
240°
b
a

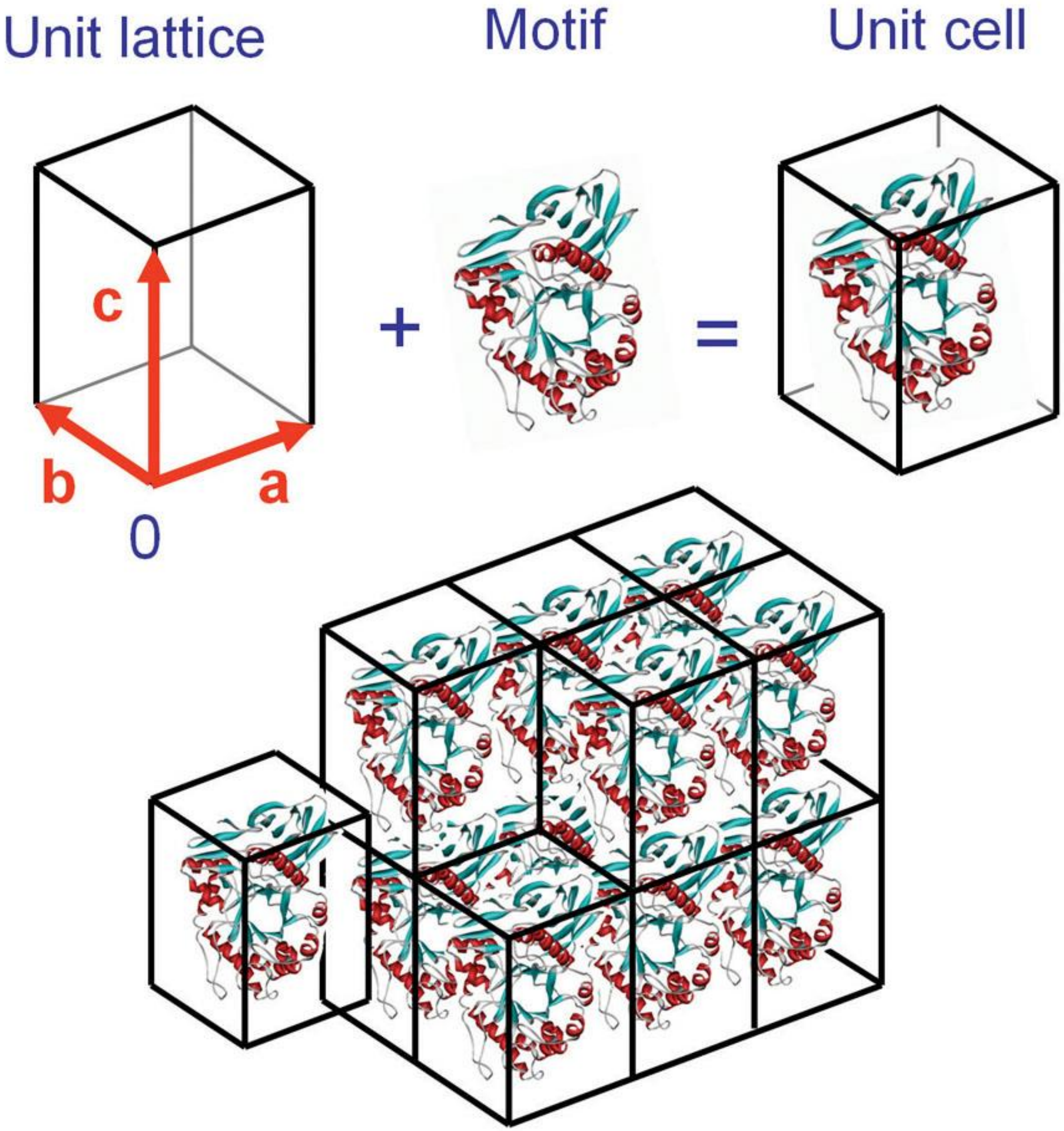

Unit lattice

Motif

Unit cell

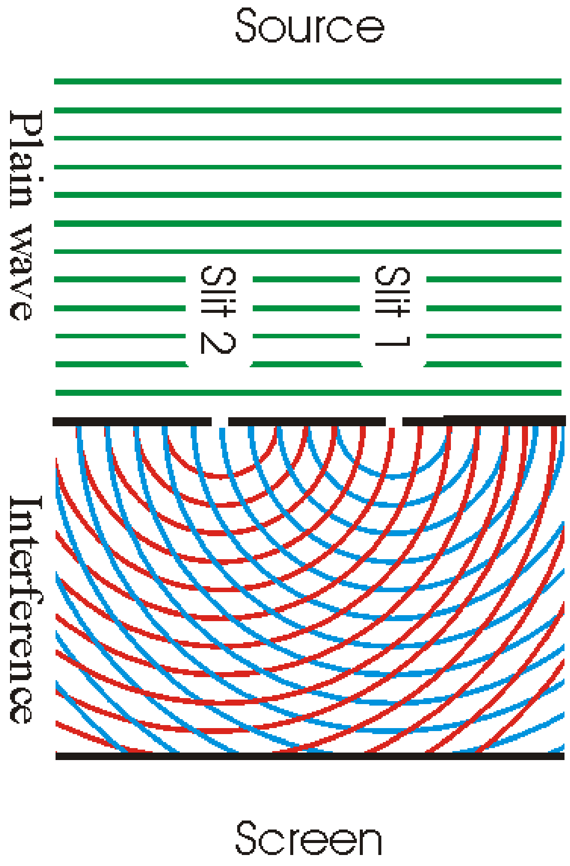
Source
Plain wave
Slit 2
Slit 1
Interference
Screen

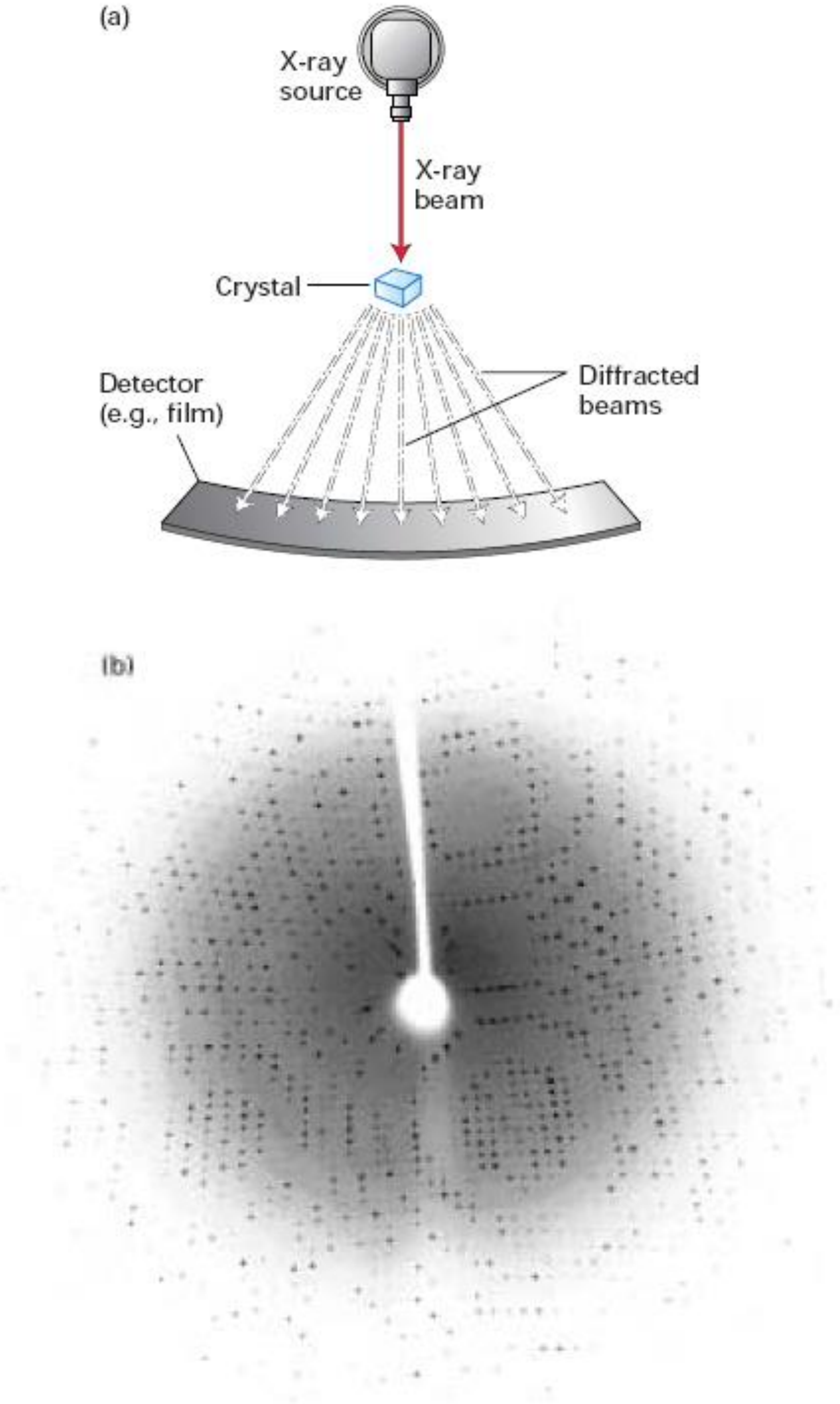
(a)
X-ray source
X-ray beam
Crystal
Detector (e.g., film)
Diffracted beams
(b)

Crystallography

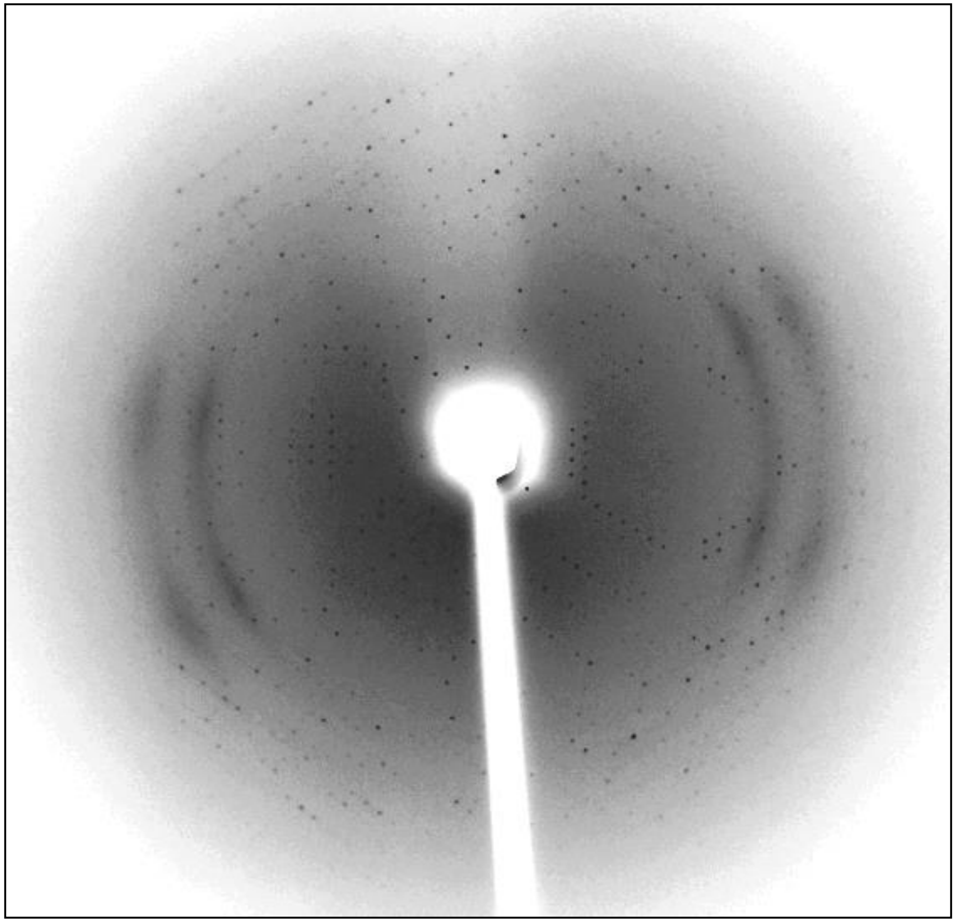

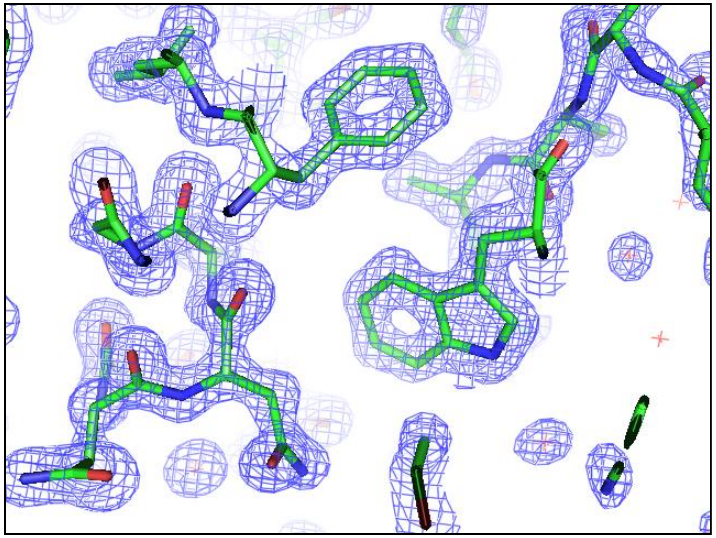

Rozdzielczość: 1,5 Å

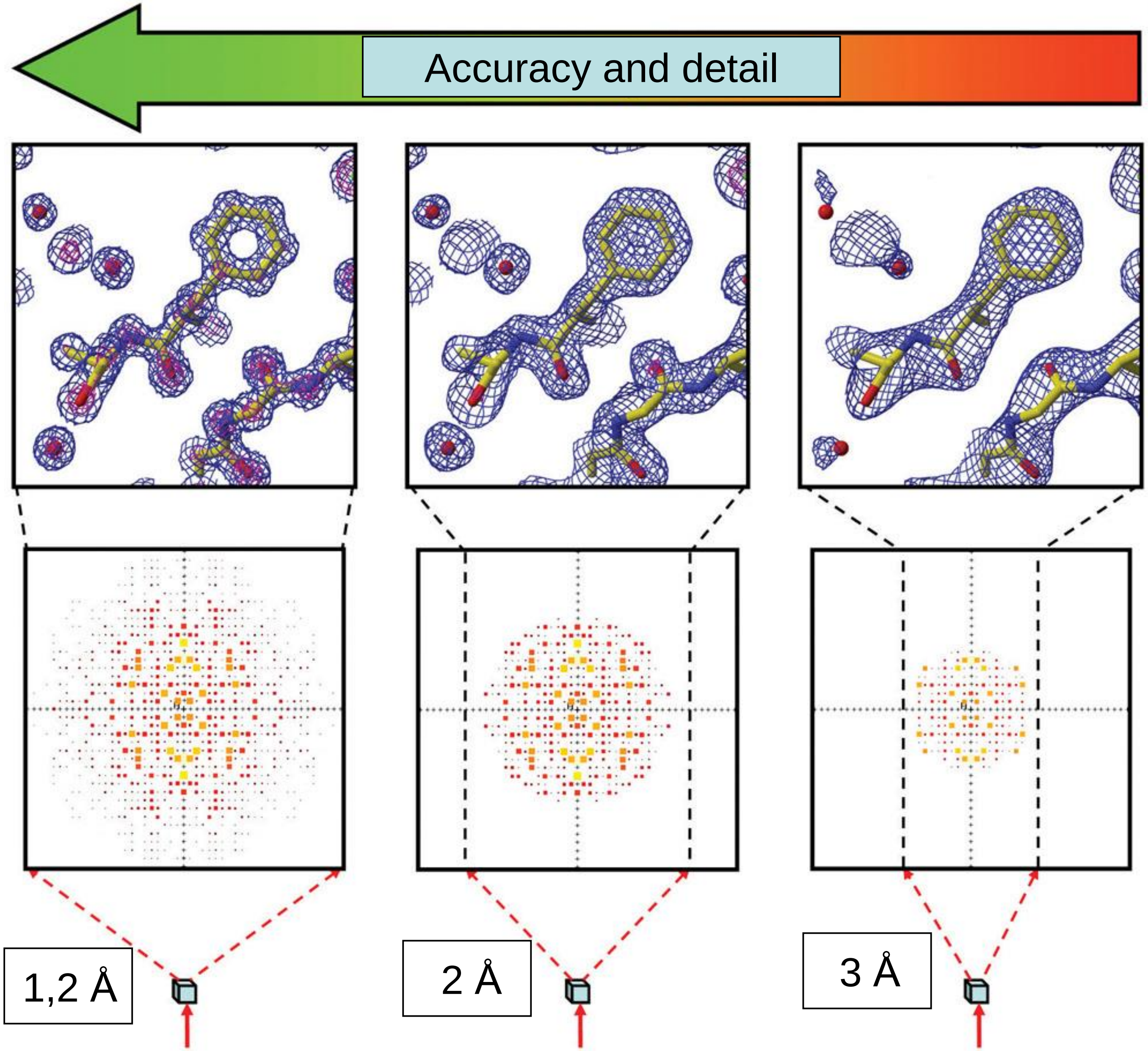

Accuracy and detail

1,2 Å

2 Å

3 Å

$$\rho(x,y,z)=\frac{1}{V}\sum_{-h}^{h}\sum_{-k}^{k}\sum_{-l}^{l}F_{hkl}\cdot\exp[-2\pi i(hx+ky+lz-\alpha_{hkl})]$$

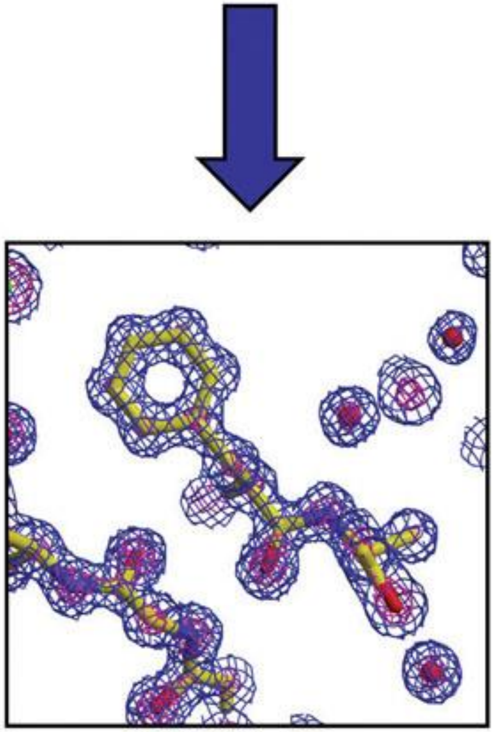

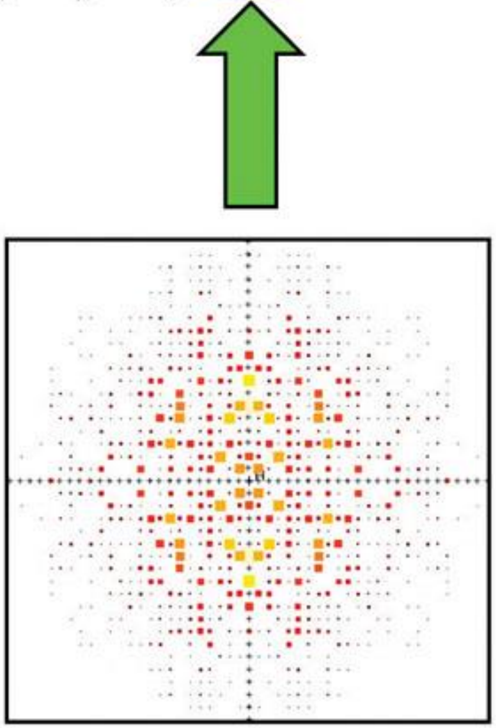

The crystallographic phase problem

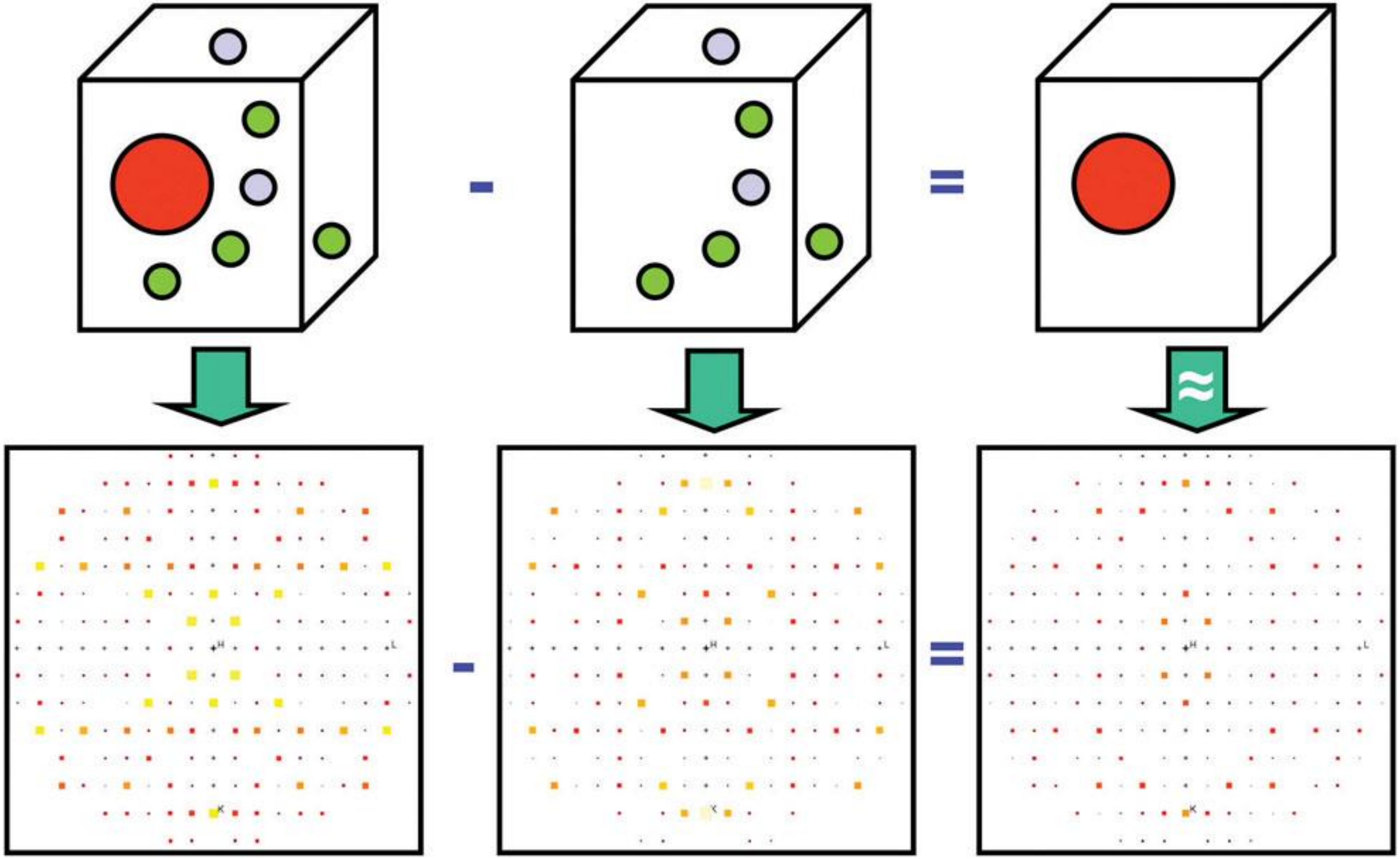
-
=
≈
-
=
H
L
K
H
L
K
H
L
K

Biomolecular Crystallography: Principles, Practice, and Application to Structural Biology

Bernhard Rupp

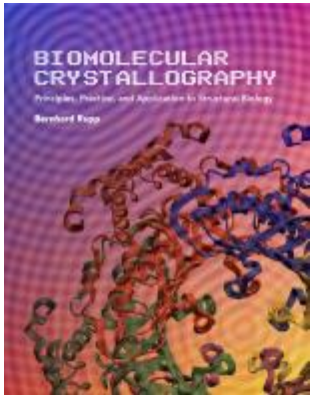

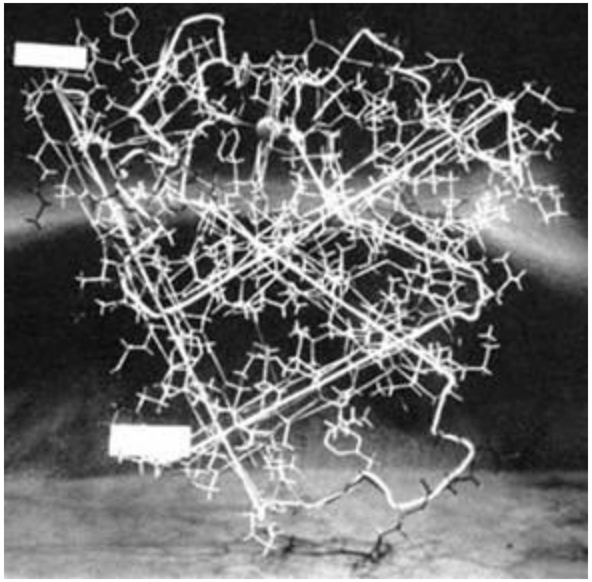

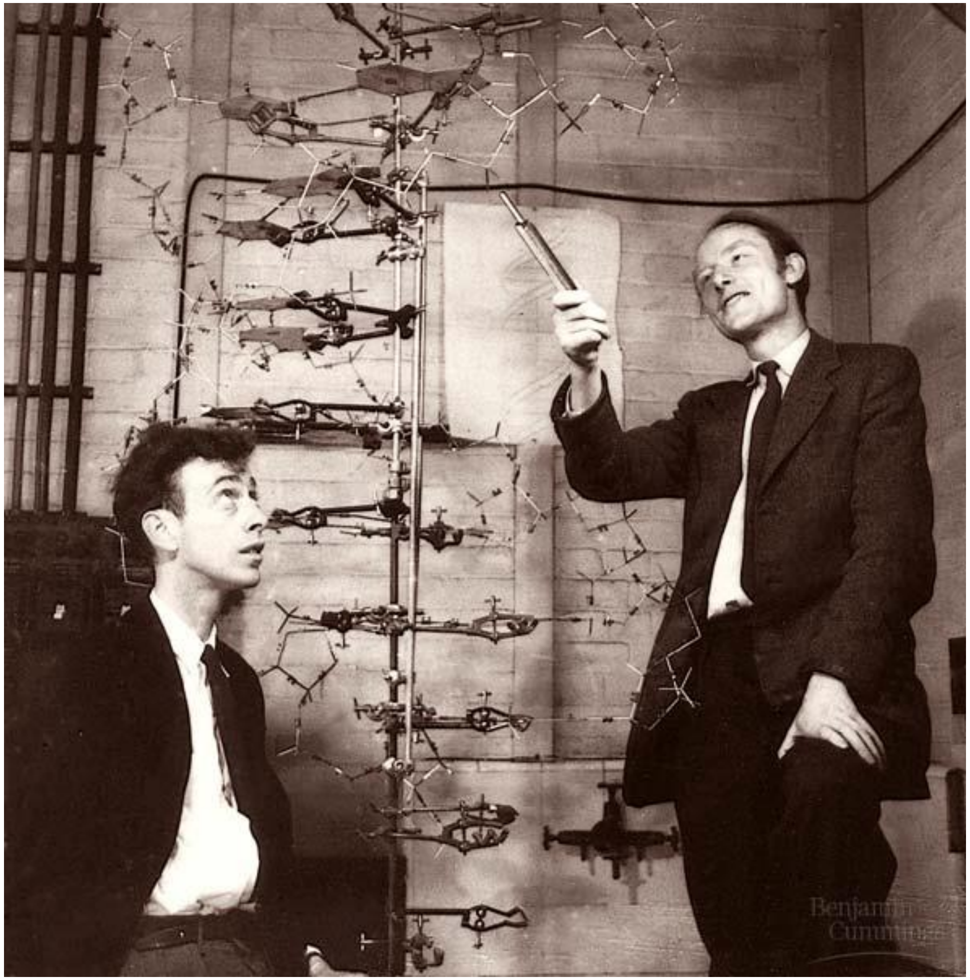

RNA crystallography

The first structure - tRNA (1974)

After 2000 - ribosomes, group I introns, P ribonuclease

A limitation of crystallography is the heterogeneity of RNA conformations, which often makes it impossible to obtain crystals

RNA crystallization difficult - out of about 80000 structures solved, about 1000 RNA alone and 1000 RNA-protein complexes

Dedicated Nucleic Acid Structure Database (ndbserver.rutgers.edu)
Allows identification of recurring motifs

EXAMPLES

Ribosome

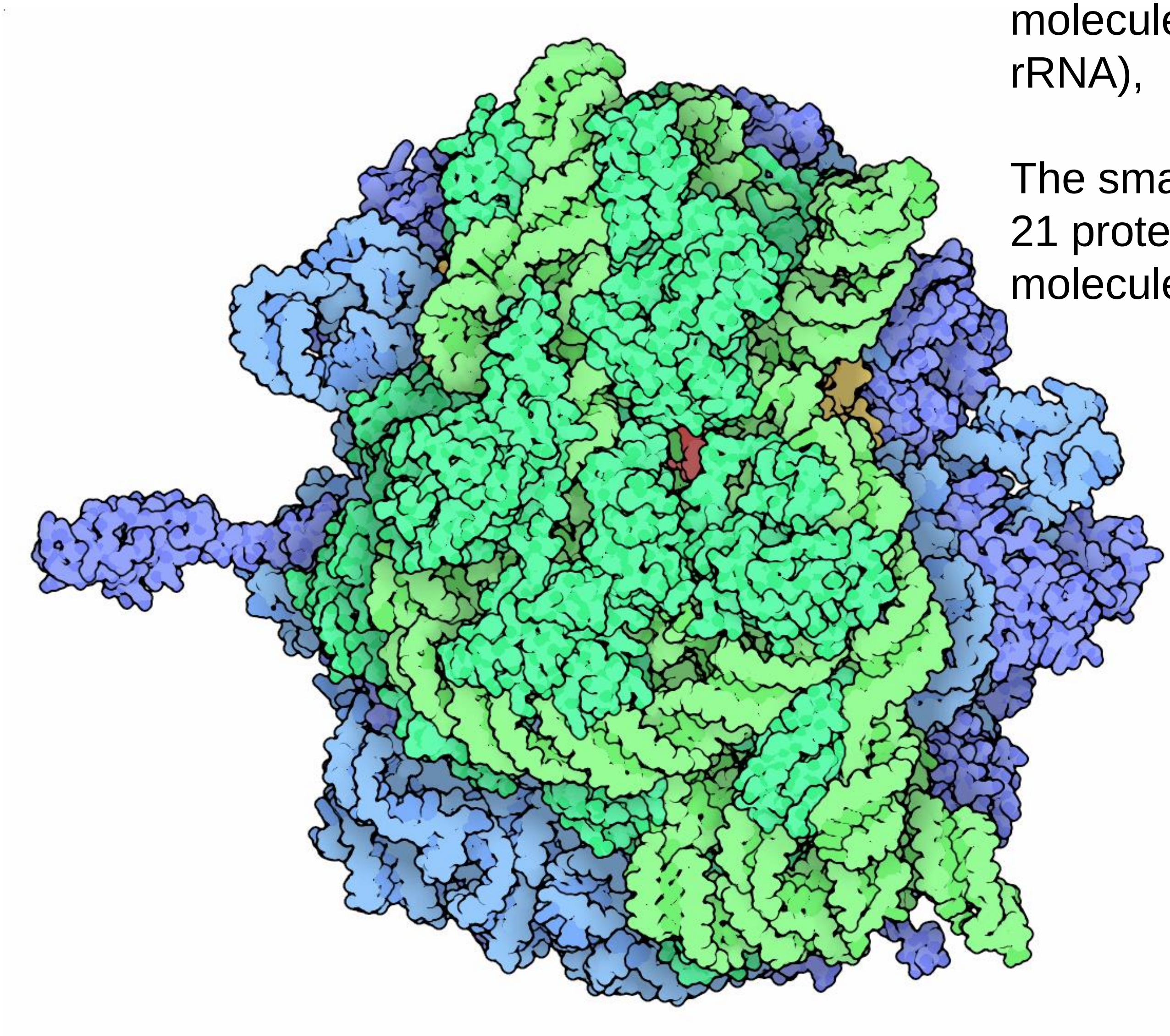

In prokaryotes there are 70S ribosomes

The large subunit (50S) contains 34 proteins and two rRNA molecules (5S rRNA and 23S rRNA),

The small subunit (30S) contains 21 proteins and one rRNA molecule (16S rRNA).

Ribosome

Bacterial ribosome composed of 30S and 50S subunits

A flexible nanomachine that adopts multiple conformations during the peptide bond synthesis cycle

First reconstructions of ribosome structure based on EM in 1970s, first detailed ones around 1995 (Joachim Frank, Holger Stark)

EM has provided a wealth of information about ribosome complexes with tRNA, mRNA elongation factors, and conformational changes of the ribosome during its cycle

EM structures are now available for, among others, bacterial, yeast, and mammalian ribosomes

The first X-ray-scattering bacterial ribosome crystals were obtained in the late 1980s (Ada Yonath)

In 1991, 50S crystals were presented that scattered up to about 3 Å.

In 2000, the first structure of a large subunit from *H. marismortui* was published (T. Steitz)

In 2001, the structure of the entire ribosome from *T. thermophilus* (H. Noller)

Currently available multiple complex structures with tRNAs, accessory factors and antibiotics

Nobel Prize 2009 - Steitz, Yonath, Ramakrishnan

2010 - Structures of eukaryotic ribosomes

2014 - Structures of mitochondrial ribosomes

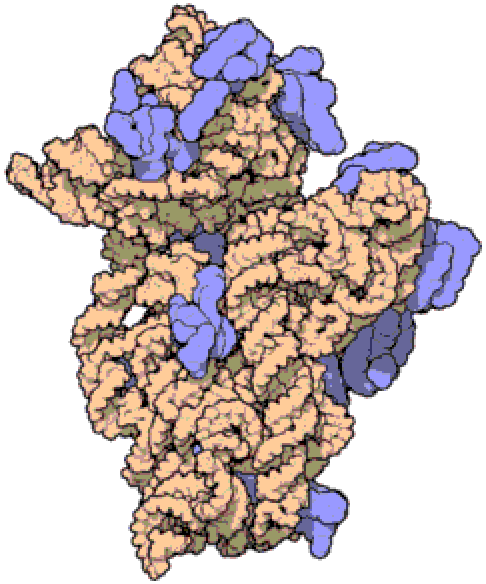

Atomic structure of the 30S Subunit from *Thermus thermophilus*. Proteins are shown in blue and the single RNA strand in orange.It is found by MRC Laboratory of Molecular Biology in Cambridge, England.

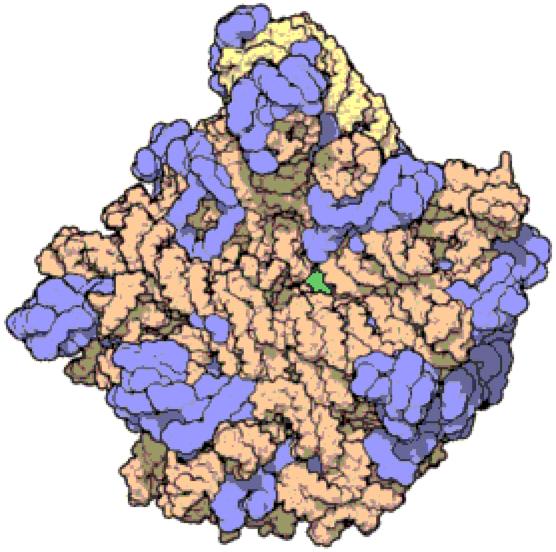

Atomic structure of the 50S Subunit from *Haloarcula marismortui*. Proteins are shown in blue and the two RNA strands in orange and yellow.[13] The small patch of green in the center of the subunit is the active site.

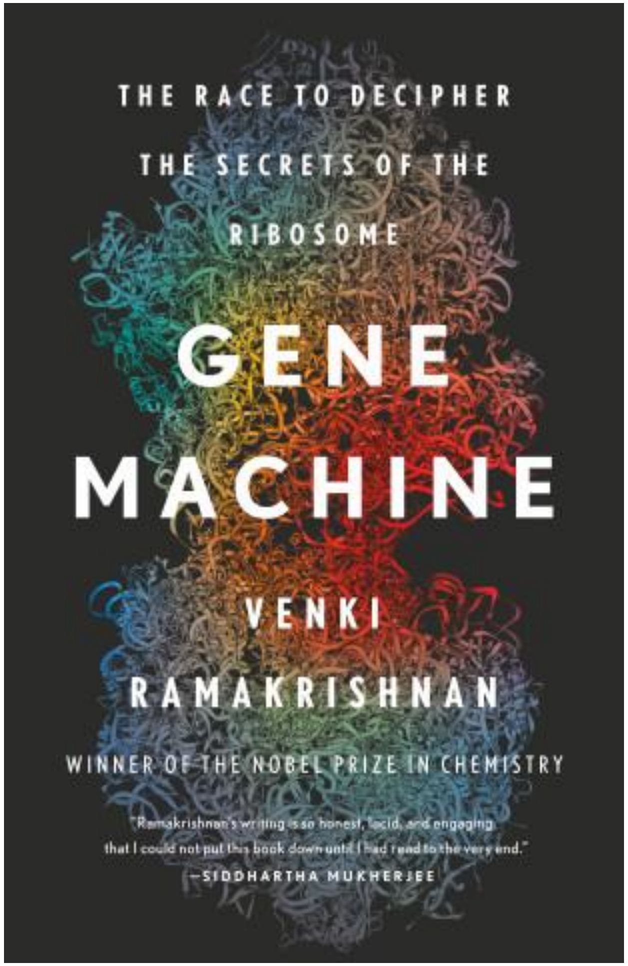

THE RACE TO DECIPHER
THE SECRETS OF THE
RIBOSOME

GENE
MACHINE

VENKI
RAMAKRISHNAN

WINNER OF THE NOBEL PRIZE IN CHEMISTRY

"Ramakrishnan's writing is so honest, lucid, and engaging
that I could not put this book down until I had read to the very end."
—SIDDHARTHA MUKHERJEE

Electron microscopy

EM's main strength is its ability to visualize large, mobile complexes - there is no upper size limit

Analysis of mobile complexes is possible - classifying different conformations of molecules

For cryo-EM, resolutions of up to 1.0 Å are achieved

EM has proven to be a very useful tool for studying ribosomes, especially their movements in the peptide bond synthesis cycle

Hybrid methods - a combination of low-resolution EM and high-resolution crystallographic structures - can be particularly useful

EM revolution since 2012

2017 Nobel Prize in Chemistry

Richard Henderson

Joachim Frank

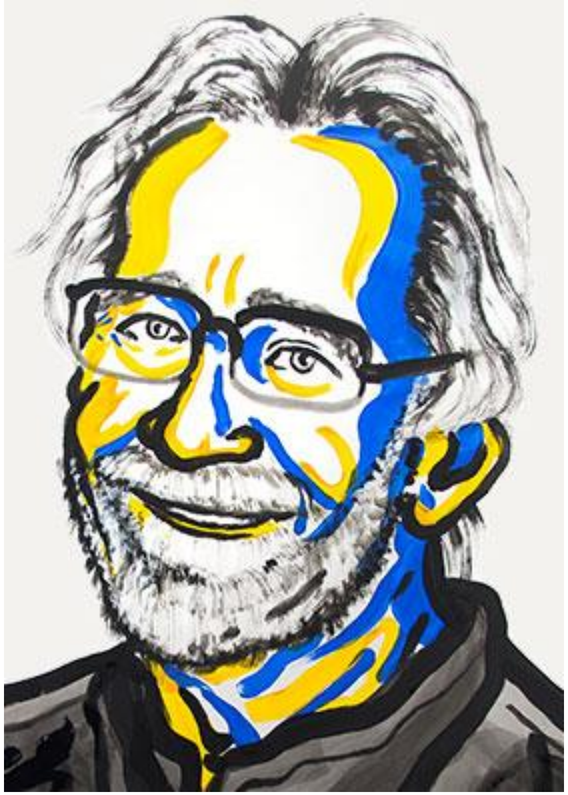

Jacques Dubochet


TECNAI


TITAN KRIOS
FEI COMPANY

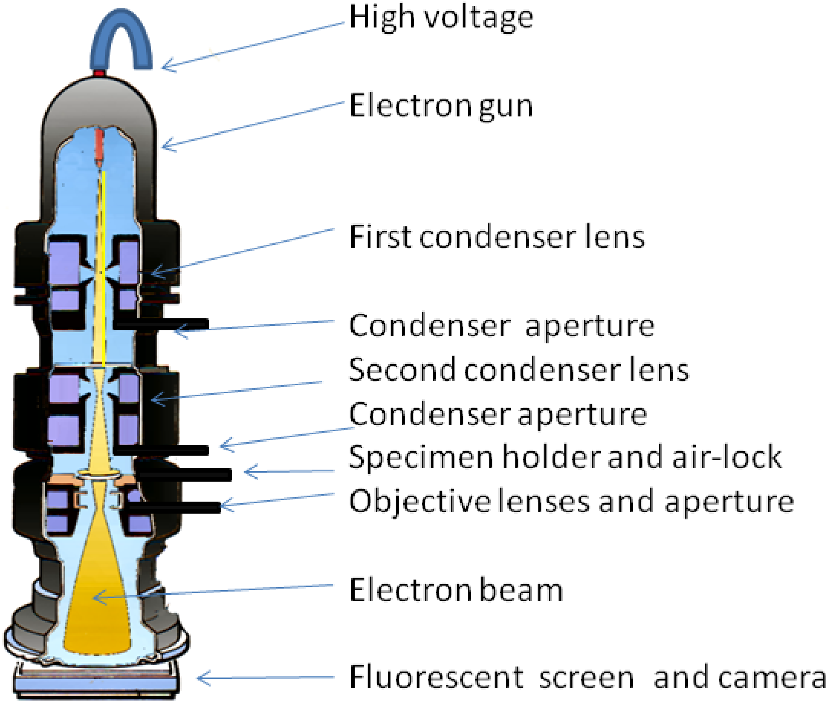

Transmission Electron Microscope

TEM microscope at 300 kV – corresponding wavelength 0.2 Å

EM lenses are poor

TEM vs SEM

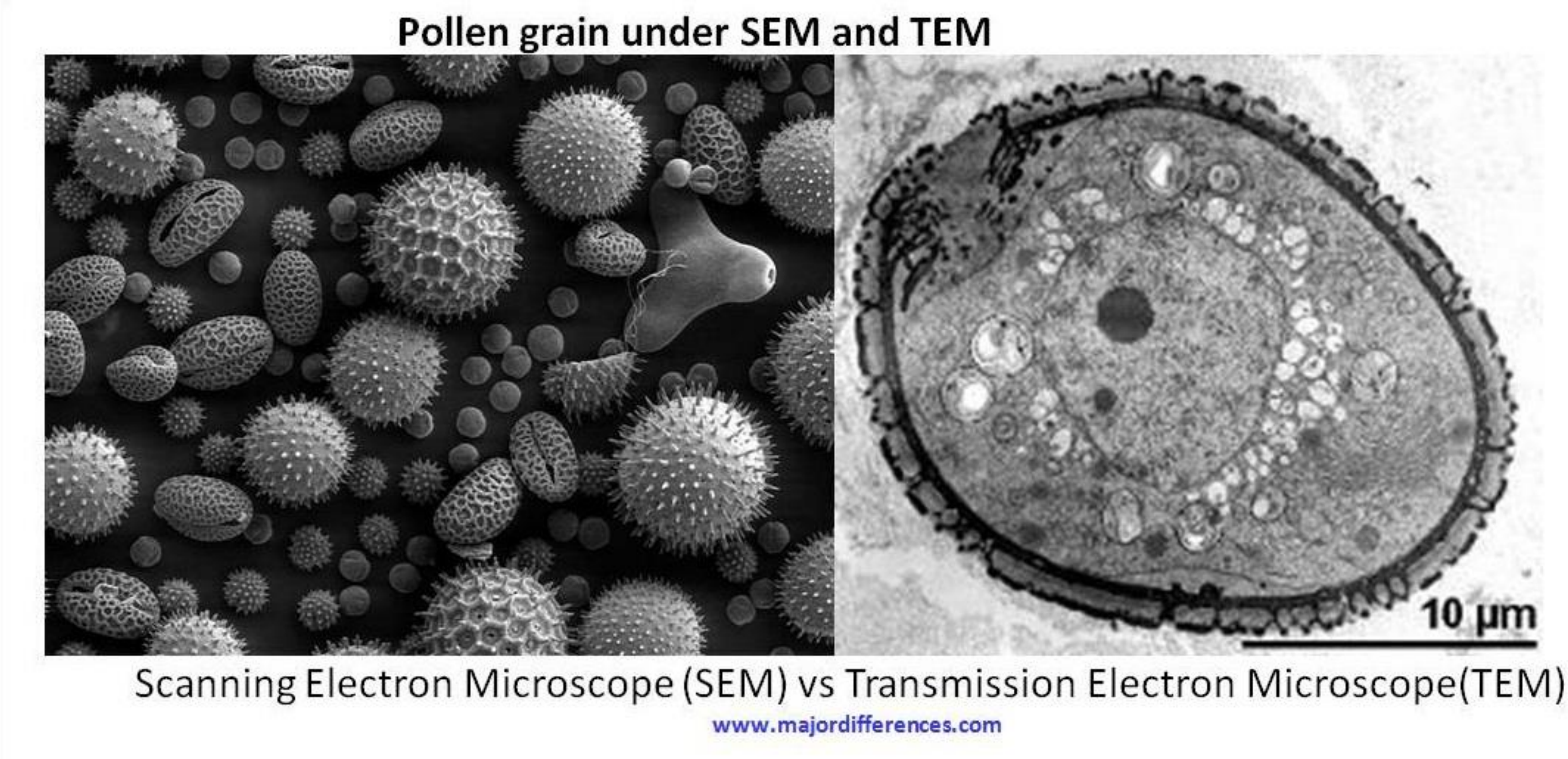

Scanning Electron Microscope (SEM) vs Transmission Electron Microscope(TEM)

www.majordifferences.com

SEM (Scanning Electron Microscope):
- Based on scattered electrons
- surface and composition
- 3D shape
- Lower resolution

TEM (Transmission Electron Microscope):
- Based on transmitted electrons
- Internal structure/composition
- 2D projection
- Higher resolution

Electrons vs matter

- Coulombic interactions
  - with electrons AND nucleus
- SEM:
  - secondary electrons
- TEM: electrons scattered:
  - elastically → image formation
  - inelastically → radiation damage
- Sources of contrast in TEM:
  - Amplitude contrast
  - Phase contrast

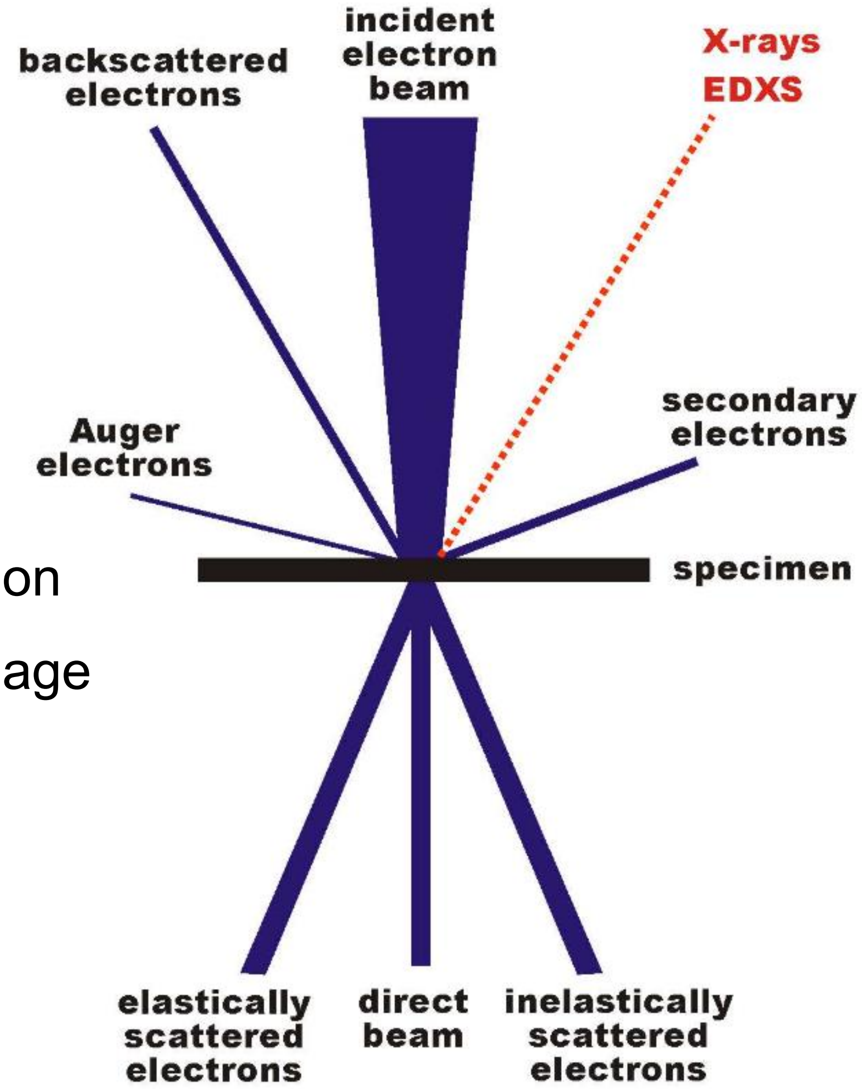

source: Frank Krumeich; Properties of Electrons, their Interactions with Matter and Applications in Electron Microscopy; www.microscopy.ethz.ch

Contrast – summary

- Amplitude contrast (=mass/scattering contrast)
  - deflected electrons lead to regions of reduced amplitude
  - applicable to strongly scattering and thick samples
- Phase contrast
  - changes in the wavefront phases
- Detectors can only record amplitudes
  - in a in focus and perfect (aberration free) optical system phase objects are invisible to detectors
  - amplitude contrast can be achieved by introducing interferences in the wavefront
  - → defocus!!!

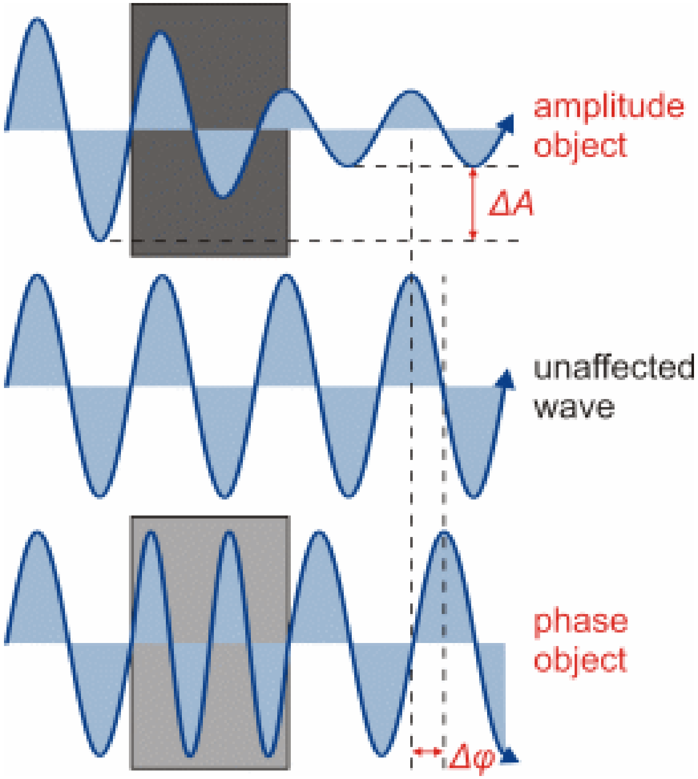

source: http://home.uni-leipzig.de/pwm/web/?section=introduction&page=phasecontrast

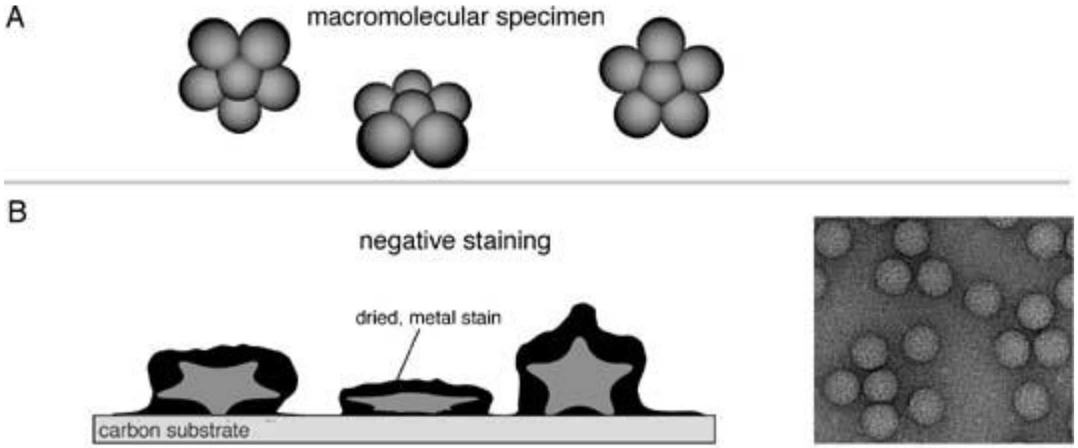

Negative stain

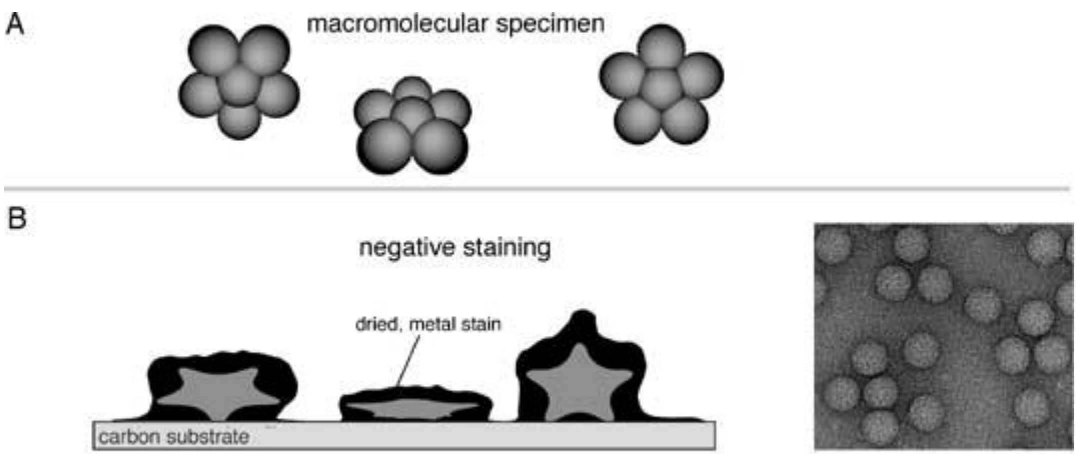

Negative stain

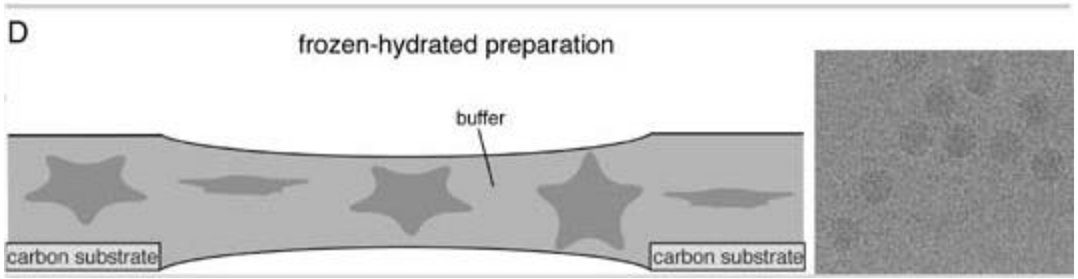

Cryo-EM


C
1
GROSZ

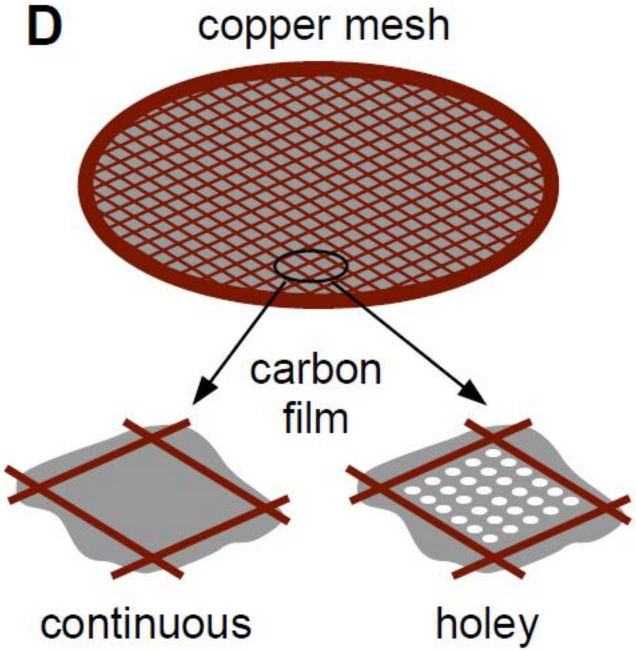
D
copper mesh
carbon film
continuous
holey

Preparation of cryo-EM specimen

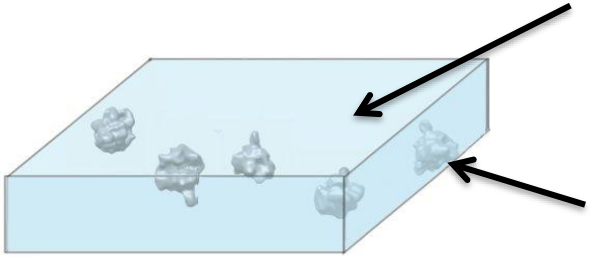

vitreous ice

protein

Cryo-EM grid

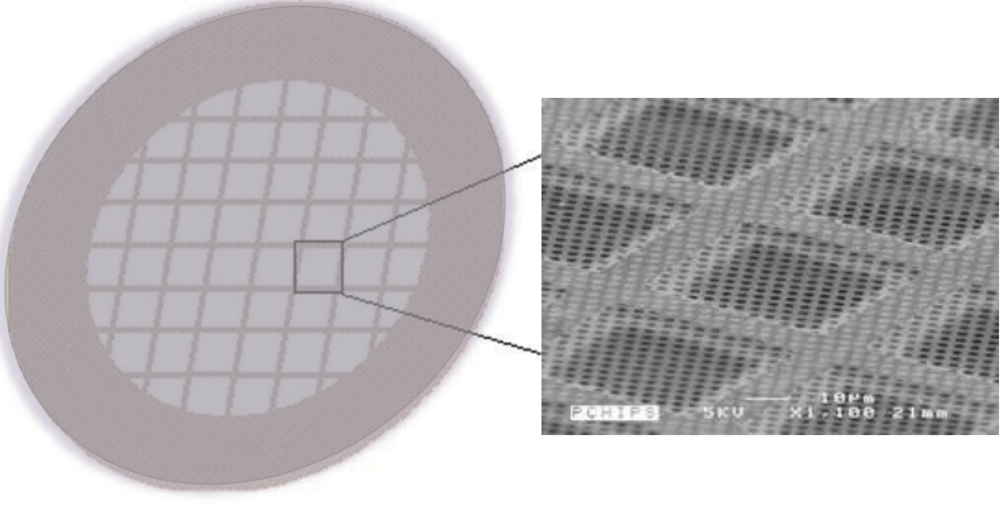

http://www.emsdiasum.com

Ania Piasecka

Cryo-EM specimen preparation

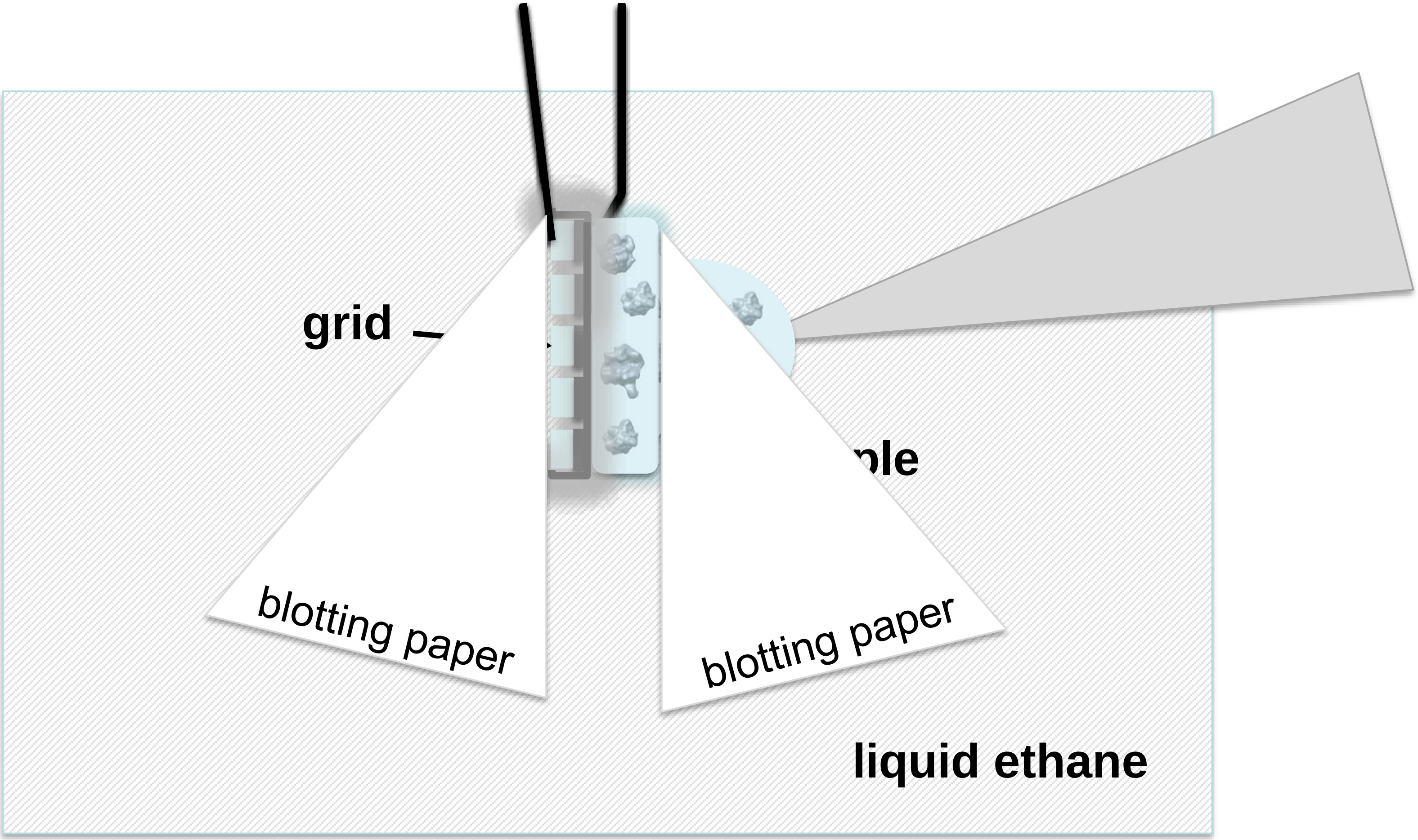

Ania Piasecka

SPR – principles

- TEM images: projections of particles
- What kind of projections do we need?
  - many projections of identical particles with different, known orientations

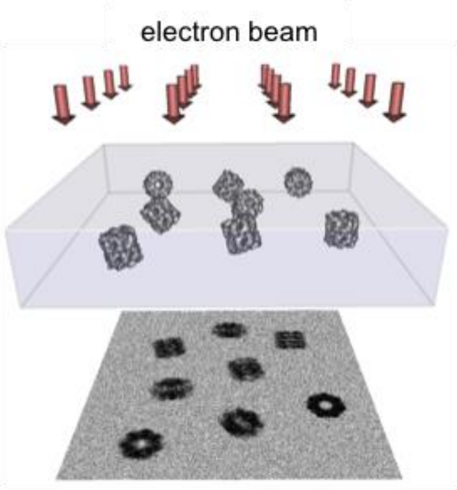

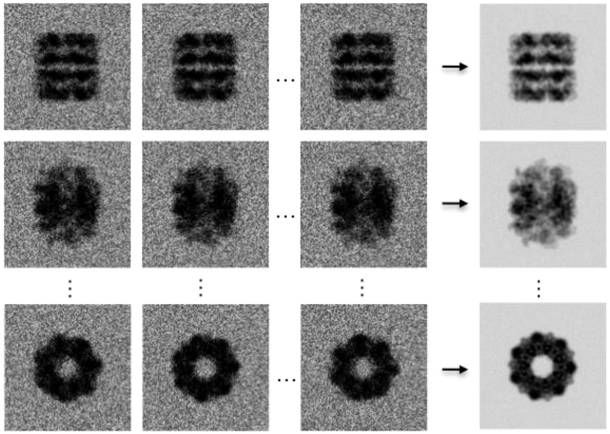

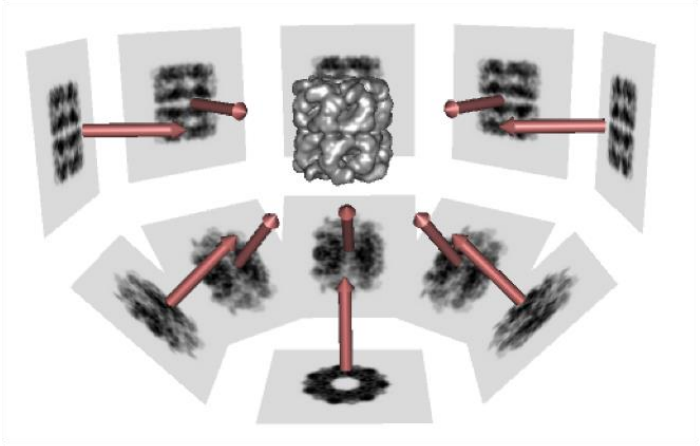

Image source: https://people.csail.mit.edu/gdp/cryoem.html

SPR – size limits

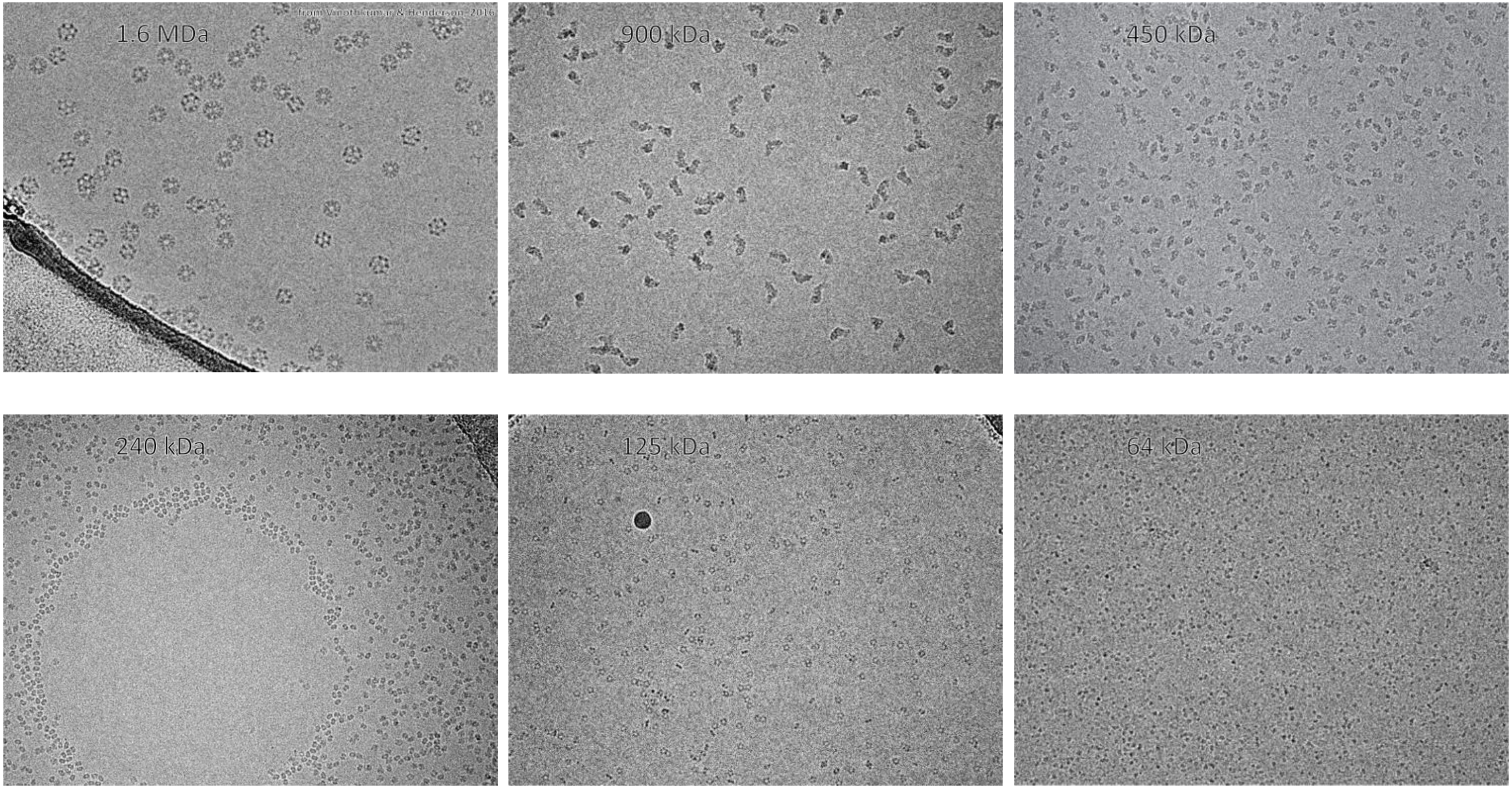

source: Cryo-EM17 Lecture 01 Past Present Future; Richard Henderson, MRC Lab, 2017

PROBLEMS:

- Low contrast of biological samples
- Radiation damage
- Sample vibrations

Resolution

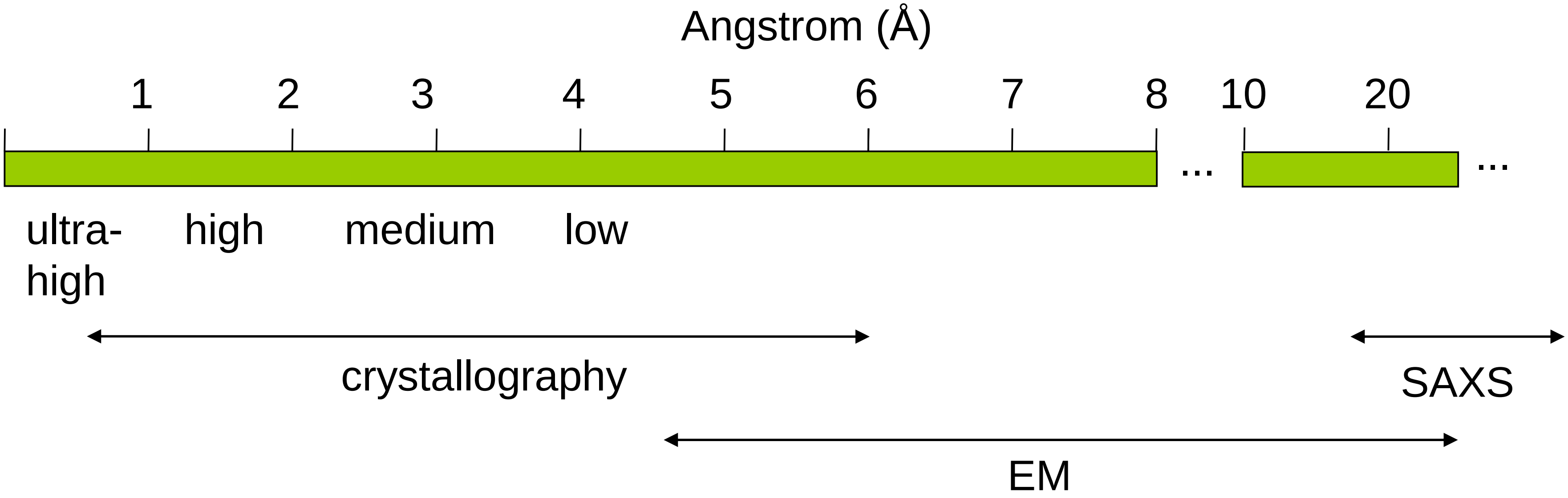

Angstrom (Å)

1 2 3 4 5 6 7 8 … 10 20 …

ultra-high

high

medium

low

crystallography

SAXS

EM

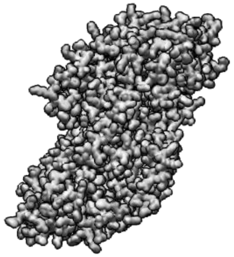

2.5 Å

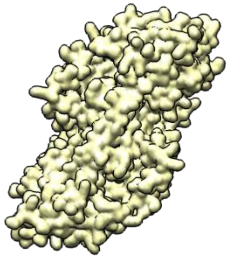

4 Å

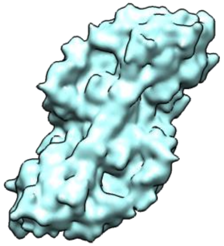

8 Å

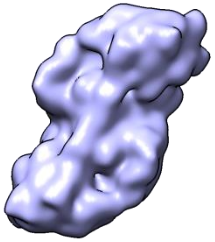

12 Å

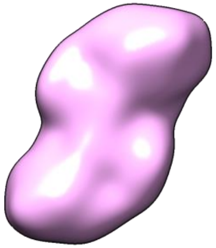

25 Å

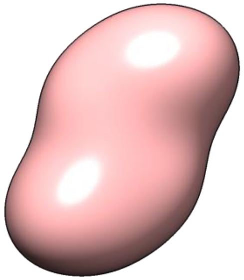

50 Å

Resolution

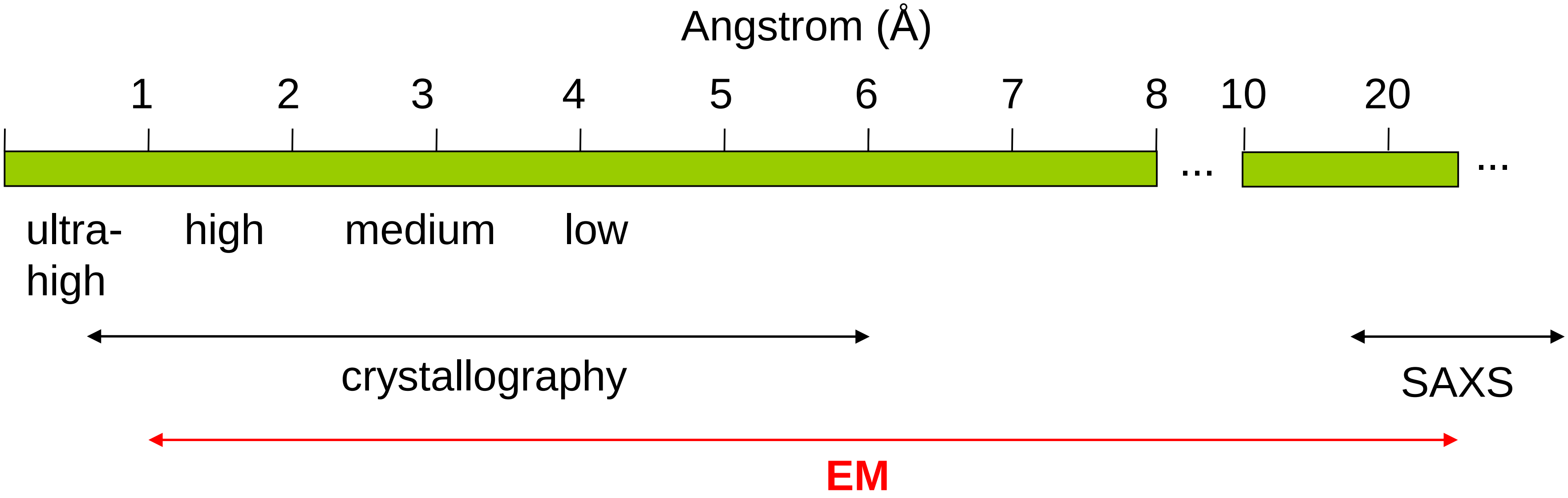

Angstrom (Å)

1 2 3 4 5 6 7 8 ... 10 20 ...

ultra-high

high

medium

low

crystallography

SAXS

EM

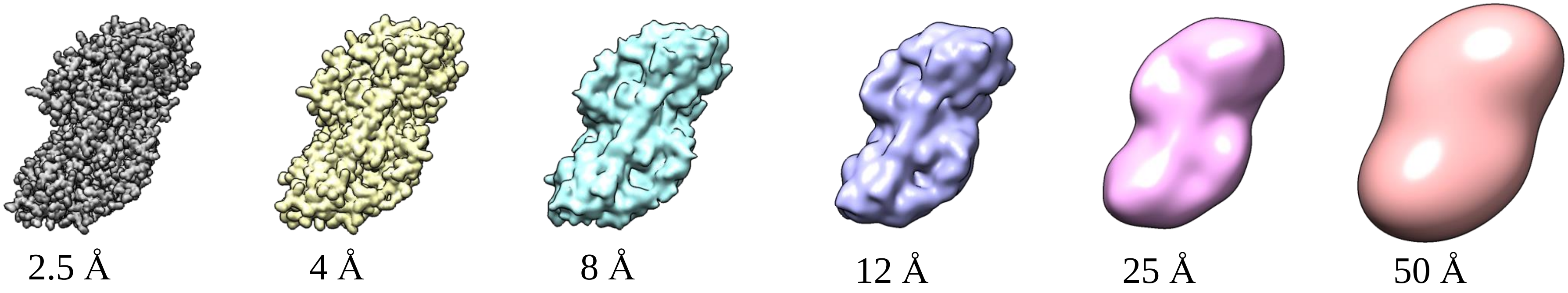

2.5 Å

4 Å

8 Å

12 Å

25 Å

50 Å

Direct detectors

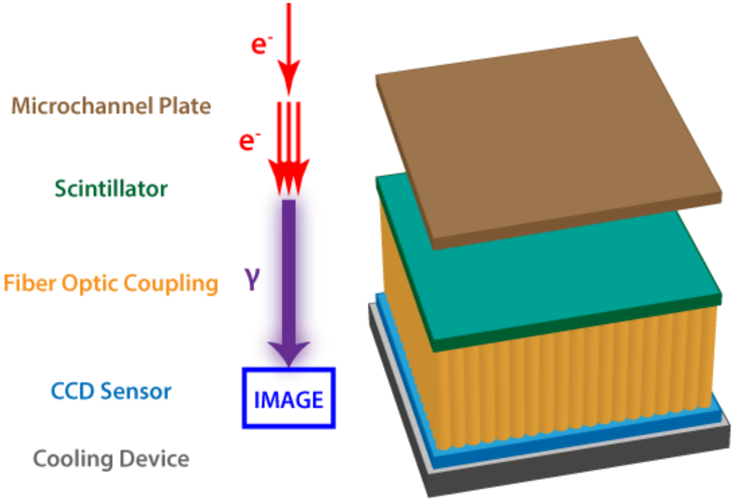

MCP + CCD

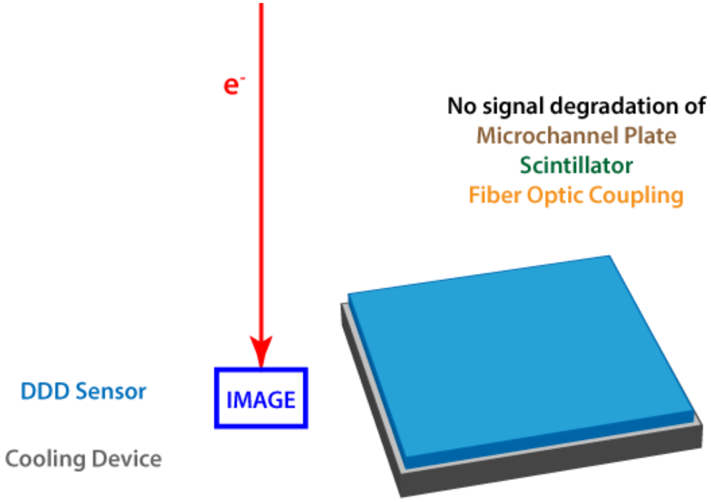

Direct Detection Camera

PROBLEMS:

- Radiation damage
- Sample vibrations

MOVIES

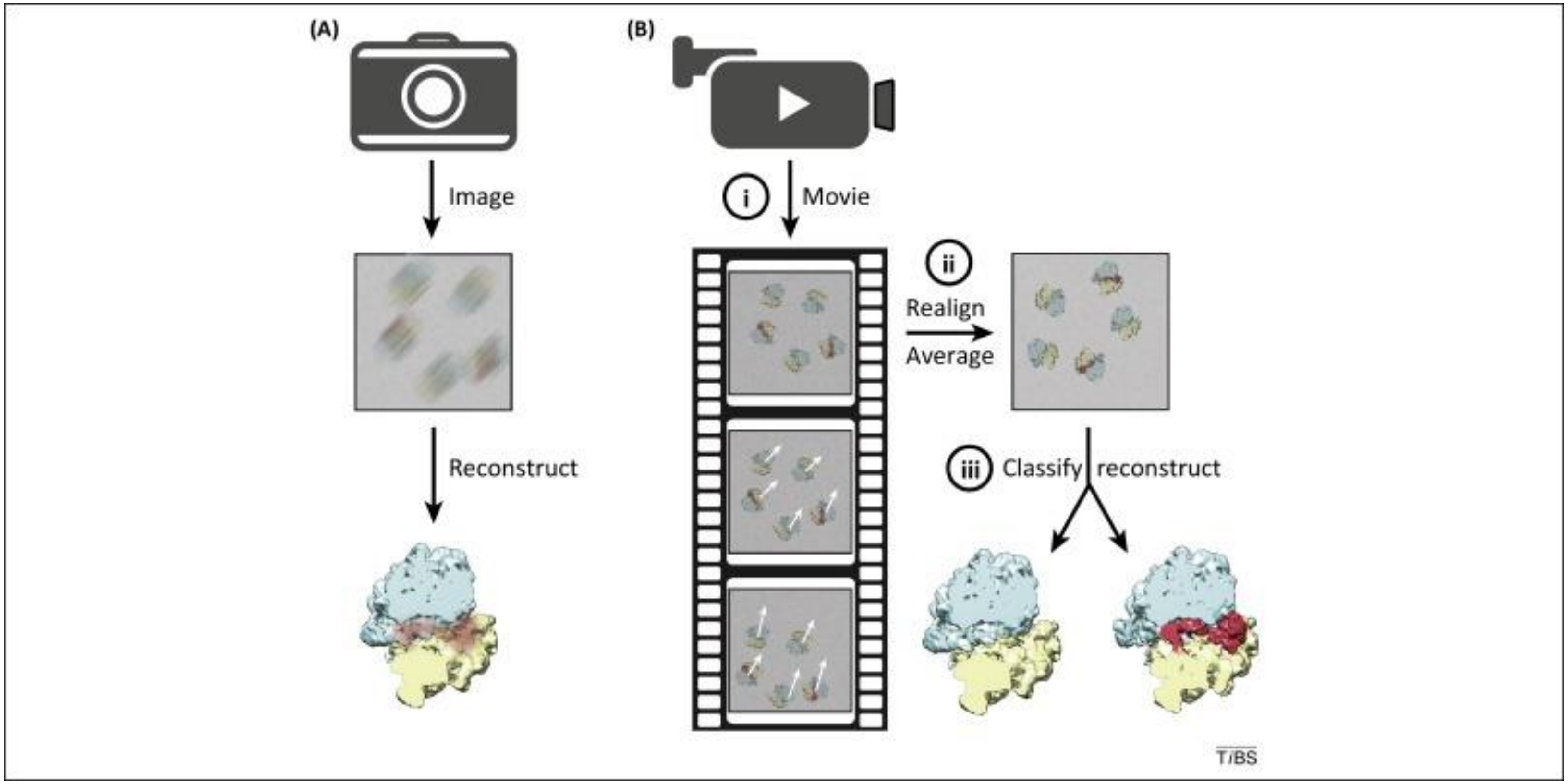

Software packages

- CryoSPARC (very fast commercial software)
- cisTEM (Computational Imaging System for Transmission Electron Microscopy)
- SIMPLE (Single-particle IMage Processing Linux Engine)
- RELION REgularized LIkelihood OptimizatioN

source: https://www.ebi.ac.uk/pdbe/emdb/statistics_software.html/
more info:
https://en.wikibooks.org/wiki/Software_Tools_For_Molecular_Microscopy
http://www.emdatabank.org/emsoftware.html

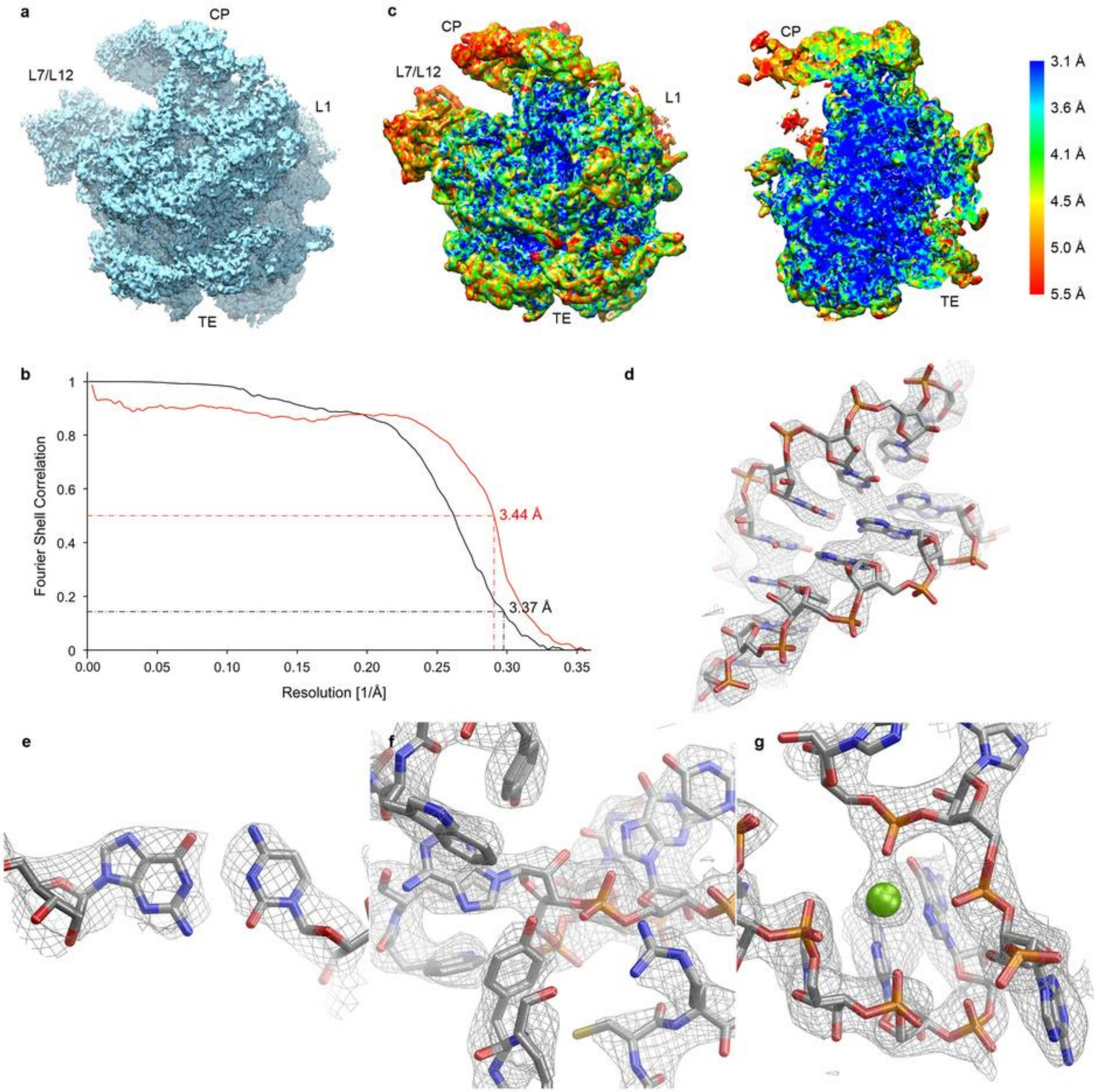

Basil J. Greber, et al. The complete structure of the large subunit of the mammalian mitochondrial ribosome
Nature 515, 283–286 (13 November 2014)

SPR – progress

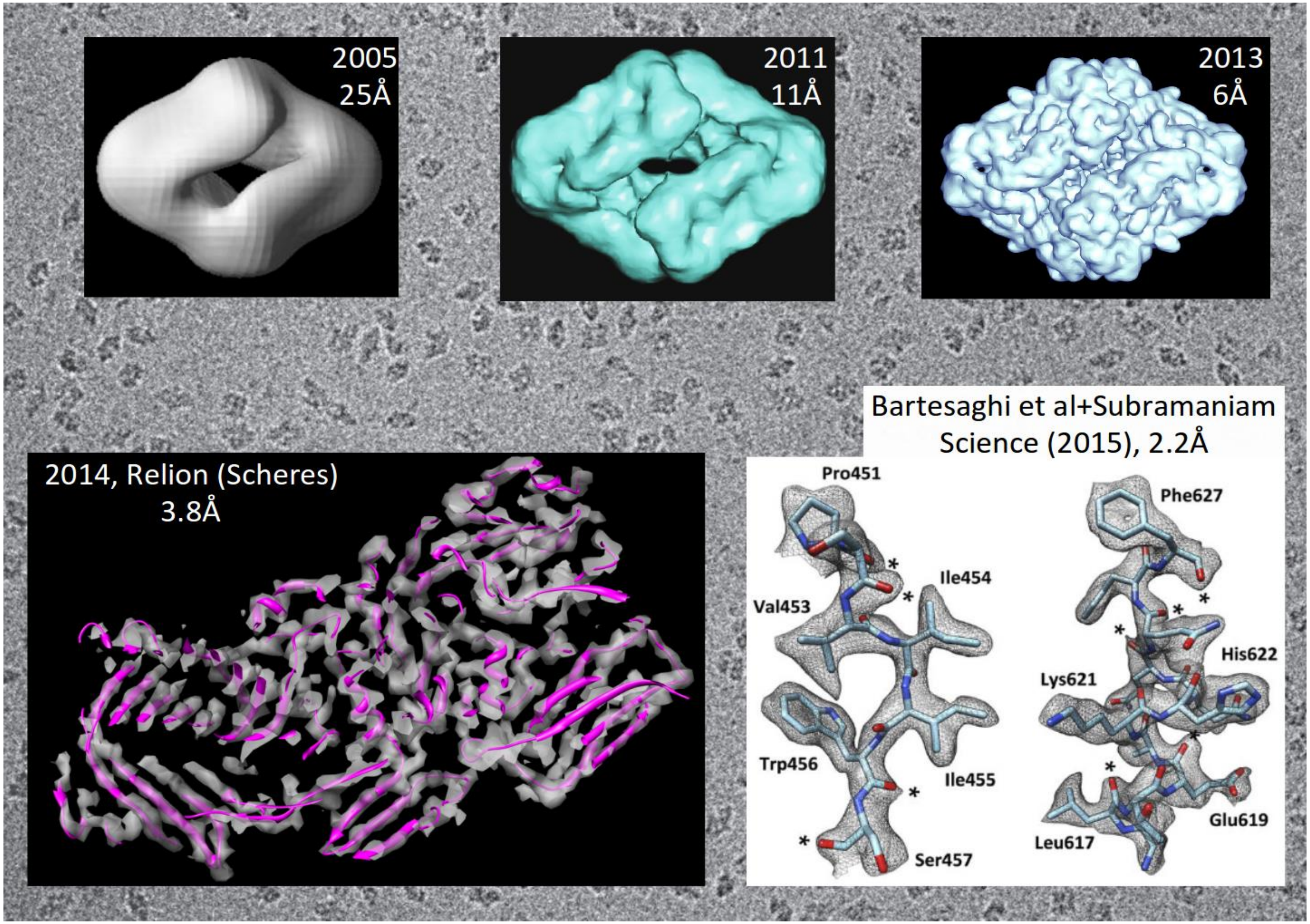

source: Cryo-EM17 Lecture 01 Past Present Future; Richard Henderson, MRC Lab, 2017

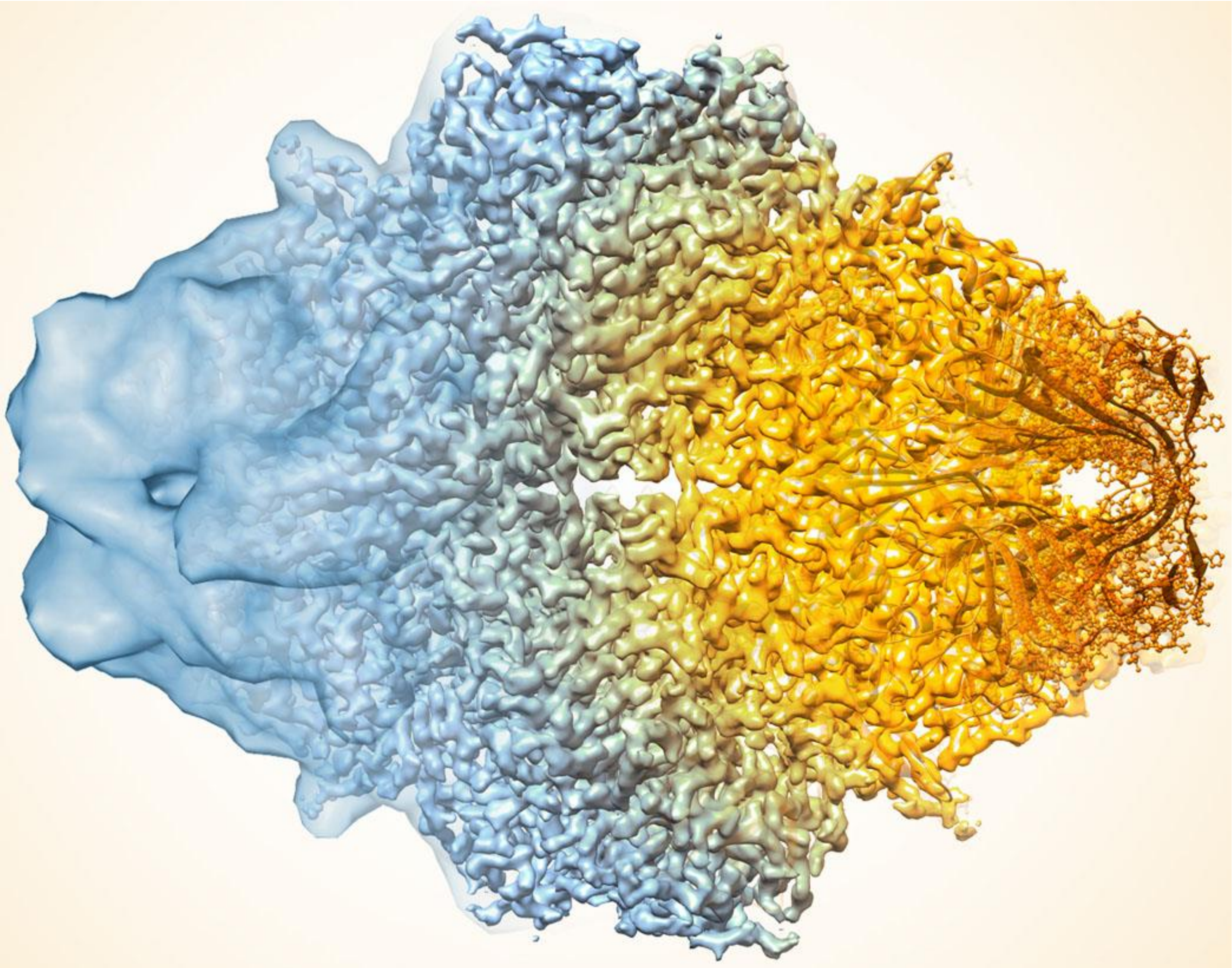

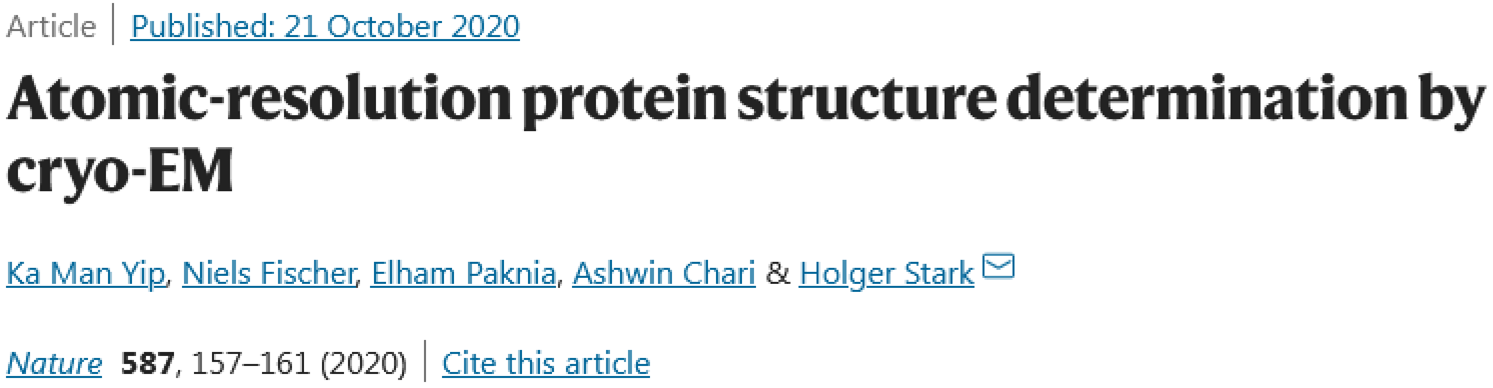

Article | Published: 21 October 2020

Atomic-resolution protein structure determination by cryo-EM

Ka Man Yip, Niels Fischer, Elham Paknia, Ashwin Chari & Holger Stark

Nature **587**, 157–161 (2020) | Cite this article

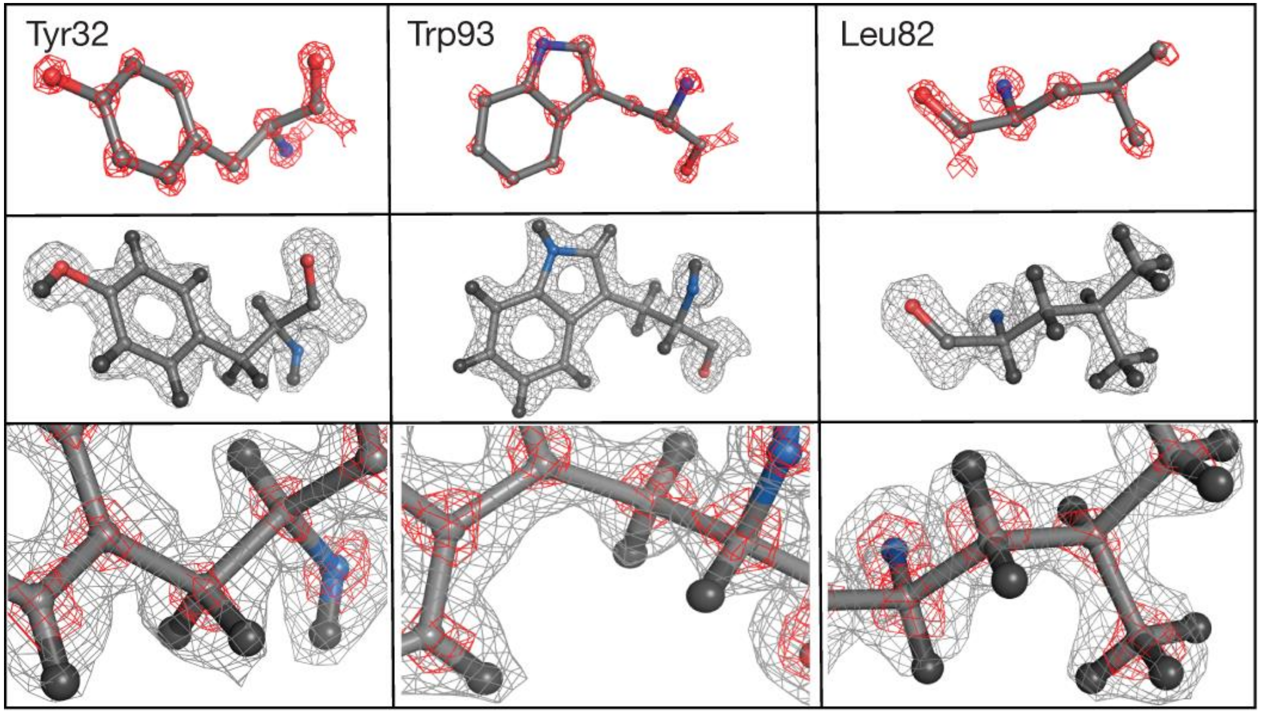

Title: Translation dynamics in human cells visualized at high-resolution reveal cancer drug action

Authors: Huaipeng Xing[1,2], Reiya Taniguchi[1], Iskander Khusainov[1], Jan Philipp Kreysing[1,3], Sonja Welsch[4], Beata Turoňová[1], Martin Beck[1]*

Affiliations:

[1]Department of Molecular Sociology, Max Planck Institute of Biophysics, 60438 Frankfurt am Main, Germany.

[2]Faculty of Biochemistry, Chemistry and Pharmacy, Goethe University Frankfurt am Main, 60438 Frankfurt am Main, Germany.

[3]IMPRS on Cellular Biophysics, 60438 Frankfurt am Main, Germany

[4]Central Electron Microscopy Facility, Max Planck Institute of Biophysics, 60438 Frankfurt am Main, Germany.

*Corresponding author. Email: martin.beck@biophys.mpg.de

Translation cycle

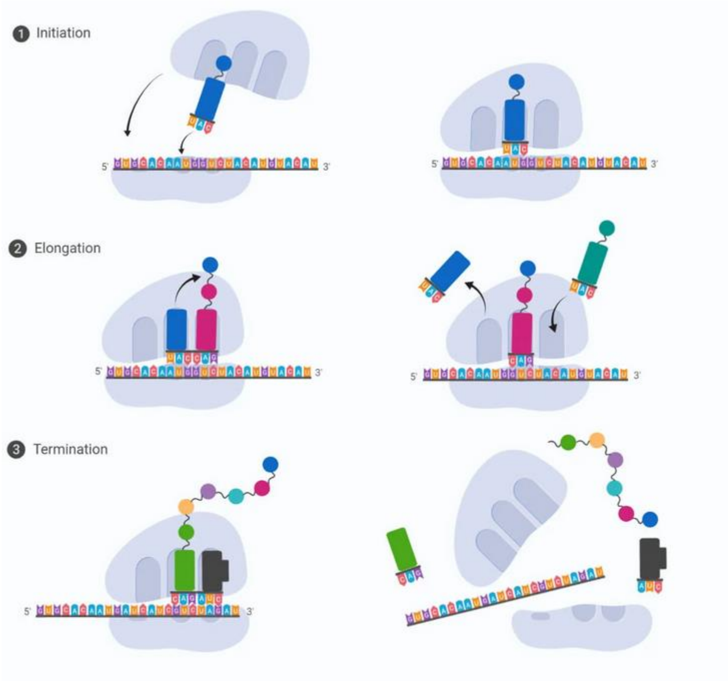

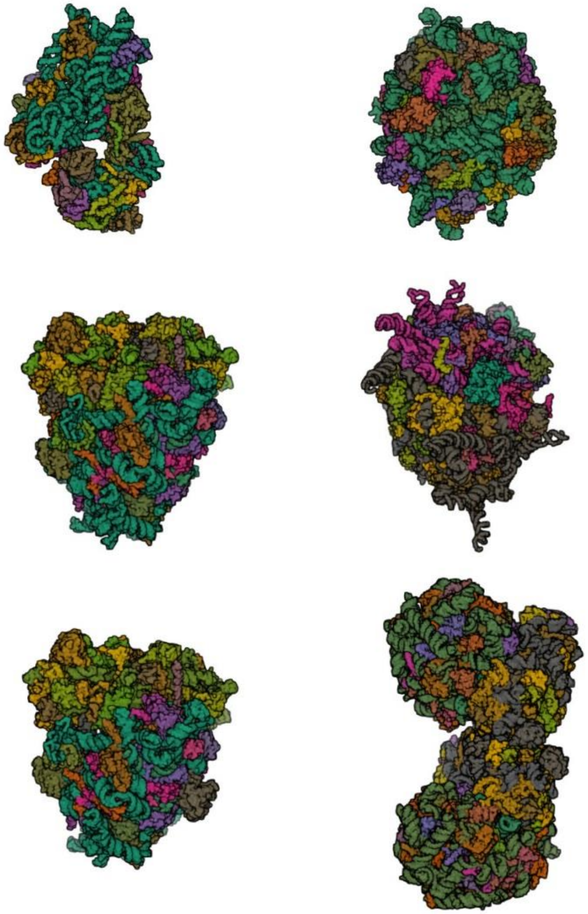

Methodology

cryo-focused ion beam (cryo-FIB) milling

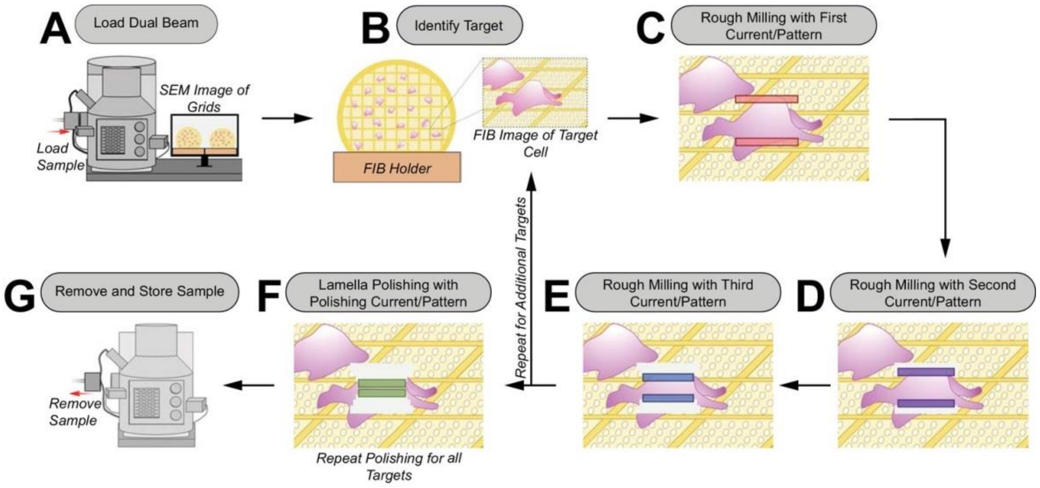

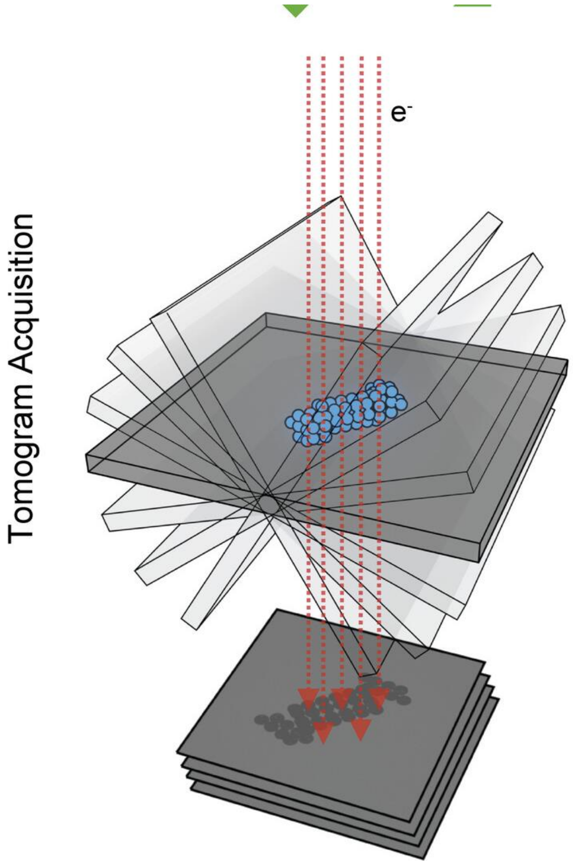

35 cells --- 358 tomograms

Overall ribosome structure

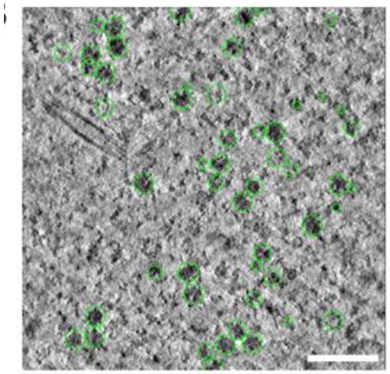

○ Initial ribosomal candidates (1080 particles)

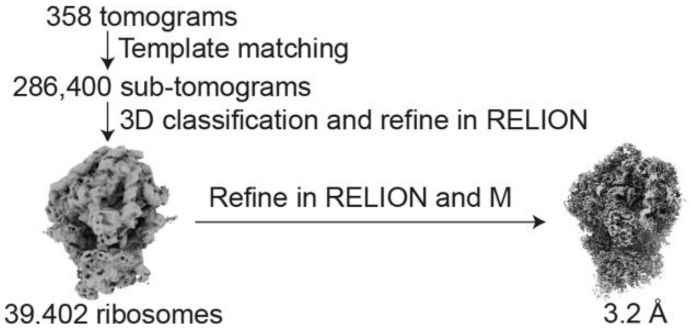

358 tomograms

↓ Template matching

286,400 sub-tomograms

↓ 3D classification and refine in RELION

39.402 ribosomes

Refine in RELION and M →

3.2 Å

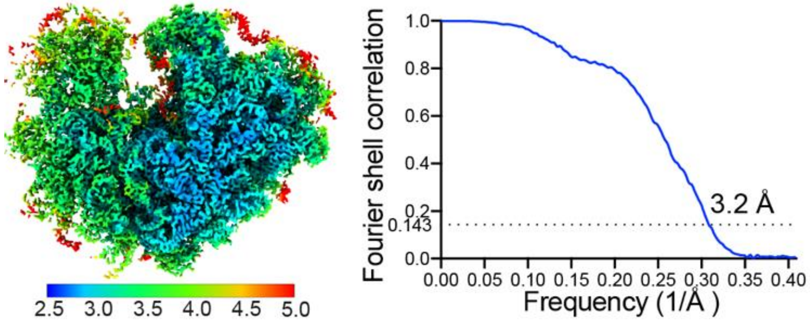

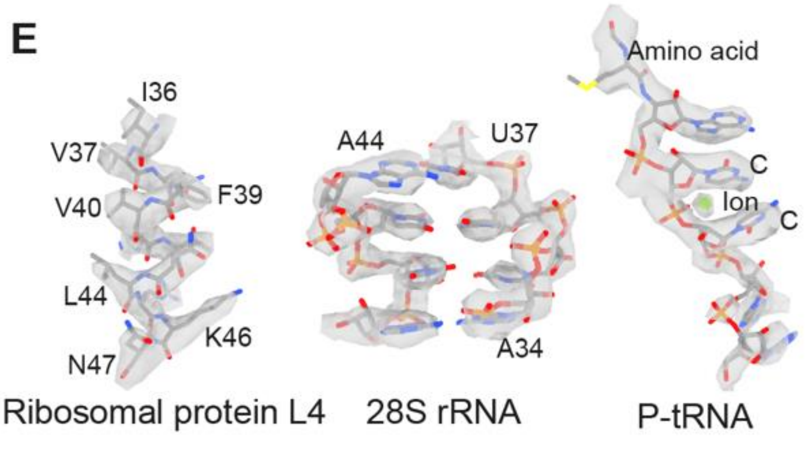

Peptidyl transferase center (PTC)

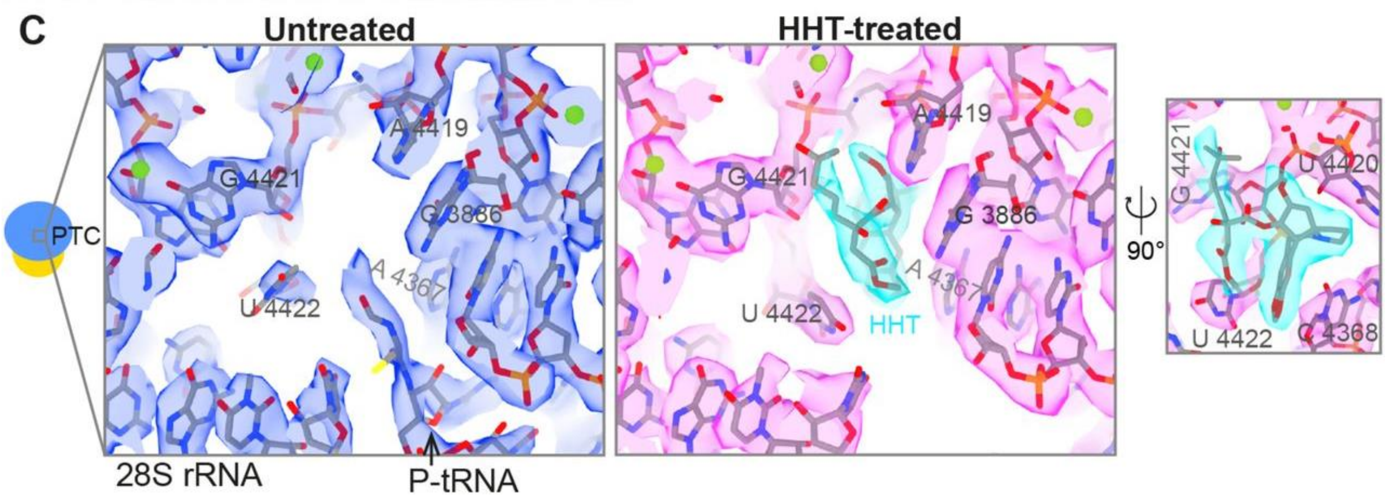

- HHT (homoharringtonine) - natural compound that binds to the ribosome and inhibits protein synthesis
  - drug for chronic myeloid leukemia
  - the exact mechanism of inhibition of protein synthesis not known

Translation elongation landscape in human cells

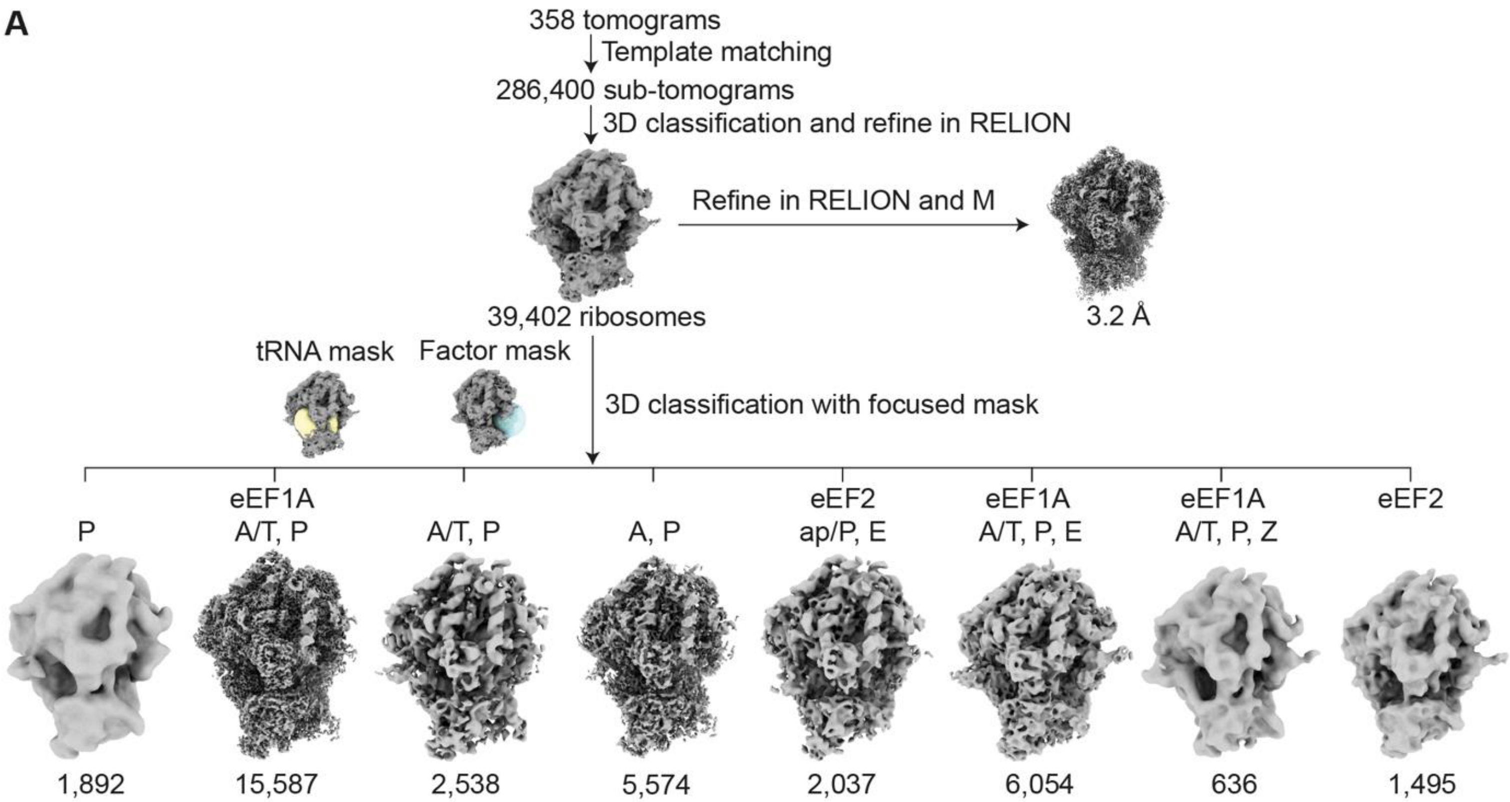

14.7 Å 3.4 Å 8.3 Å 5.0 Å 9.6 Å 8.7 Å 16.4 Å 11.7 Å

Translation elongation landscape in human cells

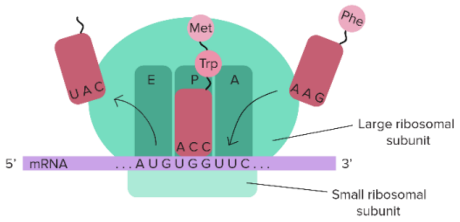

A – amino-acyl site
P – peptidyl site
E – exit site

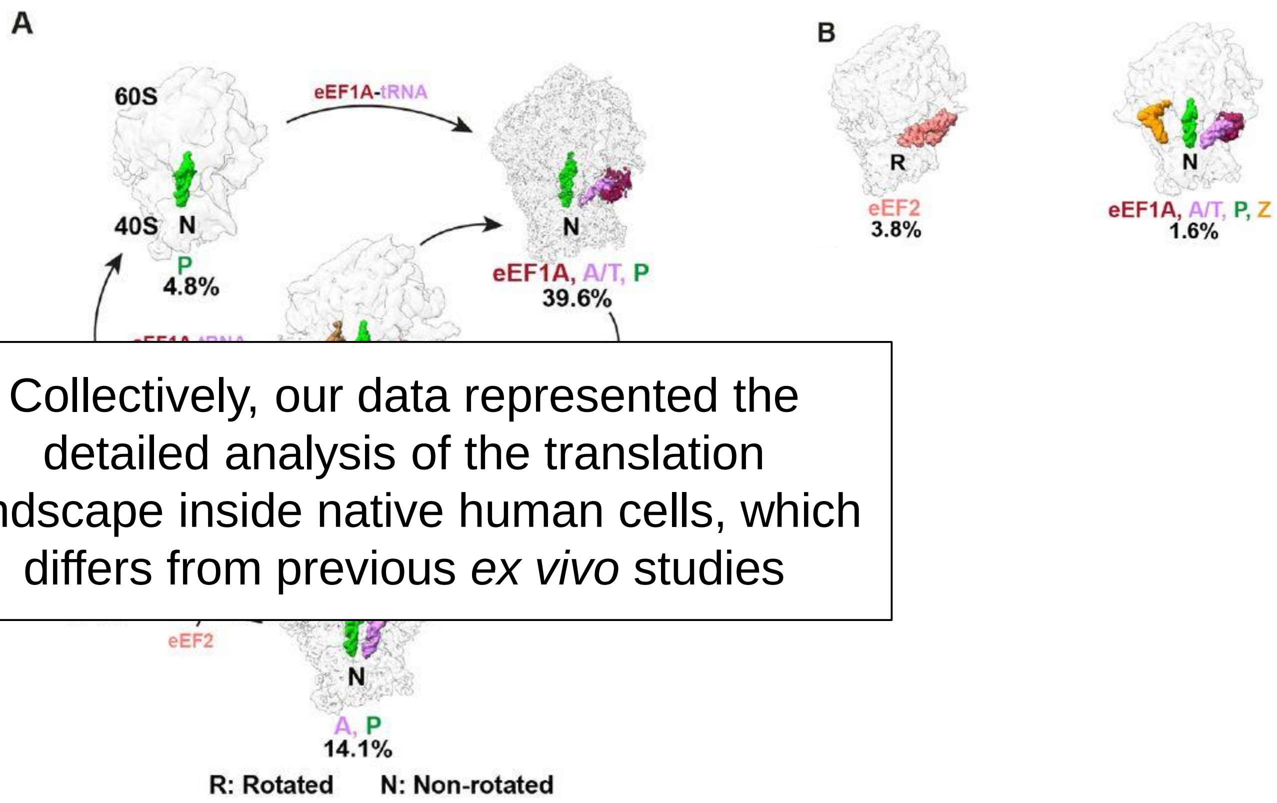

Collectively, our data represented the detailed analysis of the translation landscape inside native human cells, which differs from previous *ex vivo* studies

HHT modifies the translation elongation landscape

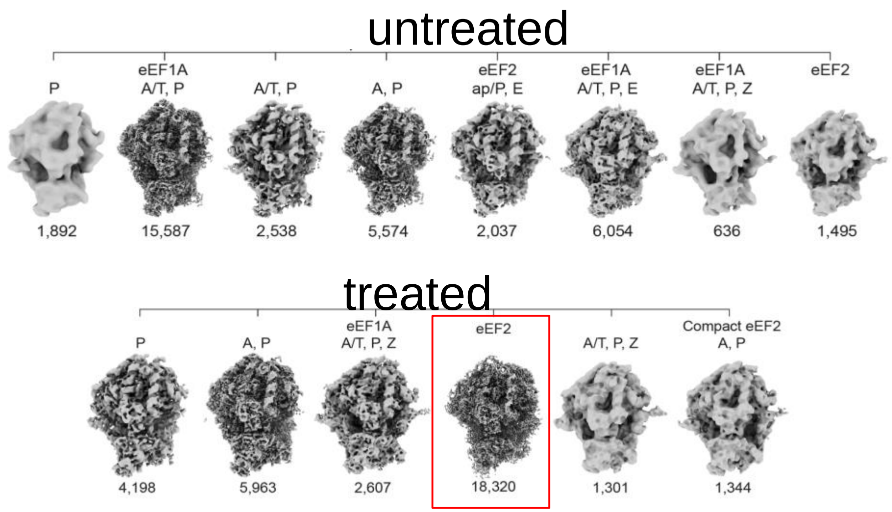

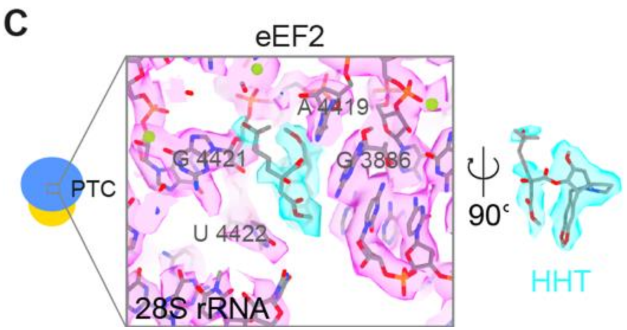

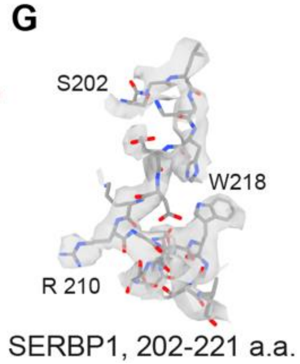

SERBP1(SERPINE1 mRNA-binding protein 1) – marker for hibernating ribosomes

HHT treatment results in the accumulation of ribosome hibernation, which may be representative of the mechanism of the drug action in cancer therapy.

Cryo-EM

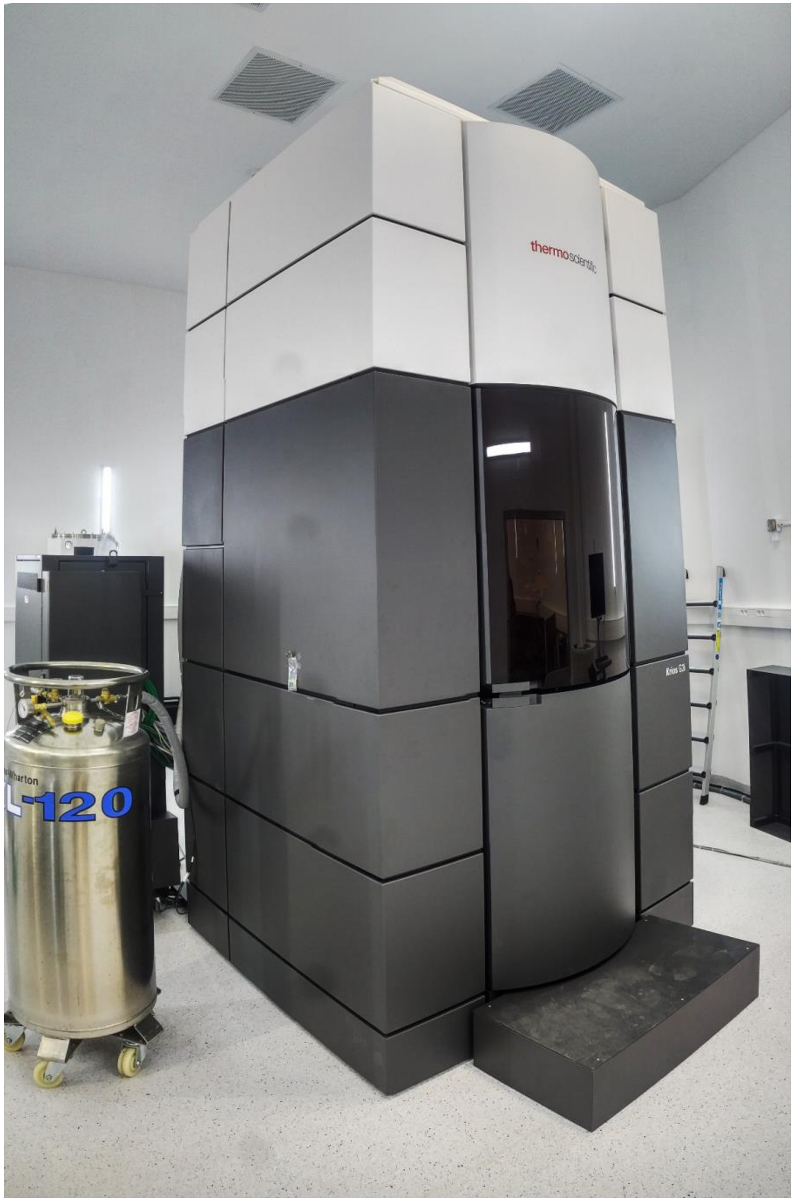
thermo scientific
Krios G3i
L-120

Protein Data Bank

www.pdb.org

PyMOL

http:// pymol.org

http://www.imb-jena.de/www_bioc/

RNAs form complex 3D structures that govern their mechanisms of action

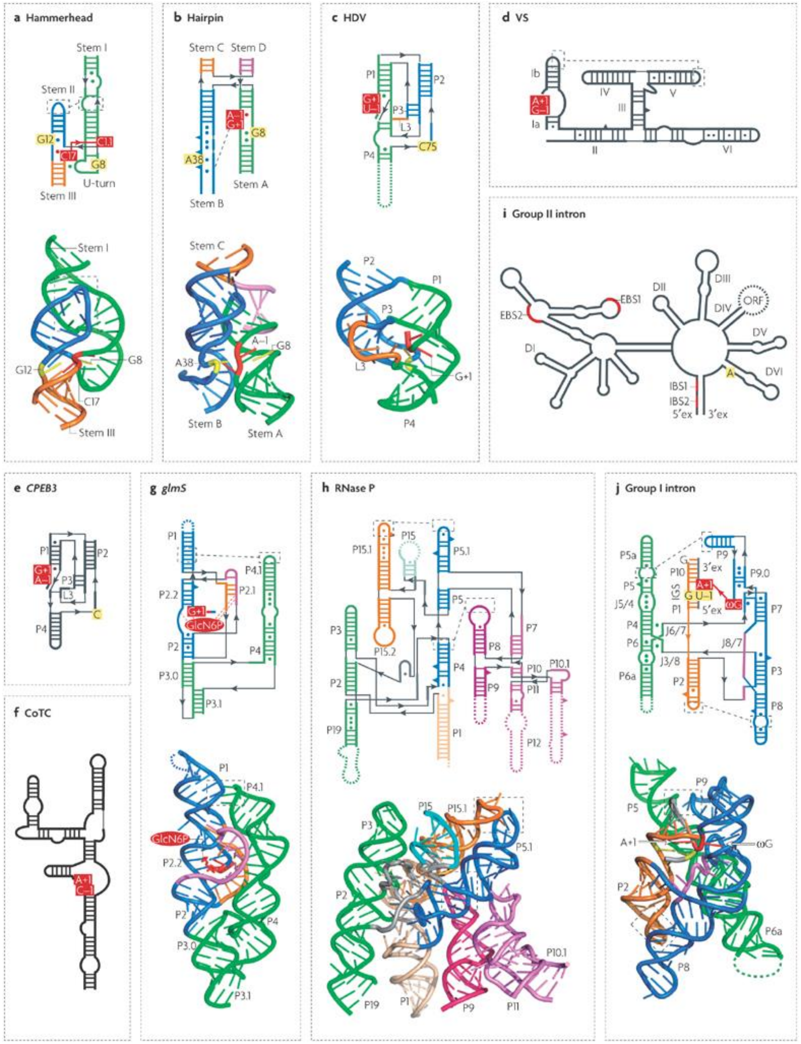

Nature Reviews | Genetics

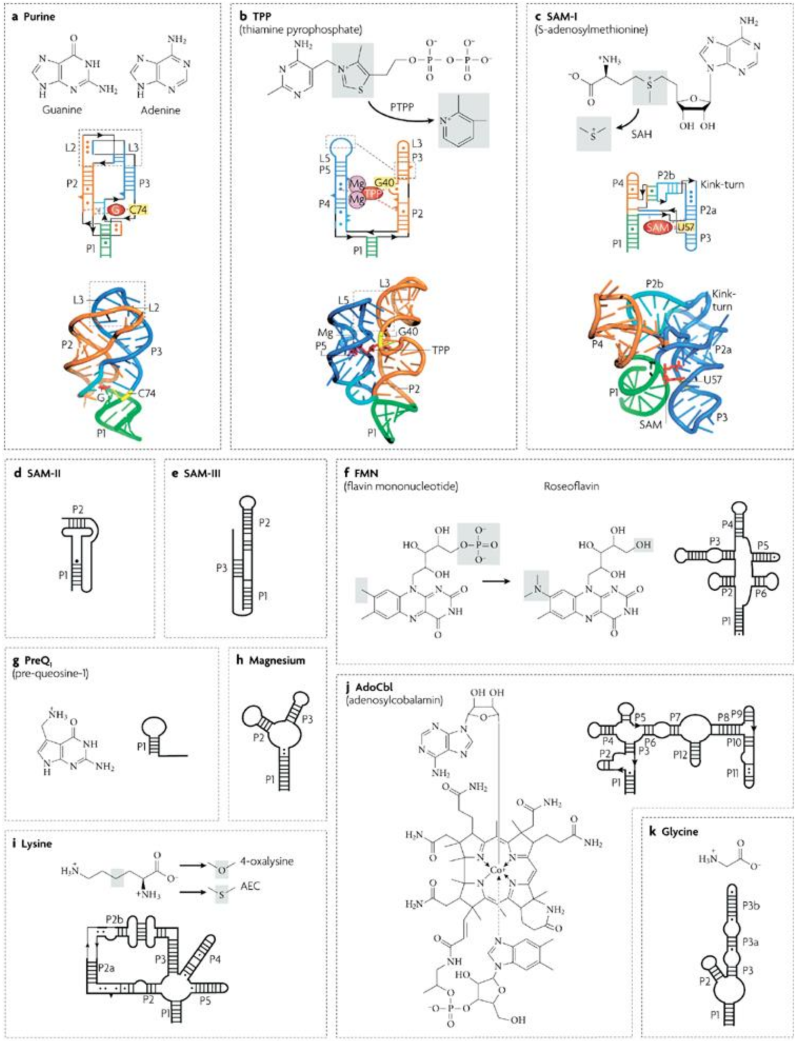

Nature Reviews | Genetics

Serganov A, Patel DJ
Ribozymes, riboswitches and beyond: regulation of gene expression without proteins
Nature Rev Genet 2007, 8, 776–790

Niektóre jądra atomowe posiadają moment magnetyczny:

- Ten moment jest równoległy i proporcjonalny do spinu jądra
- Dla spinu ½ możliwe są dwa stany energetyczne – równoległy i antyrównoległy do zewnętrznego pola magnetycznego
- Przejścia między tymi dwoma stanami są obserwowane z NMR
- częstotliwość odpowiadająca przechodzeniu między tymi dwoma stanami jest nazwana częstotliwością Larmora

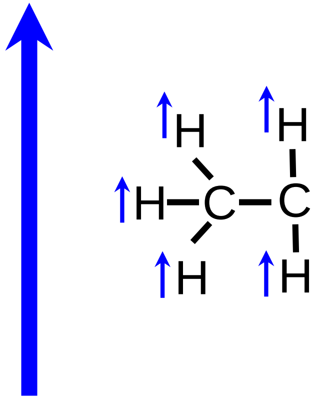

Przesunięcia chemiczne

Prądy generowane przez chmury elektronowe osłaniają jądro od zewnętrznego pola magnetycznego modyfikując częstotliwości Larmora o milionowe części.

Jedynie ^{1}H, ^{13}C, ^{15}N, oraz ^{31}P mogą być zastosowane w NMR

Jednowymiariowe widma dla tetrapętli (region protonów iminowych)

Dwuwymiarowe widma HSQC

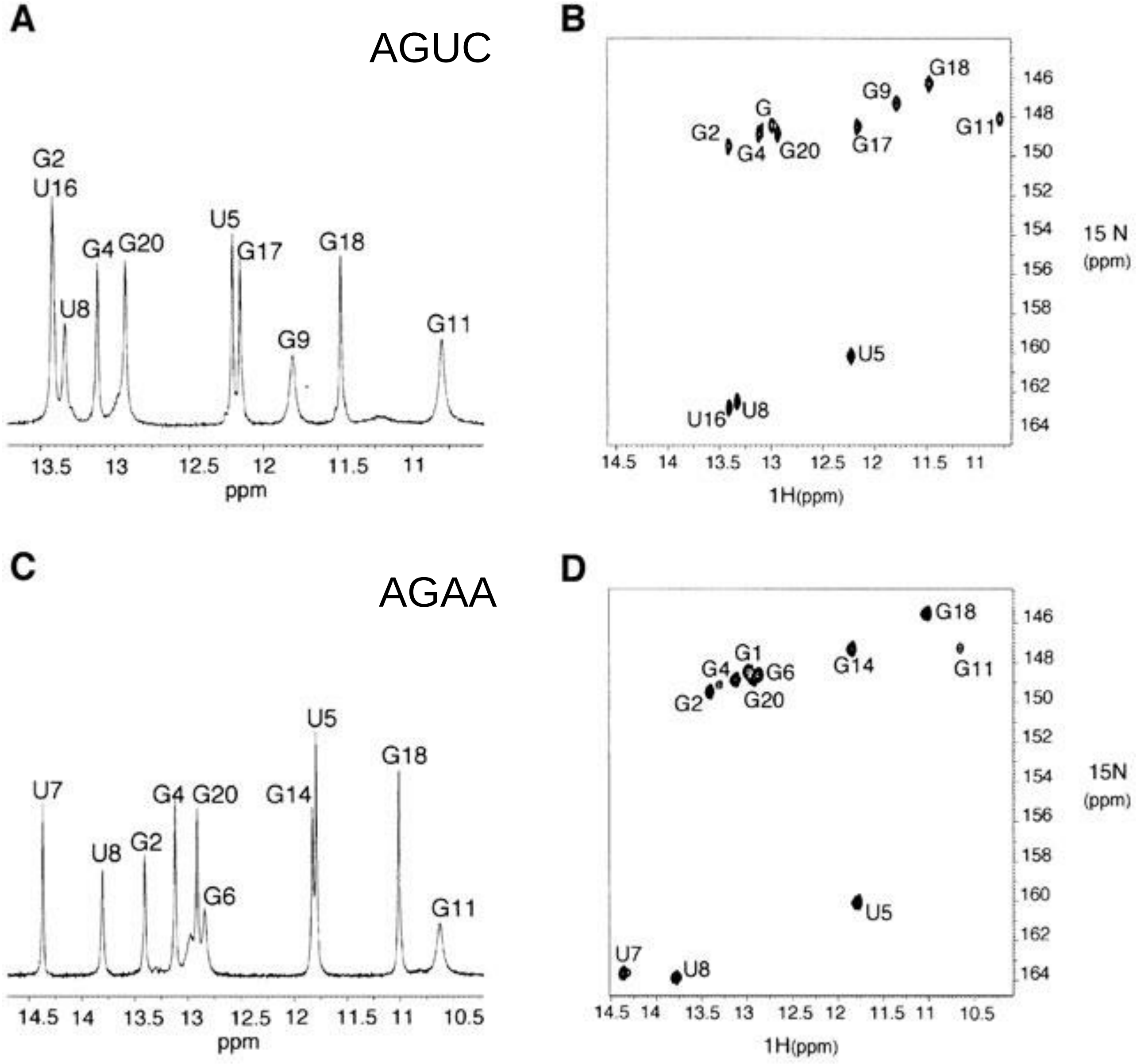

AGUC

AGAA

Stałe sprzężenia

W najprostszym przypadku oczekujemy pojedynczych sygnałów od poszczególnych protonów w cząsteczce.

Proton, który obserwujemy (H_A) znajduje się w pobliżu innego protonu (H_B). Moment magnetyczny HB jest również ułożony równolegle lub antyrównolegle ułożony względem pola zewnętrznego. Połowa H_A będzie się znajdować obok H_B ułożonego równolegle do pola i „odczuwa” nieco większe pole, a połowa obok H_B ułożonego antyrównolegle i „odczuwa” nieco mniejsze pole.

Stała sprzężenia (coupling constant) mierzona w Hz opisuje oddzielenie składników multipletu

Pośrednie sprzężenia spinowo-spinowe w NMR są przenoszone wiązania między atomami (dwa lub trzy; sprzężenia przez cztery wiązania są często poniżej poziomu detekcji).

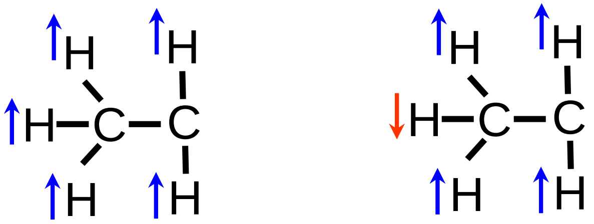

Obserwowane rezonanse występują w multipletach - singlet, dublet, kwartet itd.

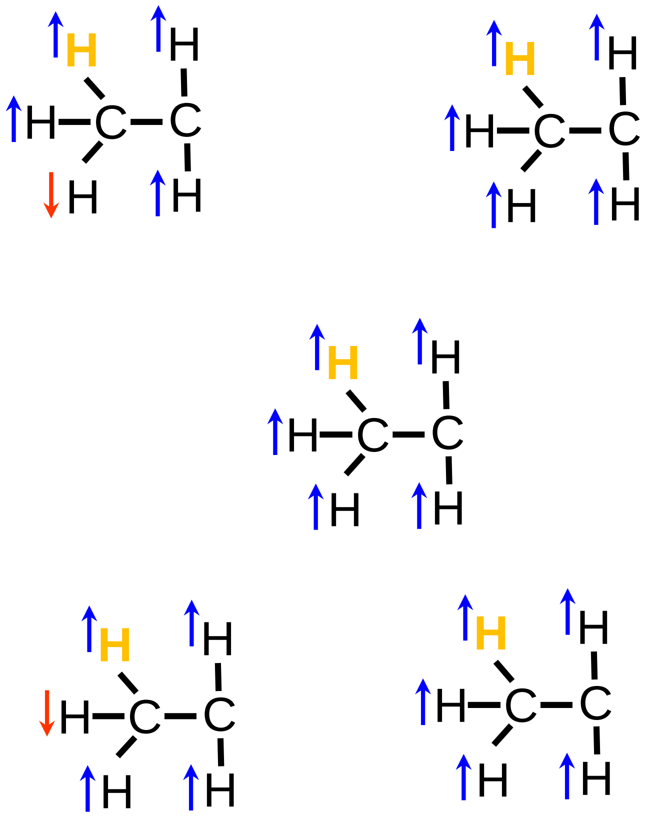

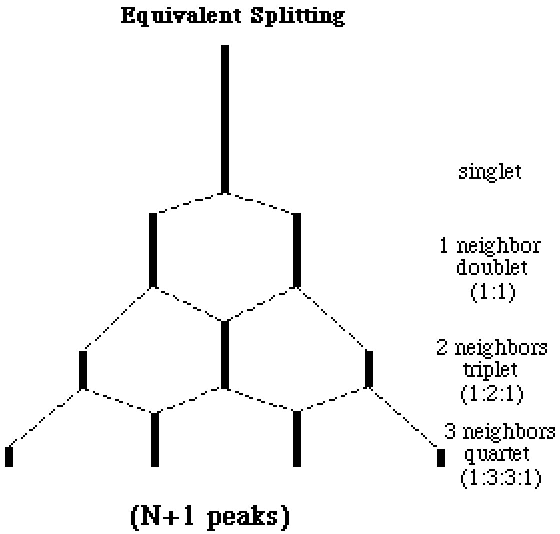

Duże znaczenie dla określania struktury przestrzennej cząsteczek mają też stałe sprzężenia wicynalne (przez trzy wiązania), których pomiar pozwala na określanie kątów dwuściennych w cząsteczkach poprzez tzw. równanie Karplusa

Innym mechanizmem sprzężenia pomiędzy momentami magnetycznymi jąder jest **bezpośrednie sprzężenie spinowo-spinowe** lub dipolowe (stała tego sprzężenia jest oznaczana D), która zachodzi przez przestrzeń. W cieczy, ruchy cząsteczki powodują, że sprzężenie bezpośrednie ulega uśrednieniu do zera

Zależne od odległości jąder - ~ $1/r^6$

Można ja jednak mierzyć jako tzw. resztkowe sprzężenie dipolowe w częściowo zorientowanych cieczach (np. zawierających polimery, wirusy etc.)

Sprzężenia dipolowe prowadzą również do zmian intensywności sygnałów NMR – jądrowy efekt Overhausera, którego wielkość jest odwrotnie proporcjonalna do odległości dwóch protonów (<6 Å)

Nagroda Nobla - Kurt Wutrich 2002

Doświadczenia rozpoczynają się od przygotowania cząsteczek wyznakowanych izotopami ^{13}C and ^{15}N.

Widma dwu- i trójwymiarowe są rejestrowane, aby zidentyfikować systemy spinowe i przypisać sygnały do poszczególnych reszt

Informacja strukturalna jest uzyskana przez pomiar tzw. efektu jądrowego Overhausera (NOESY)

Pomiary stałych sprzężeń pozwalają zmierzyć kąty w szkielecie fosforanowym RNA

Zmierzone więzy są następnie użyte w protokole minimalizacji struktury dynamiki molekularnej z simulated annealing
Wygenerowana zostaje grupa struktur (ensemble), która spełnia założone więzy

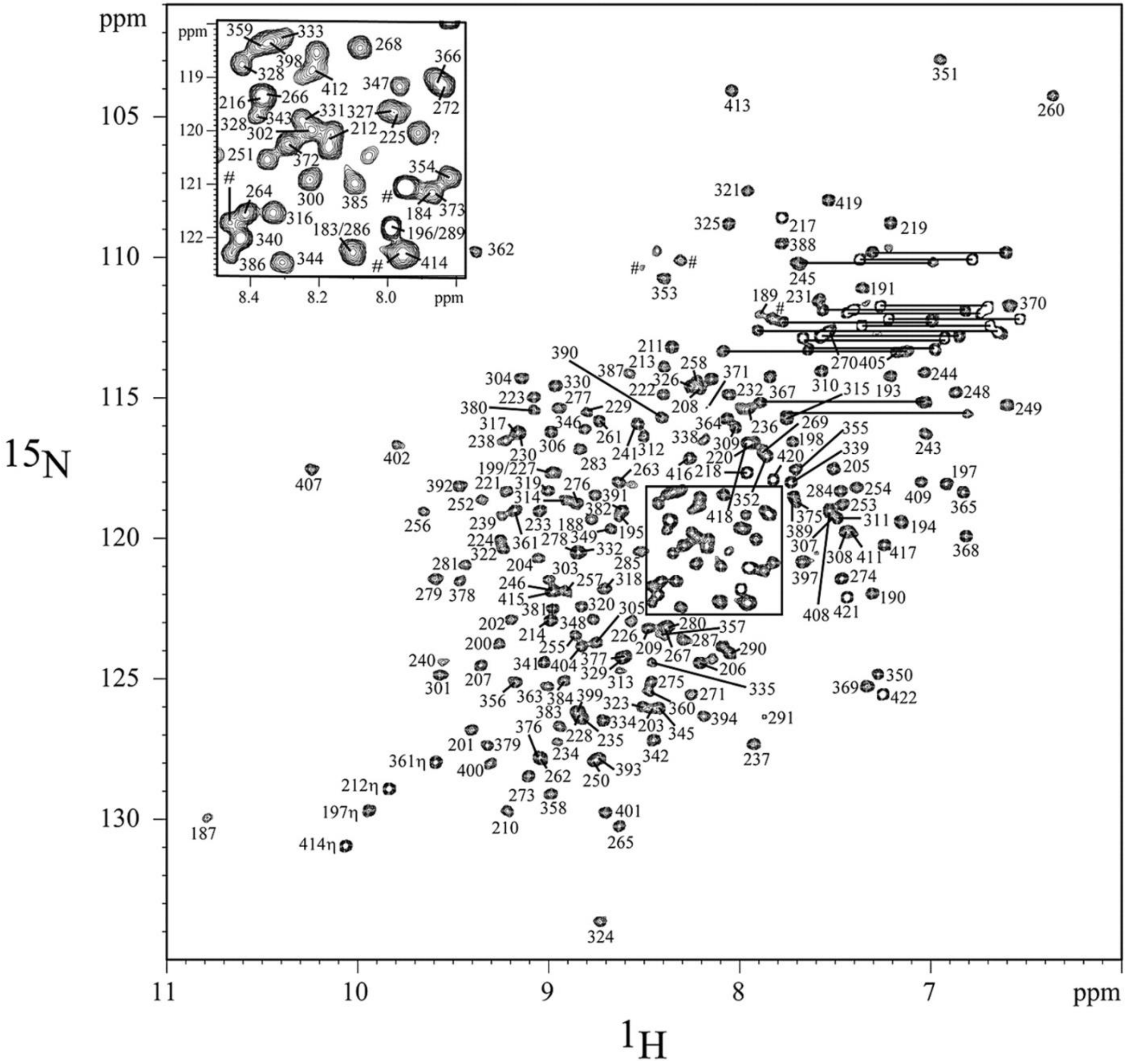
ppm
105
110
115
120
125
130
15N
11
10
9
8
7
ppm
1H
ppm
119
120
121
122
8.4
8.2
8.0
ppm
359
333
398
328
268
366
412
347
272
216
266
331
327
328
343
212
302
225
?
251
372
354
#
264
300
385
#
184
373
316
122
183/286
196/289
340
386
344
#
414
351
413
260
321
419
325
217
219
388
362
#
#
245
353
191
189
231
#
370
270
405
211
244
390
387
213
258
371
310
315
193
248
304
330
326
222
208
232
367
223
277
229
249
380
317
346
261
364
236
269
355
238
306
338
309
198
339
243
402
230
241
312
220
420
197
199/227
263
416
218
205
407
392
221
319
276
391
284
254
409
252
382
352
253
365
256
239
314
233
188
195
418
375
311
194
224
361
349
389
417
322
278
332
307
308
411
368
281
204
285
397
274
303
318
246
257
408
421
190
279
378
415
320
305
381
348
280
357
202
214
226
209
287
290
200
255
267
240
404
377
206
341
329
335
207
313
301
275
350
356
363
271
369
422
384
399
323
360
383
334
203
291
394
345
201
379
228
235
342
376
237
361η
400
234
393
262
250
212η
273
358
401
197η
210
265
187
414η
324

Doświadczenia rozpoczynają się od przygotowania cząsteczek wyznakowanych izotopami ^{13}C and ^{15}N.

Widma dwu- i trójwymiarowe są rejestrowane, aby zidentyfikować systemy spinowe i przypisać sygnały do poszczególnych reszt

Informacja strukturalna jest uzyskana przez pomiar tzw. efektu jądrowego Overhausera (NOESY)

Pomiary stałych sprzężeń pozwalają zmierzyć kąty w szkielecie fosforanowym RNA

Zmierzone więzy są następnie użyte w protokole minimalizacji struktury dynamiki molekularnej z simulated annealing
Wygenerowana zostaje grupa struktur (ensemble), która spełnia założone więzy

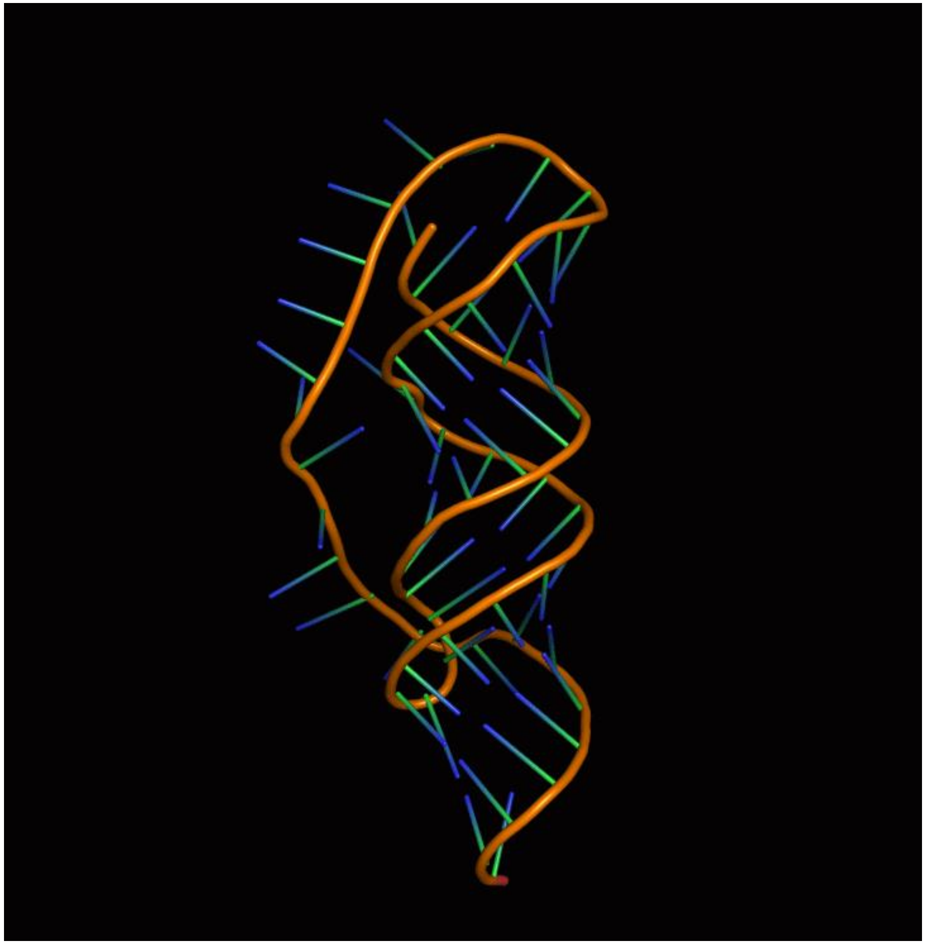

„Klasyczny” NMR dla RNA – ograniczenie do ok. 15 kDa
Ostatnie udoskonalenia NMR dla RNA to zastosowanie resztkowych sprzężeń dipolowych oraz selektywne izotopowe znakowanie RNA – obecny limit to 30 kDa (ok. 100 nukleotydów)

Zaletą NMR jest badanie cząsteczek w roztworze oraz możliwość badania ich dynamiki

Pierwsze struktury RNA rozwiązane NMRem - 1991

W ogromnej większości dostępne struktury RNA NMRowe to krótkie fragmenty (dupleksy itp.)

JEOL CRYO ARM 300

FEI TALOS ARCTICA

TITAN KRIOS

Time-consuming steps

Data transfer :)	many hours
Motion correction	GPU: few hours
CTF	GPU: few hours
Particle picking	GPU: few hours
Manual inspection	hours-days
2D classification	GPU: few hours
3D classification	GPU: few hours (or more)
3D refinement	GPU: hours/days (or more)
– Up to 100 000 CPU hours!	

Challenges

- Improve the contrast – phase plates
- Reduce sample movements
- Quality cirterion (equivalent of R_{free})
- Further developement of cryo-EM tomography

pre-mRNA splicing

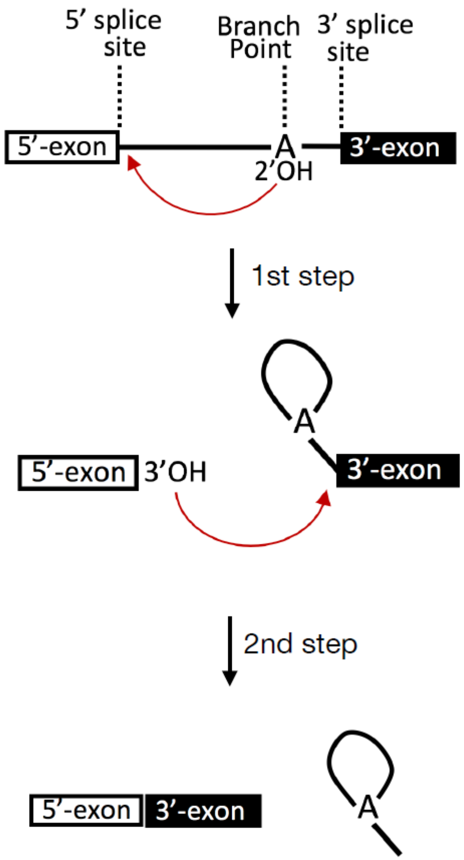

Will and Lührmann (2011)

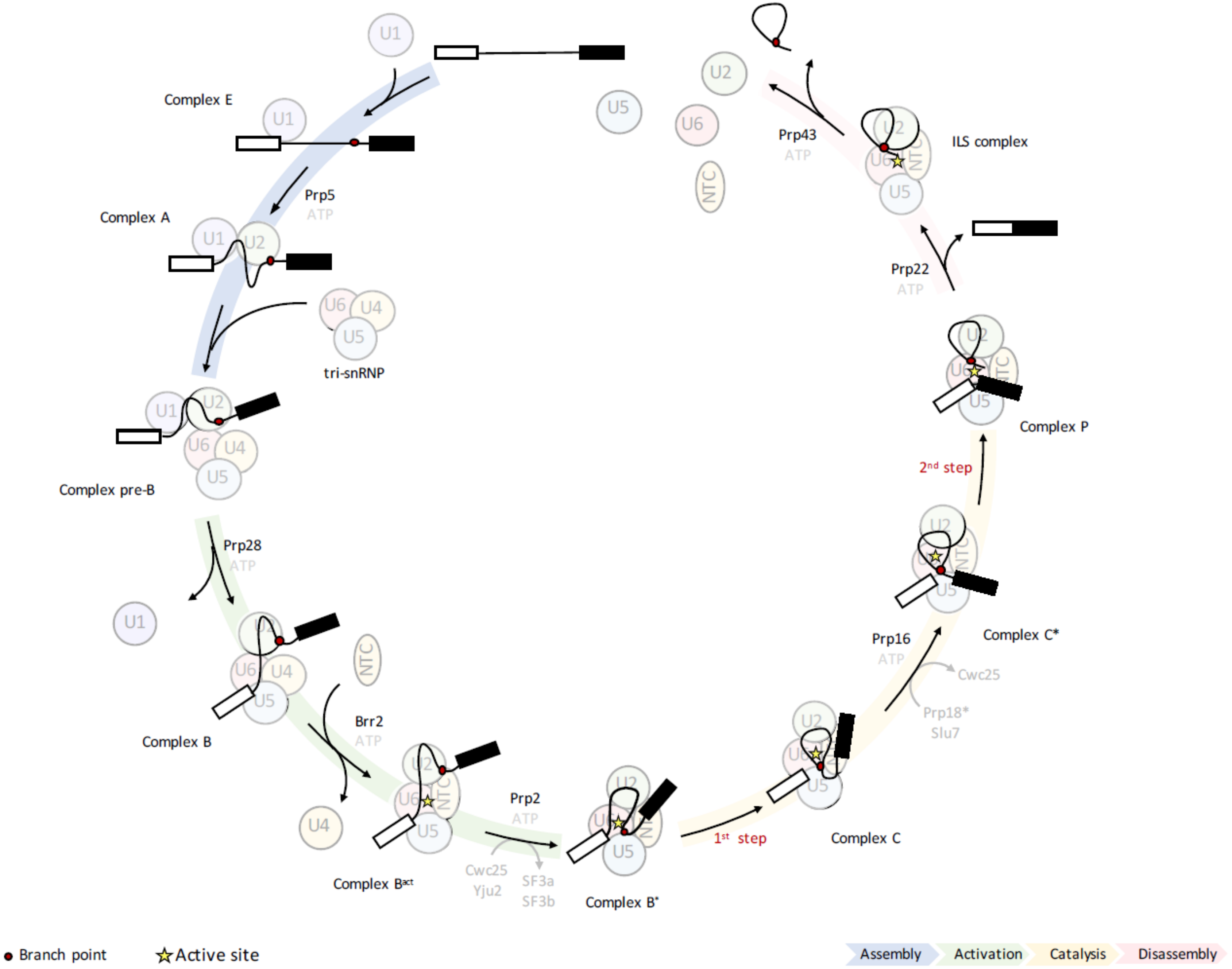
U1
Complex E
U1
Prp5
ATP
Complex A
U1
U2
U6
U4
U5
tri-snRNP
U1
U2
U6
U4
U5
Complex pre-B
Prp28
ATP
U1
U2
U6
U4
U5
Complex B
NTC
Brr2
ATP
U4
U2
U6
NTC
U5
Complex B^act
Prp2
ATP
Cwc25
Yju2
SF3a
SF3b
U2
U6
NTC
U5
Complex B*
1st step
U2
U6
U5
Complex C
Prp16
ATP
Cwc25
Prp18*
Slu7
U2
U6
NTC
U5
Complex C*
2nd step
U2
U6
NTC
U5
Complex P
Prp22
ATP
U2
U6
NTC
U5
ILS complex
Prp43
ATP
U2
U5
U6
NTC
Branch point
Active site
Assembly
Activation
Catalysis
Disassembly

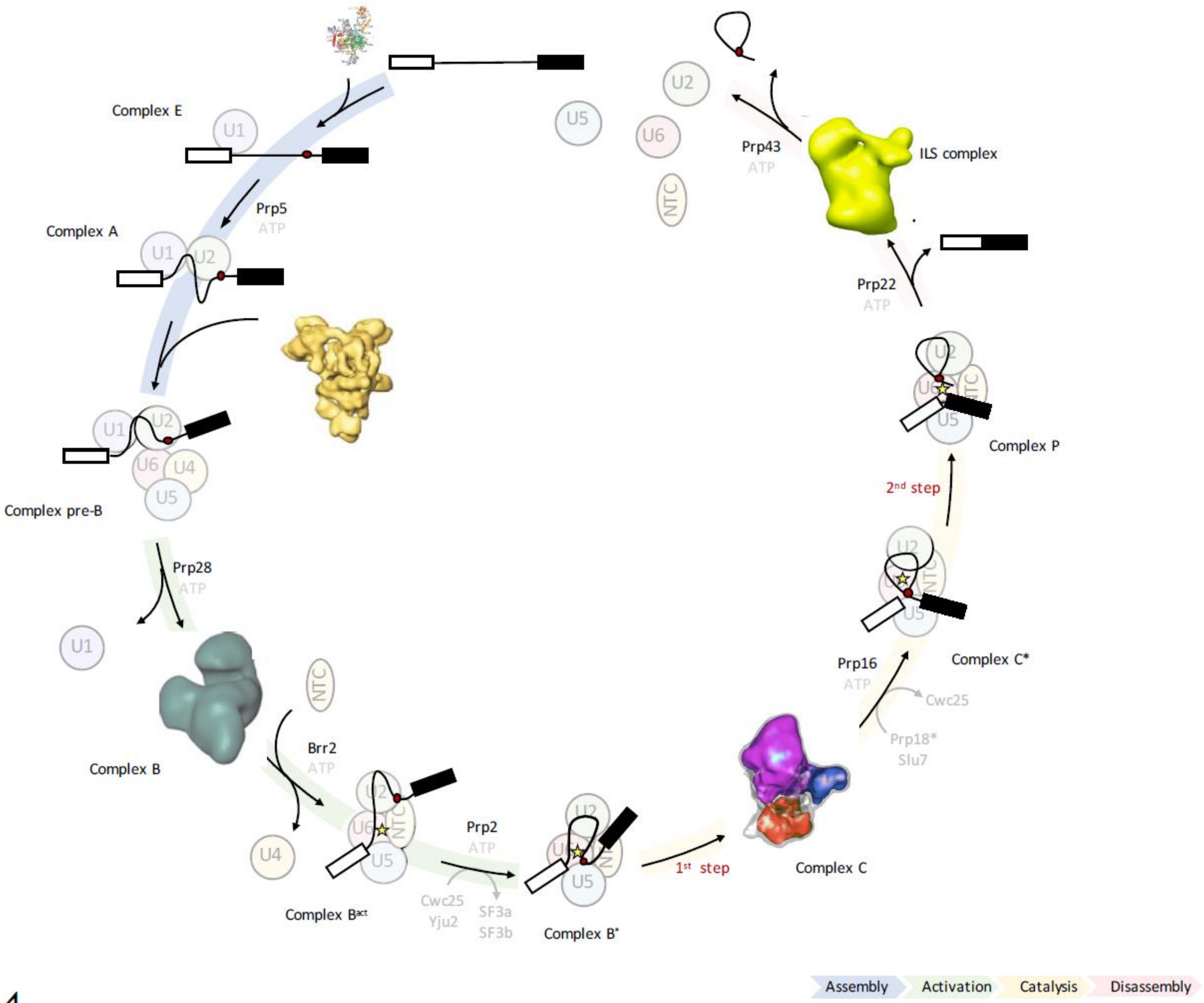
Complex E
U1
Prp5
ATP
Complex A
U1
U2
U1
U2
U6
U4
U5
Complex pre-B
Prp28
ATP
U1
Complex B
NTC
Brr2
ATP
U4
U2
U6
NTC
U5
Complex B^act
Prp2
ATP
Cwc25
Yju2
SF3a
SF3b
U2
U6
NTC
U5
Complex B*
1st step
Complex C
Prp16
ATP
Cwc25
Prp18*
Slu7
U2
U6
NTC
U5
Complex C*
2nd step
U2
U6
NTC
U5
Complex P
Prp22
ATP
ILS complex
Prp43
ATP
U2
U5
U6
NTC
Assembly
Activation
Catalysis
Disassembly

Year 2014

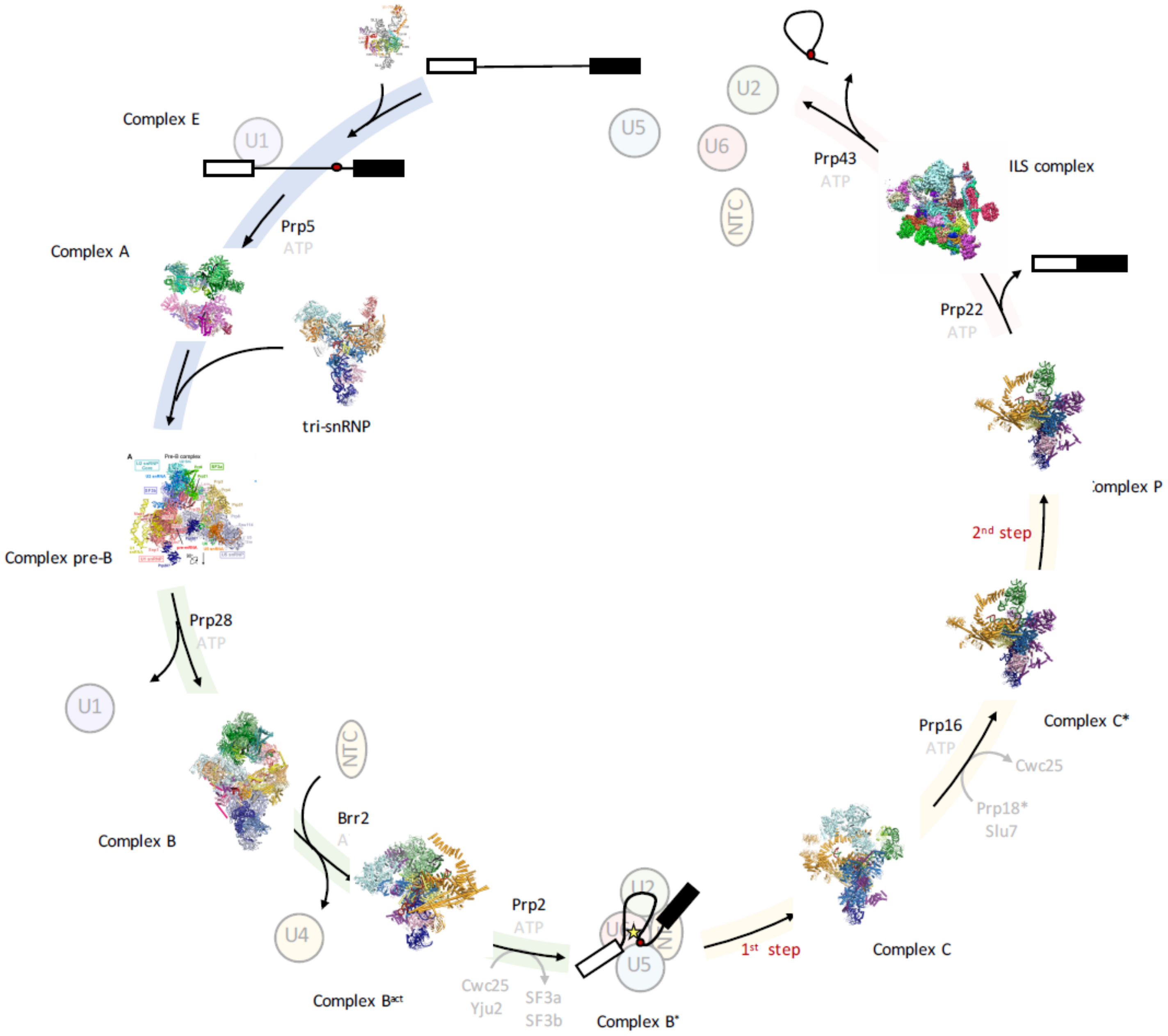

Complex E

U1

Prp5
ATP

Complex A

tri-snRNP

Complex pre-B

Prp28
ATP

U1

Complex B

NTC

Brr2
ATP

U4

Complex B^{act}

Prp2
ATP

Cwc25
Yju2

SF3a
SF3b

U2
U6
NTC
U5

Complex B*

1st step

Complex C

Prp16
ATP

Cwc25

Prp18*
Slu7

Complex C*

2nd step

omplex P

Prp22
ATP

ILS complex

Prp43
ATP

U2

U5

U6

NTC

Assembly → Activation → Catalysis → Disassembly

Year 2018

c

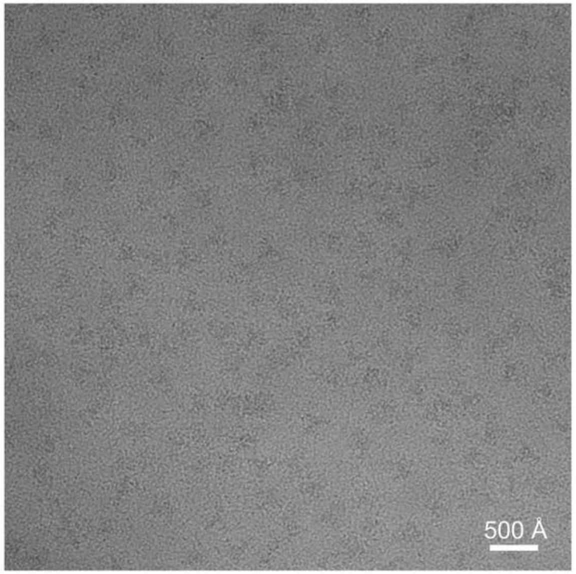

d

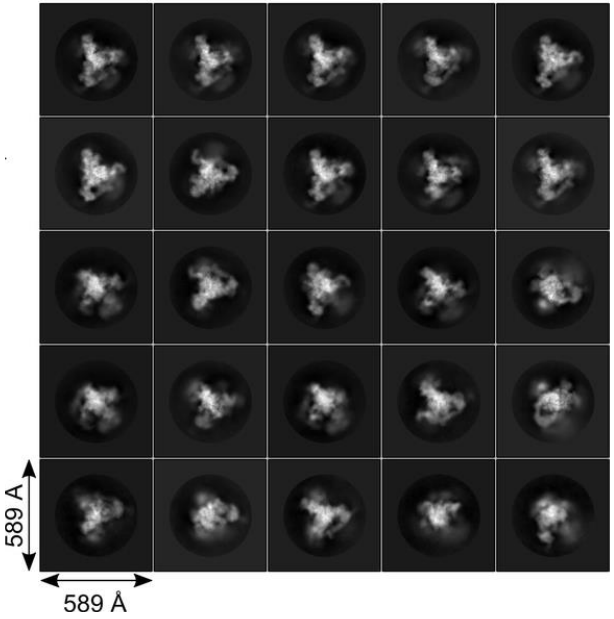

Galej W, Nature, 2016

a

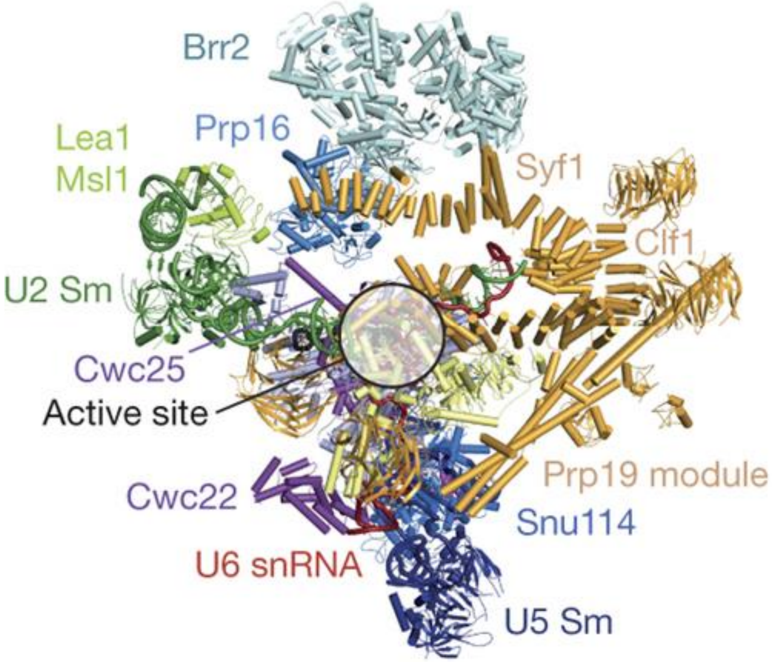

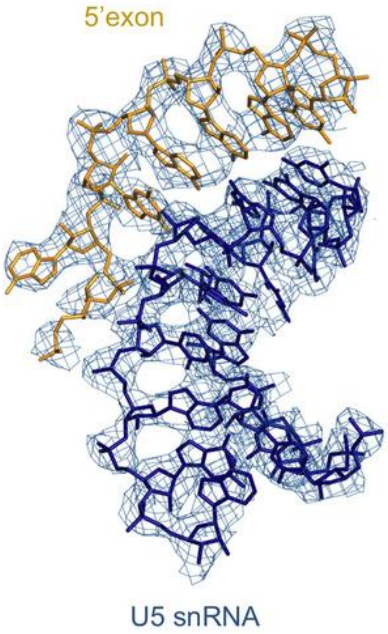

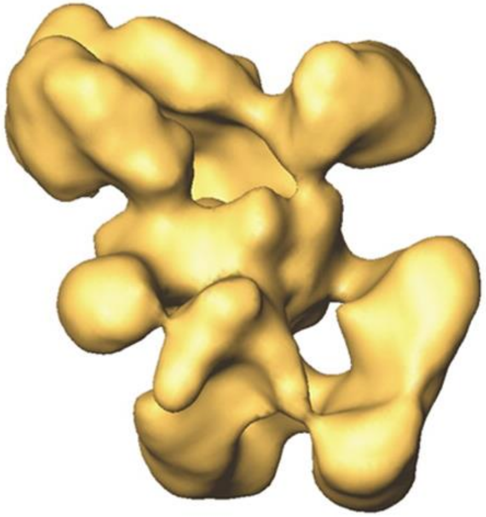

Golas MM, Mol Cell, 2010

Galej W, Nature, 2016

https://www.annualreviews.org/doi/suppl/10.1146/annurev-biochem-091719-064225